Development of a finite rate chemistry solver with tabulated dynamic adaptive chemistry

Anurag Surapaneni

Delft University of Technology

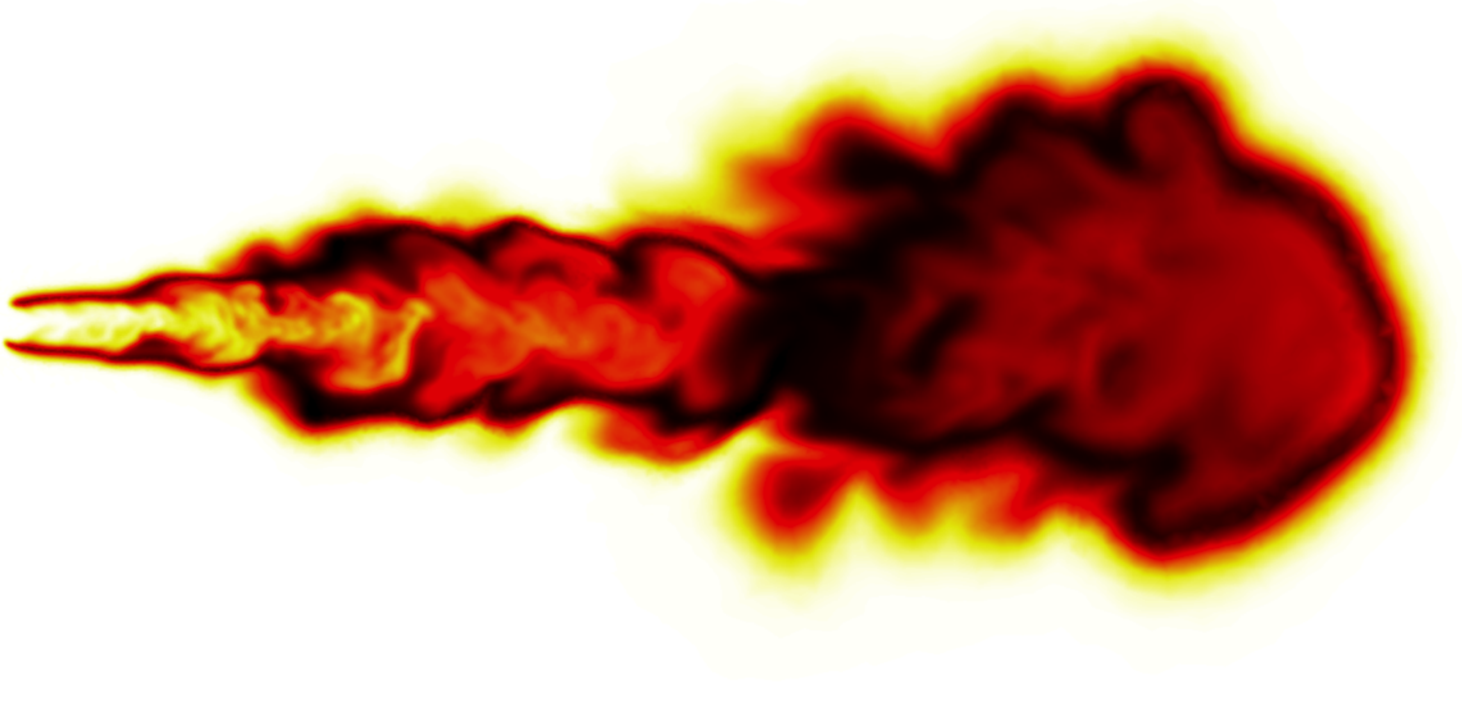

Delft University of Technology

Challenge the future

Development of a finite rate chemistry solver with tabulated dynamic adaptive chemistry

by

Anurag Surapaneni

to obtain the degree of Master of Science
at the Delft University of Technology,
to be defended publicly on 13/12/2019

Student number:	4717694	
Project duration:	January 1, 2019 – October 30, 2019	
Thesis committee:	Dr. Daniel Mira Martinez	CASE - Barcelona Supercomputing center, supervisor
	Dr. A. G. Rao,	Power and Propulsion - TU Delft supervisor
	Dr. D. J. E. M. Roekaerts,	Process and Energy - TU Delft
	Dr. S. J. Steven Hulshoff,	Aerodynamics - TU Delft

This thesis is confidential and cannot be made public until 13/12/2021.

Preface

The current study would not have been possible without the support an guidance of the following people. I would like to thank Dr.Daniel Mira for being my supervisor and constantly supporting and guiding me through every aspect of my thesis. I express my gratitude to Dr. Arvind Rao for being my supervisor at Delft and initially exposing me to the field of combustion in the field of aerospace engineering. I am in debt to Prof. Dirk Roekaerts and Dr. Nijso Beishuizen for teaching me the theory and practical applications of numerical combustion. I would like to thank Ambrus Both for his critical inputs and help with the daily logistics of the thesis. I am grateful to André Perpignan for his inputs on my thesis and literature review. I appreciate all the effort and support I received from the CASE department at the Barcelona Supercomputing Centre.

I would like to thank my friends and housemates who have supported me throughout my TU Delft journey. I am grateful to the open-source community, and hope that the community keeps growing. Finally I an forever in debt to my parents Srinivas and Manjula Rao for their constant support and love.

Anurag Surapaneni
Barcelona, October 2019

Abstract

Despite the onset of peta-scale computing, simulations of reacting flows with detailed chemistry is still considered computationally expensive. Better understanding of the chemistry of various fuels has led to increase in the complexity of the simulations in an effort to compute flows with real complex fuels. The increase in complexity makes CFD simulations prohibitively expensive even for the next generation of exa-scale computing. To have accurate reacting flow simulations with detailed chemistry at realisable costs some sort of cost mitigation strategy is to be applied. Solution of the chemistry in reacting flows is one of the most expensive steps of such simulations as it involves solving a system of highly non-linear stiff equations. There have been various methods proposed to reduced this computational costs at the expense of some assumptions. These methods can be broadly classified into two categories: (1) methods based on tabulation which include ISAT and Flamelet methods, and (2) methods based on adaptive chemistry. Former methods are developed to work on specific regimes of combustion and are known to predict reacting flows accurately, but when used outside this regime they may fail.

The present project falls under the adaptive chemistry category and aims to develop a numerical framework for the study of turbulent flames at various regimes using high-fidelity numerical simulations with on-the-fly adaptive kinetics. The chemistry reduction process is based on the Path Flux Analysis (PFA) enforcing Adaptive Chemistry (AC) based on local conditions.

PFA is a chemistry reduction method based on truncating reaction pathways. Key species are defined, usually reactants, major products, and species of specific interests like pollutants. PFA classifies reaction pathways between theses key species and eliminates pathways which fall below a specified threshold. PFA algorithm is formulated in a way that multiple generations of intermediate species can be tracked. In literature a universal threshold is specified, however, as the reaction pathways and their weights depend on the local chemical state, a universal definition of the threshold would lead to different levels of reduction and can lead to over-reduced/under-reduced regions. In this work the definition of the threshold is modified to be dependent on the local thermodynamic state, this ensures a uniform level of reduction.

Current state-of-the-art model of dynamic adaptive chemistry rely on an error estimator which decides when and where in the computational domain the reduction algorithm to be applied. This error estimator, usually a correlation function between specific chemical species is user specified and has a great impact on the reduction. This makes it necessary for the user to have an *a priori* understanding of problem and its chemistry. The methodology developed in this project eliminates the need for this error estimator as the reduced chemistry is tabulated based on a set of controlling variables. These controlling variables have global definitions and are identified for different regimes of combustion. The expensive operation of chemistry reduction is tabulated, hence reducing the computational time needed for chemistry reduction significantly.

State of the art reduction models and the proposed model are tested in: (1) laminar steady-state cases: premixed free flame, counterflow diffusion, and partially premixed flames; and (2) transient cases: auto-ignition, flame kernel propagation in stratified mixtures, flame vortex interaction, and a reacting Taylor-Green vortex. The proposed model is found to predict solutions with the same accuracy as the state of the art models in steady state cases and performs better in transient cases due to its nature of chemistry reduction which makes it applicable to a variety of combustion problems without any tuning. Computationally the proposed model was found to be between 5 to 20 % faster for specific cases than the respective reference case with no chemistry reduction.

Contents

Acronyms

CFD Computational Fluid Dynamics.

CFL Courant Friedrichs Lewy.

CODAC Correlated Dynamic Adaptive Chemistry.

CSP Computational Singular Perturbation.

DAC Dynamic Adaptive Chemistry.

DNS Direct Numerical Simulation.

DRG Direct Related Graph.

DRGEP Direct Related Graph Error Propagation.

ECDAC Error Controlled Dynamic Adaptive Chemistry.

EOL End of Life cycle.

FVI Flame Vortex Interaction.

GPS Global Pathway Selection.

HCCI Homogeneous Charge Compression Ignition.

HPC High Performance Computing.

IEA International Energy Agency.

ILDM Intrinsic Low Dimensional Manifold.

ISAT In-Situ Adaptive Tabulation.

LES Large Eddy Simulation.

MAD Mixtured Averaged Diffusion.

MST Multi Species Transport.

NTC Negative Temperature Coefficient.

ODE Ordinary Differential Equation.

OPR Overall Pressure Ratio.

PaSR Partially Stirred Reactor.

PFA Path Flux Analysis.

PSR Perfectly Stirred Reactor.

PV Progress Varibale.

QSSA Quasi Steady State Assumption.

RANS Reynold’s Averaged Navier-Stokes.

TDAC Tabulated Dynamic Adaptive Chemistry.

TGV Taylor Green Vortex.

List of Figures

1 Introduction

Combustion is a branch of science which affects every aspect of human life today and also played a key role in physiological and sociological human evolution. Today combustion is used ubiquitously in various applications like applied heating, transportation, power generation among numerous others. Our dependence on combustion is absolute and human life can not be sustained without it. This dependence however, comes with its own implications of excessive usage of fossil fuels as a source for combustion leading to depletion of sources and emission of harmful gases. Despite the advancements in the non-renewable energy sector which include sources of energy like hydel, nuclear, wind and solar power major fraction of energy up to 85 % still comes from fossil fuels. The reliance on fossil fuels as a source for combustion is likely to be present in the near future due to issues concerning convenience, technological advancements and economics associated with use and development of non conventional sources of energy. The transportation sector is one the largest consumers of the global energy demand with about 25 % of the global fossil fuel usage and an increase of about 1.4 % an year [11]. Societies are pushing towards decarbonising the transportation sector with replacement fuels that are cleaner and greener than conventional fuels allowing for a carbon-neutral growth in the near term. Efforts are being made to find alternative energy sources that can be used with the current engine technologies and supply infrastructures. Fuels such as ethanol [14] or biodiesel [29] stand out as suitable options and are currently being employed in internal combustion engines and gas turbines, but their widespread use is limited by the the availability of required technology and infrastructure. On the other hand there is a rapidly growing sector of electrically powered vehicles. These vehicles aim to reduce fossil fuel consumption by using a combination of batteries and electric motors for propulsion rather than a traditional internal combustion engine. Conceptually this method would seem to work but majority of the electricity is produced by burning fossil fuels. This would then mean that the process of burning the fuel is being shifted from the vehicle to a power plant. An End of Life Cycle EOL analysis reveals that the net production of carbon during manufacturing and usage of these vehicles till their end of life is higher than convention vehicles using fossil fuels. This is due to a very high dependence on fossil fuels for electricity generation and a lack of technology in the manufacturing process and economics concerning supply and demand. A growth in the usage of renewable energy and further research into manufacturing of the batteries and related components should makes these vehicle more efficient. Despite these issues the electric vehicle industry is growing every year leading to better manufacturing process and lower overall emissions.

The Aviation sector which makes up a 15 % of the total energy demand is committed to reducing its carbon emissions by 50% from their 2005 level by 2050 [31]. To achieve this feasible choices in the near future for alternative jet fuels must be considered as drop-in-fuel [31]. This means substitutes of conventional jet fuels must be completely interchangeable and compatible with conventional jet fuels without requiring engine or fuel system modifications. Aviation biofuels which are blends of low carbon sustainable fuel with fossil jet fuel is one such alternative to Jet A. The use of aviation biofuel is reflected in the International Energy Agency IEA's Sustainable Development Scenario, aviation biofuel is anticipated to reach around 10% of total aviation fuel demand by 2030, and increase to 20% by 2040. The number of flights using the blended biofuel is more that 150,000 since the first flight in 2008, supporting IEA's predictions.

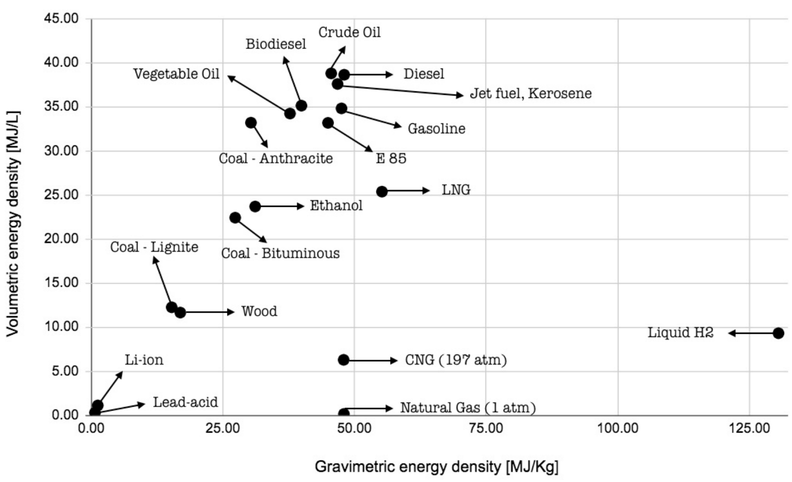

Figure 1.1: Volumetric V/s gravimetric energy density (adapted from [28])

The cluster of fuels which are currently being used in the aviation industry lie in the high volumetric and gravimetric energy density region, this is due to restrictions in the volume of the fuel that can be stored on board to be used in flight. Though sources like hydrogen have high gravimetric energy densities their volumetric density is quite low and hence would either need to be pressurised or be stored in larger volumes, this opens up new difficulties in considering hydrogen at a fuel. Predictions show Figure 1.2 that liquid fossil fuels will continue to dominate the transportation sector as a the primary energy source for the next 50 years or even longer [51]. The International Air Transport Association predicts a 100 % growth in the aviation industry in the next 20 years [24]. This leads to a scenario where there is an increase in energy supply for the transportation sector which reflects in its sustainability ,price, security and availability. Additionally worldwide concerns about the impact of current and future transportation related greenhouse gas emissions and pollutants on public health and climate change has made it necessary to come up with more efficient combustion systems.

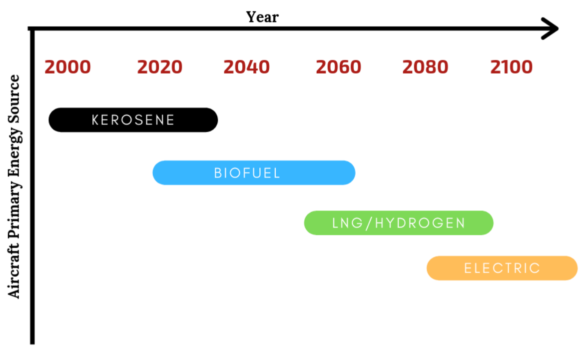

Figure 1.2: Trend showing primary fuel in the civil aviation industry (adapted from [16])

As is seen in Figure 1.2 until the turn of the next century blends of kerosene with ethanol (biofuels) and hydrogen will act as the primary sources of energy for aviation before giving way to electrically powered aircrafts. It is then important to have research in areas to improve existing aircrafts, one such research area is the combustion process. There have been numerous studies done towards improving existing combustion systems by designing more efficient combustion systems which would also minimise the production of pollutants.

The aviation industry to comply with the pollution standards specified by ACARE and the Paris agreement [1] which specified the reduction of greenhouse gas emissions is taking major strides towards cleaner engines. Efforts are aimed towards increasing the Overall Pressure Ratio OPR in the turbine, the OPR is the overall ratio of stagnation pressures as measured across the compressor of a gas turbine engine. The increase in the OPR improves the thermal efficiency of the system as more work can be extracted from the flow [30]. However, the increase in OPR leads to increase in combustion chamber temperatures which increase the production of NO_X, specifically thermal NO_X. The simultaneous increase in efficiency and reduction in emissions is contradicting and, hence the design of efficient combustion chambers needs to be a trade-off between the two. A lean combustor with a high bypass ratio would fit the design requirements, as it would reduce the production of pollutants while increasing the overall efficiency of the gas turbine. Lean combustion is associated with many complex phenomena such as thermo-acoustic instabilities, lean blow-outs to name a few. Predicting these complex behaviour in experimental set-ups is quite tricky and hazardous, hence numerical combustion plays a pivotal role in prediction of such phenomenon and aid combustion system design.

1.1. Numerical combustion

Further understanding of the physics and chemistry of the combustion process is fundamental to achieve improvements in fuel efficiency, reduce greenhouse gas emissions and pollutants and aid in a smooth transition to alternative fuels. The interest in such fronts is evidenced by the IEA's Technology Collaboration Program on Emissions Reduction in Combustion [3], where fundamental and prospective research in combustion and fuels are carried out. The development of calculation models that are capable of reproducing fundamental process is a central task to the program, which will allow the improvement of future powertrain designs. Especially in gas turbines where the design and development of combustion experiments in realistic conditions is very challenging due to the high power and flow conditions.

To predict the performance of novel combustion chambers with cleaner fuels further understanding and more accurate characterisations of the fuels on practical applications is to be evaluated. Compared to traditional design of combustion systems, based upon both experimental knowledge and simplified often semi-empirical models, Computational Fluid Dynamics CFD tools have reached a point where they can guide the design and development of more efficient and cleaner applications. This is especially critical in the case of complex combustion problems, which entails a list of complex simultaneous processes that are very difficult to isolate and therefore to adequately quantify.

The process of combustion is extremely complex, occurs in multiple scales and is a combination of different branches of science such as fluid dynamics and chemistry. Testing and design of combustion systems is quite tricky and expensive as they usually function in extreme conditions such are high temperature and/or high pressure. Accurate measurements at these critical conditions is difficult and computational approaches can assist experimental data. This would mean that combustion system can be tested and be designed by using computers to simulate their behaviour at various conditions numerically. Accurate numerical description of complex chemistry phenomenon are among the most taxing computer simulations. Chemistry of a fuel depends on numerous species and the highly non linear reaction mechanisms they follow. As simplistic equilibrium assumptions or single step chemistry methods fail to capture complex chemical phenomena researcher's pushed towards using more detailed mechanisms. This led to the development of detailed chemical mechanisms for numerous fuels. However, incorporating such large mechanisms into simulations is a challenge in itself. These chemical mechanisms give rise to stiffness in the simulations which make their solution computationally expensive. Methods have been developed and to reduce the computational cost with minimal sacrifice in accuracy reference in section 2.

1.1.1. Need for large kinetics

Chemical reactions schemes are developed for certain conditions and when used outside their range for applicabilities fail, this is demonstrated by an example of auto-ignition delay in N-Heptane. Auto-ignition delays usually decrease with increase in mixture temperature, however for hydrocarbons with high number of carbon atoms there exits a region where the ignition delay increases with increase in mixture temperature. This is called the negative temperature coefficient NTC region and the reason for this behaviour is explained in brief in section 5.1.1.To predict this behaviour chemical kinetics need to account for low temperature chemistry and oxidation pathways [30]. This effect is shown in 1.3a, where the differences between a mechanism with low temperature chemistry [35] and one without [27] are compared. The number of species were 188 and 99 respectively, this shows that predicting complex phenomena such as the NTC region require more detailed chemical reaction mechanisms.

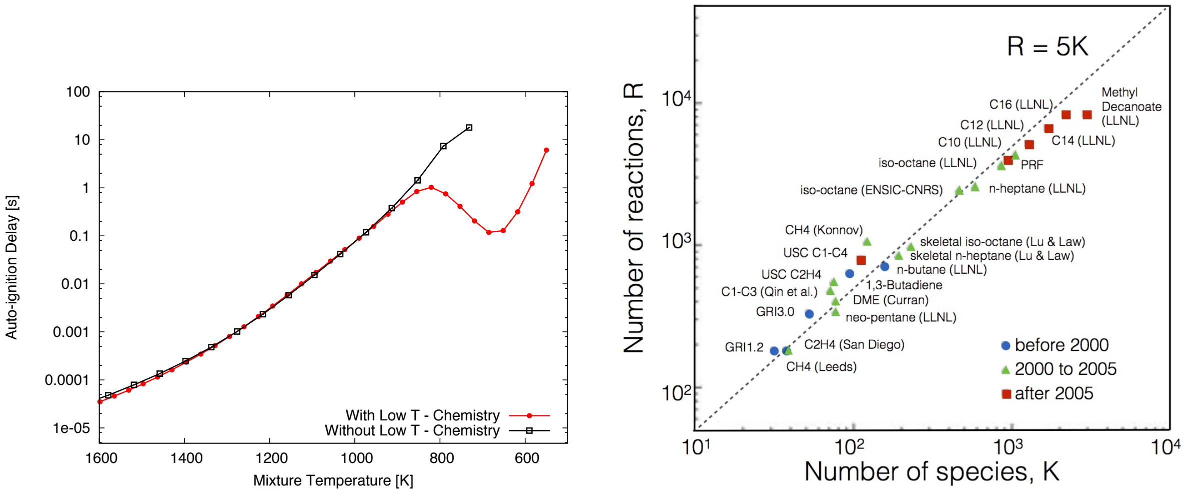

(a) Ignition delay times for N-heptane (b) Size of detailed mechanism in the past decade [36]

Prediction of pollutants also require detailed and specific reaction mechanisms, the production of NO_X occurs through pathways based on temperature (Thermal NO_X), Fenimore pathway (Prompt NO_X) and the NNH pathway among others. Soot is a very complex pollutant as it is produced and predicted from precursor aromatic compounds which in-turn have complex formation mechanisms. This leads to the need for very large chemical kinetics to predict pollutants to some degree of accuracy.

Detailed mechanisms for simpler fuels like methane or hydrogen with NO_X mechanisms still are quite extensive and are to be adapted before used in actual simulations. The problem gets amplified for higher hydrocarbons where in the size of the mechanisms makes even 0 D simulations quite expensive. Figure 1.3b show the development of detailed mechanisms for hydrocarbons since 1990. The computational costs of dealing with such large mechanisms are discussed in 1.1.2

1.1.2. Computational Expenses

The cost of a fully resolved reacting flow simulation depends on multiple factors such as the number of species characterising the reaction process, the temporal and spatial resolutions associated to the problem or the numerical schemes and algorithms used for the resolution, or the inter-node communication, among others. In practice, the resolution of the problem can be decomposed in the computation of scalar transport (advection and diffusion), the temporal derivatives, and the chemical source terms. The following computational cost analysis is adapted from [36] and aims to derive a function which would evaluate the computational costs based solely on the number of reactions and species. Apart from the actual integration of the chemical source terms the next major expensive process is computing the diffusion coefficients in the multi-component flow. Models like the Mixture Averaged Diffusion MAD and the Multi Component Diffusion MST are essential when predicting flows dominated by diffusion. The cost of the mixture-averaged as given by Lu et.al [36] scales quadratically with the number of species. The Multi Component Diffusion model MST is more detailed and involves an implicit calculation and is known to scale at least cubically with the number of species. As the chemical source terms are usually non-linear and when an implicit integration is used a Jacobian matrix needs to be computed for the Newton method. The cost of computing the Jacobian analytically is linear with the number of reactions as its computed by differentiating each reaction's rate with respect to its participating species. However, the cost of computing the Jacobian numerically scales quadratically with the number of species as reaction rates are to be computed for each perturbed mass fractions of species. Jacobian factorisation scales cubically with the number of species and can not be reduced as the Jacobian's encountered in chemically reacting flows are rarely sparse. Finally, the inter-node communication in case of a parallel code scales linearly with the number species. All these expenses can be put as Equation 1.1:

$$C = C_0 + \alpha S + \beta S^2 + \gamma S^3. \tag{1.1}$$

where S is the number of species, C is the overall cost of a simulation, C_0 is computational overhead which is neglected,α,β and γ are constants which are dominated by chemical source integration, diffusion and factorisation of the Jacobian respectively. For large mechanisms with a lot of grid points the simulations can dominate the power the current supercomputers. Lu et.al [36] recommend that for fuels with simple chemistry such as hydrogen and methane an implicit solver with Mixtured Averaged Diffusion (MAD) and an analytically computed Jacobian would be efficient. For larger mechanisms however, the implicit solutions of the Jacobian might be quite expensive and explicit methods are to be preferred. Diffusion in large mechanisms can also be simplified by assuming lewis number transport by either having lewis numbers as a constant value for all species or by setting all lewis numbers to unity (equal diffusivities for all species). Literature on reduction methods to accelerate simulations of reacting flows with respect to reduction in detailed chemistry/diffusion, implicit and explicit solver with stiffness removal techniques will be discussed in section 2

1.1.3. High Performance Computing (HPC)

The computational costs involved with numerical combustion were discussed in the previous section, traditional computers cannot provide the computing resources necessary for computing reacting flows with detailed chemistry. This is where High Performance Computing (HPC) systems come into play, HPC is generally referred as the practice of aggregating computing power to deliver higher performance than could not be achieved from a desktop machine or workstation to solve large computational problems [23]. High-fidelity numerical combustion codes require massively parallel multi-physics algorithms to address multi-scale and multi-physics processes. This is addressed using HPC architectures and scalable solvers that can run efficiently on advance heterogeneous supercomputing systems. The developments in the combustion community are hence closely linked to the development of HPC clusters, Figure 1.4 shows that the size of DNS simulations follows Moore's law. Moore's law is derived from an observation that the number of transistors on a dense circuit doubles every year, a similar trend is observed in reacting flow simulation indicating their dependence.

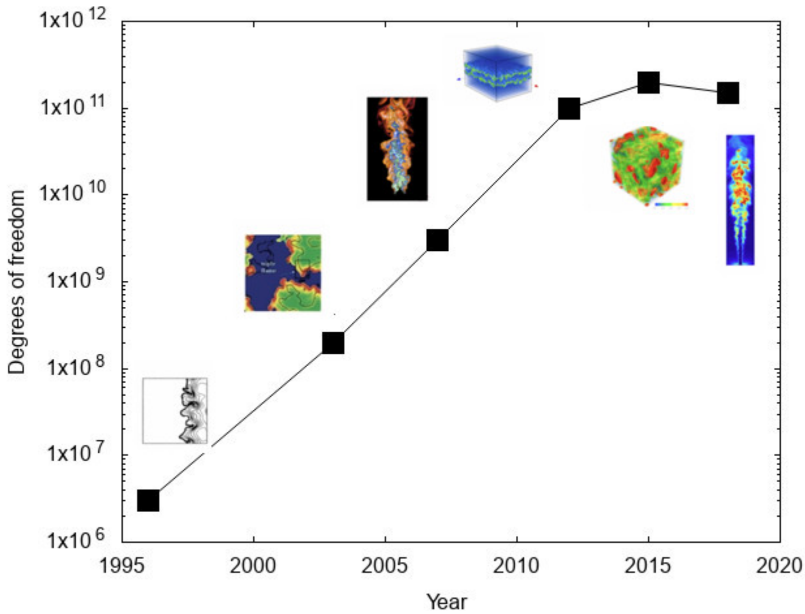

Figure 1.4: DNS simulations with time (adapted from [10])

For the current project the HPC cluster system called MareNostrum 4 at the Barcelona Supercomputing Centre was used, the project completely relied on this system for computational resources.

1.1.4. Scope of the project

The scope of the project is to develop a reacting flow solver based on finite rate chemical kinetics with on-the-fly chemistry reduction that can be applied to solve large scale LES and DNS problems.

The current project is done in collaboration with the CASE department of the Barcelona Supercomputing centre (BSC). BSC currently has 43 research groups with over 500 members working on innovative projects in the field of computer science, life sciences, earth sciences and computer applications in science and engineering. BSC's aim to promote HPC services towards novel projects fits perfectly with the scope of the current project. The outcome of the current project would enable research on the fundamentals of combustion for various existing and experimental burners. This evaluation would help designers and engineers to design more efficient and effective combustion systems.

1.2. Thesis Layout

The following section outlines the structure of the thesis.

Motivation and scope of the study is discussed in section 1. Available literature on chemistry reduction model is discussed in section 2. The literature review is broken down in two sections where in static and dynamic implementations of the reduction methods are presented. The study focuses primarily on two groups of reduction which are based on truncation of reaction pathways and tabulation methods. Based on the literature review and the motivation research objective for this study are presented. The report then discusses theory in section 3 behind reaction flow simulations which include conservation equations respective modelling choices and chemical kinetics. The implementation of the finite rate solver is then discussed in section 4, the multi-physics code Alya is presented in section 4.1 and the open source chemical kinetics solver Cantera's structure and functionalities are discussed in section 4.2. Then the coupling strategy between the transport solver (Alya) and the chemistry solver (Cantera) is presented in section 4.2.1. Performance of static chemistry reduction in canonical flame problems like premixed, counter flow diffusion flames for two fuels - Methane and N-heptane are discussed in section 5. The report then discusses the performance of Dynamic Adaptive Chemistry (DAC) in steady state laminar premixed, counter flow diffusion and partially premixed problems. A stratified flame and Flame Vortex Interaction (FVI) case provide insights on the performance of the reduction methods for transient cases. Finally, a turbulent 3D Taylor Green Vortex (TGV) case is shown to evaluate the reduction strategies in turbulent flows. The report then discusses the HPC aspect of the study discussing scalabilities and load imbalances before presenting data on the computational performance of the reduction strategies. Lastly, relevant conclusions are drawn and scope for further studies are formulated.

2
Literature review

The importance and implications of using detailed chemistry was discussed in section 1.1.1. To simulate reacting flows with detailed chemist at feasible computational costs it is necessary to adopt some method of chemistry reduction. There are many such methods for chemistry reduction which are detailed by Law et.al [37]. Though different the methods can be broadly classified as:

- Reaction path based methods
  - Chemical path reduction
  - Chemical path/states tabulation
- Chemical Lumping
- Timescale analysis

Chemical lumping is based on lumping species with similar chemical or physical properties to reduce the overall number of equations to be solved. Time-scale analysis is based on separating species as fast and slow evolving species based on the classical Computational Singular Perturbation (CSP) method applied to chemical kinetics [21] and treating them differently using a Quasi Steady State Assumption (QSSA). This method aims to reduce the stiffness of the equations that are solved. Both these methods require knowledge of the chemistry of fuel and regime of combustion of the problem. Moreover, dynamic implementations of these methods is not very straightforward and needs a lot of user input. The objective for the chemistry reduction in the context of this project was to have a reduction method which is globally applicable to any fuel at any combustion regime with minimal user input. After a literature survey was done on all the reduction methods the reaction pathway method was found to be most apt to fit the purpose of the project, the following sections talk about the different methods of reduction and their dynamic implementations.

2.1. Reaction path reduction methods

These methods are based on identifying important reaction paths in order to reduce chemistry. The Direct Related Graph (DRG) methods was proposed by Lu & Law [34] which involved identifying key/important species and constructing a relation matrix based on the reaction paths and the reaction rates between them. The relation coefficient between species A and B in given by Equation 2.1:

$$r_{AB} = \frac{\Sigma_{i=1,N} \mid v_{A,i}\omega_i\delta_{Bi} \mid}{\Sigma_{i=1,N} \mid v_{A,i}\omega_i \mid}. \tag{2.1}$$

where i is the number of reaction in the mechanism, $v_{A,i}$ is the stoichiometric coefficient of species A in reaction i, ω_i is the net rate of progress of reaction i and $\delta_{Bi} = 1$ or 0 if species A in involved in reaction i or not respectively.

A threshold is set and species which fall below this value are eliminated from the mechanism. Lu et.al [34] reduced a detailed mechanism for methane from 70 species to 33 species based on this method and evaluated its performance in laminar premixed and auto ignition problems. As pointed by Lu et.al [34] the key parameter in this method is the specification of the cutoff threshold, as the relation matrix changes with changes in mixture composition temperature and pressure a global threshold could not be easily defined in all cases. The reduced mechanism could also lead to truncated reaction paths which would lead to accumulation or depletion of species. To overcome such ambiguities in the DRG method P.Pepiot et.al [40] proposed a modified implementation of the DRG method which accounted for an Direct Related Graph Error Propagation (DRGEP). This method computes the error in the prediction of a certain species of that is incurred by neglecting a reaction path. The coefficients are scaled to have a bounded value between 0 and 1, this is done so that the coefficients become relative and an universal threshold can be specified. The formulation of the relation matrix is given by Equation 2.2

$$r_{AB} = \frac{\Sigma_{i=1,N} \mid v_{A,i}\omega_i\delta_{Bi} \mid}{max(P_A, C_A)}. \tag{2.2}$$

where

$$P_A = \Sigma_{i=1,i} max(0, v_{A,i}\omega_i), \tag{2.3}$$
$$C_A = \Sigma_{i=1,i} max(0, -v_{A,i}\omega_i). \tag{2.4}$$

An assumption is made that the longer the error has to propagate the smaller the effect it has and this target specific reduction leads to greater and more efficient reduction of mechanisms. In the end an integrity check is performed on the mechanism to make sure that there are no truncated pathways or pathways which lead to accumulation of certain species. It was pointed out by Sun et.al [49] that the DRG method which selects species based on absolute reaction rates makes the relation matrix non-conservative. Sun also mentions that the DRGEP method included error propagation in multiple generations, however It fails to include the reaction paths where the intermediate species occur in parallel. Further on The DRGEP method fails to capture species with both fast and slow dynamics, Sun gives and example of the catalytic effect NO_x on ignition enhancement [49]. To mitigate these issues a combination of of DRG and DRGEP with species sensitivity was proposed by Niemeyer et.al [39], this however was computationally very expensive due to the addition of the species sensitivity calculations. To address all these issues Sun et.al came up with a multi-generation Path Flux Analysis (PFA) [49] including both consumption and production pathways. The formulation of the relation matrix was altered to account for multiple generations of simultaneously produced/consumed intermediate species for a second generation PFA the formulation is as follows.

$$r_{AB} = r_{AB}^{p-1st} + r_{AB}^{c-1st} + r_{AB}^{p-2nd} + r_{AB}^{c-2nd}. \tag{2.5}$$

where r_{AB}^{p-1st} , r_{AB}^{c-1st} ,r_{AB}^{p-2nd} and r_{AB}^{c-2nd} are the corresponding production and consumption paths from species A to B for $1st$ and $2nd$ generation species respectively. second generation coefficients:

$$r_{AB}^{p-2nd} = \Sigma_{M_i \neq A.B}(R_{AM_i}^{p-1st} R_{MB_i}^{p-1st}), \tag{2.6}$$
$$r_{AB}^{c-2nd} = \Sigma_{M_i \neq A.B}(R_{AM_i}^{c-1st} R_{MB_i}^{c-1st}). \tag{2.7}$$

first generation coefficients:

$$r_{AB}^{p-1st} = \frac{P_{AB}}{max(P_A, C_A)}, \tag{2.8}$$
$$r_{AB}^{c-1st} = \frac{C_{AB}}{max(P_A, C_A)}. \tag{2.9}$$

The definition of P_A and P_B is the same as in the DRGEP formulation, however, the additional variables P_{AB} and C_{AB} are defined as

$$P_{AB} = \Sigma_{(i=1,i)} max(0, v_{A,i}\omega_i\delta_{iB}), \tag{2.10}$$
$$C_{AB} = \Sigma_{(i=1,i)} max(0, -v_{A,i}\omega_i\delta_{iB}). \tag{2.11}$$

where δ_{i_B}) is an boolean operator to determine if species B exists in reaction i. The performance of PFA was compared against the DRG method in autoignition problems for n-decane/air mixtures. It was found by Sun et.al that the reduced mechanisms generated by PFA were more effective in predicting auto-ignition delays, it was also found that PFA could identify species in catalytic cycles. Although Sun's implementation of PFA only included one generation of intermediate species the algorithm of PFA can be extended to more generations. The increase in computational cost as give in Sun is $(NumberofSpecies)^{Generations}$. As seen by Sun the computational cost of PFA at higher number of generations increases very rapidly hence it was found not be feasible include more than second generation relations. This still meant that a method to quantify the relation between various species of a mechanism is still a problem to be solved. The Global Pathway Selection (GPS) [17] algorithm aimed to address this issue. The main assumption of the method are that if a significant portion of species pass through a hub species then it needs to be kept in the mechanism irrespective of its influence on key species. Secondly, species which are important to build the chemical pathway to produce or consume these hub species must also be included. The GPS approach consists of constructing elemental flux graphs for all the elements in the detailed mechanism. Then the so called hub species are selected such that they transfer a significant amount of the elemental fluxes and finally global pathways between products and reactants through each hub species are found based on the elemental fluxes graphs. Gao's implementation of this algorithm in [17] shows better performance at auto-ignition delay studies for n-heptane and iso-octane than the methods mentioned earlier. Also as pointed out by Gao et.al the GPS method also could be used to reduce mechanism based on mixtures of different fuels.

2.2. Reaction path/states tabulation methods

In the following sections literature on methods based on tabulating reaction pathways/chemical states are presented.

2.2.1. In-Situ Adaptive Tabulation (ISAT)

ISAT approach as presented by Pope et.al [42] aims to reduced the number of degrees of freedom of a problem by on-the-fly tabulation of chemistry. An accessed region is defined which contains a set of all possible compositions which are most likely to occur in the problem. The problem in then tabulated based on the low dimension accessed region which is used to represent the higher dimension problem. The accessed region depends on local condition both chemical and flow conditions, hence the tabulation is done on-the-fly rather than as an *a priori* process. The table is filled for a given composition and stored for later use at similar compositions. The next step is the linear mapping step which interpolates between a stored value ϕ_{tab} to a query point ϕ_{query}. The table stores ϕ, $R(\phi)$ and also the gradients $\frac{\partial R(\phi)}{\partial \phi}$. The approximation at a query point q is then determined by

$$R(\phi^q) \approx R^l(\phi^q) \equiv R(\phi^O) + \delta R^l. \tag{2.12}$$

where

$$\delta R^l = \delta R + O(\mid \delta\phi \mid^2). \tag{2.13}$$

An error threshold is defined which makes sure that the difference between actual and the linearised mapping between a tabulated point and a query point is below the given threshold. If this criteria is not fulfilled chemical sources are integrated rather than being interpolated and are stored. Areas in the computational domain can be defined with different levels of thresholds to achieve higher accuracies in regions of interest. A speed-up factor of 1000 was achieved when this method was tested with a perfectly stirred reactor case for methane with 14 species. ISAT was found to be efficient in predicting premixed flames and flame structures closer tabulated data, but in case of non-premixed flows involving a large kinetic mechanism with a broad temperature region and large concentration gradients populating and retrieving the data the binary table was computationally expensive.

2.2.2. Intrinsic Low Dimensional Manifold (ILDM)

The ILDM method proposed by Maas et.al [38] of accelerating solution of chemistry for reacting flows is based on decoupling slow and fast dynamics based on an eigenvector analysis of a 0D Perfectly Stirred Reactor (PSR) system. This method considers enthalpy, pressure and N number of species as characteristic quantities which define the state of the system. The system is then defined by these reduced number of variable, rest of the variables are mapped to these controlling variables. The justification for this reduction in the number of variables that define a system is based on the observation that in a closed adiabatic and isobaric system kinetic pathways in the phase space crossover. It would then make sense to define a subspace and find the said intersections with other quantities based on the subspace. As the effects of transport are neglected the solution of the actual solution of the chemical kinetic manifold may be different for the one that is tabulated in the ILDM method. To overcome this issue it was suggest by Oijen et.al [52] and Gicquel et.al [18] that the tabulation be done with 1D premixed or diffusion flames. In these methods a set of controlling variables is defined as is done in ILDM the most common choice of these controlling variables are the mixture fraction and the chemical progress variable. The mixture fraction (Z) defines the degree of mixing between the fuel and the oxidiser and is expressed by the Bilger's formula as:

$$Z = \frac{\beta - \beta_O}{\beta_F - \beta_O}. \tag{2.14}$$

with

$$\beta = \sum_{i=1,N_E} W \sum_{j=1,NS} a_{i,j} \frac{W_i Y_j}{W_j} i. \tag{2.15}$$

Mixture fraction is passive scalar and when lewis number equals unity its transport is given by:

$$\frac{\partial \rho Y_Z}{\partial t} + \frac{\partial \rho u_j Y_Z}{\partial x_j} = \frac{\partial}{\partial x_j}\left(\rho D \frac{\partial Y_Z}{\partial x_j}\right). \tag{2.16}$$

The second controlling variable is the chemical progress variable and this represents the progress of the reaction. The definition of the progress variable should be such that it should be monotonically increasing or decreasing through the flame. This is to make sure that a unique solution is found when a look-up to the other quantities is made. It usually is defined as combination of mass fractions of products with some specified weights. The transport of the progress variable follows the Advection-Diffusion-Source equation:

$$\frac{\partial \rho Y_C}{\partial t} + \frac{\partial \rho u_j Y_C}{\partial x_j} = \frac{\partial}{\partial x_j}\left(\rho D \frac{\partial Y_C}{\partial x_j}\right) + \dot{\omega}_C. \tag{2.17}$$

Additional controlling variables can be added to capture more complex phenomena such as including total enthalpy as a controlling variable to capture heat loss etc. For given initial conditions a N-dimensional table is constructed with the solution of 1D flames using detailed chemistry. For condition beyond the flammability limits equilibrium computations can be performed and stored.

2.3. Dynamic Adaptive Chemistry (DAC)

Static *a priori* reduction methods such as the DRG [34], DRGEP [40] or the PFA [49] require some sort of user input in the form of key species and extract reduced mechanism based on local thermo-chemical conditions. This means that the transient evolution of the neglected species is not considered which can lead large errors. Furthermore, even if some of the non-key species are not chemically reacting themselves they could be important for some third body and pressure dependent reactions. Liang et.al [32] found that exclusion of these third body species can effect prediction of N_2, CO_2 and H_2O under low temperature conditions. Liang et.al proposed a dynamic method of reduction to reduced the size of the ODE's to be solved and also account for third body reactions under transient conditions. The method of reduction used was the DRGEP method which splits the vector of species into key and non-key species. ODE's which are to be solved after reduction are formulated only on the basis of the key species, however when the rate functions are computed all the species are considered avoiding the need to include third body species into the reduced mechanism. Liang et.al also studied the effects of the critical threshold on a n-heptane Homogeneous Charge Compression Ignition (HCCI) problem and found that for chemistry in the pre-ignition stage its effect was more pronounced. Though Liang et.al presented and evaluated the DAC method for reduction, there were still some unanswered questions regarding the efficient implementation of the DAC method i.e, the frequency at which the reduction needs to be performed. There were also questions relating to the effectiveness of the DAC method to predict turbulence chemistry interaction and predict pollutants. In [57] Yang et.al addressed these issues and came up with relations between reaction time-step and reduction time-step. Yang et.al also checked the accuracy of the DAC method with DRG reduction to predict turbulence chemistry interaction and pollutants. The reaction time-step (Δt) depends on the flow and has a typical range of $10^{-}6$ to $10^{-}4$ for turbulent flows. In previous HCCI simulations by Liang [32] the time window between successive DRG reductions (Δt_r) has been taken equal to (Δt). This means that a reduced mechanism is valid for one complete flow time-step and assumes that the chemistry of the flow does not changes in the interval. This is a valid assumption for smaller flow time scales ($10-5$) but for larger time scales ($10-3$) the chemistry of the flow might change during the interval, which would effect the performance of the reduced mechanism. Two viable approaches were proposed by Yang et.al, the first approach was to have a very low value for the threshold and have the same skeletal mechanism for the complete flow time-step. The second approach was to have multiple reductions in one flow time-step with a very high threshold. Performances of both these approaches for a Partially Stirred Reactor (PaSR) were evaluated by Yang in [57]. Yang et.al found for large reaction time steps its computationally expensive to preform multiple reductions within a flow time step rather than reducing the threshold. Yang et.al quantified the errors in the prediction of NO, CO and temperature by the DAC method with a relatively small threshold to be to be 6%, 0.3% and 0.04% respectively and this reduction provided a speed up factor of 6 which is quite significant. The speed up factor as given by Yang et.al is inversely proportional to the square of the reduction ratio, which is the fraction of the species retained after the reduction.

Based on Liang's and Yang's definition of the DAC methods various modification have been found in literature which enhanced performance of the DAC method. One ambiguity in Yang's implementation of the DAC method was the definition of the threshold. This cut off threshold greatly varied among different test cases and have a huge impact on the quality and efficiency of the reduction. A more intuitive way to describe the cutoff threshold was defined in the Error Controlled Dynamic Adaptive Chemistry (ECDAC) by Gou et.al [20]. Gou suggested to tabulate the threshold value with respect to a reaction progress variable and an controlling error. The reaction progress variable would be a parameter which would uniquely define the chemistry at a given condition. Gou et.al suggested that for laminar flows a single definition of the reaction progress variable would be sufficient, typically mass fraction of certain key species. However, for high Reynolds number turbulent flames turbulent mixing might change the local mixture fraction and the reaction progress variable then needs to have multiple definitions which have to be used simultaneously to define the chemistry. The controlling error on the other hand is simply the maximum error in the mass fractions of key species or temperature between the detailed and the reduced mechanism. This form of tabulation would mean that on the basis on initial conditions, the value of the reaction progress variable and an user specified controlling error (1%) a threshold value can be obtained form the pre-generated table. Another modification of the DAC method is the Correlated Dynamic Adaptive Chemistry (CODAC) [48] is a combination of chemistry agglomeration as discussed by Jangi [26] and the DAC method. The CODAC method uses similarities in chemistry to draw correlations among cells in the computational domain with respect to both time and space. If the cells are found to be correlated then the same reduced mechanism is used for all of them. This method avoids the need for performing reduction at every time-step for each of the cells. The total time taken for the integration of chemistry for a mechanism is given as

$$t_{int} \propto N_t N_g. \tag{2.18}$$

where N is the number of species in the mechanism, t is the number of time-steps and g is the number of grid points. Time taken to perform DAC on the fly is given as:

$$t_{DAC} \propto N_d I_d N_t N_g. \tag{2.19}$$

where N_d and I_d are the number of species and reactions in the detailed mechanism respectively. It can be seen that for large mechanisms $t_{DAC} \geq t_{int}$. Hence performing the reduction on every time step and at every cell would be quite expensive. The computational time by performing the reduction only on the non correlated cells is give as

$$t_{CO-DAC} \propto N_d I_d (\epsilon_t N_t)(\epsilon_g N_g). \tag{2.20}$$

where ϵ_t and ϵ_g are a values less than one.

Sun et.al also identify the following parameters to determine correlation, they are the mass fractions of the fuel, CH_2O, $HO2$ and OH and the temperature. Sun defined the temporal correlation based on these parameters as

$$\Delta = max\left(\frac{T_{n+1} - T_n}{\epsilon_t}, \frac{lnY_{Fuel_{n+1}} - lnY_{Fuel_n}}{\epsilon_{Fuel}}, \frac{lnY_{CH_2O_{n+1}} - lnY_{CH_2O_n}}{\epsilon_{CH_2O}}, \frac{lnY_{OH_{n+1}} - lnY_{OH_n}}{\epsilon_{OH}}, \frac{lnY_{HO_{2n+1}} - lnY_{HO_{2n}}}{\epsilon_{HO_2}}\right). \tag{2.21}$$

where □is an user defined vector of tolerances. If max(Δ) < 1 the states are said to correlated in time. A similar formulation is obtained for space as well. The CODAC method was found to be on average two-orders faster than the DAC implementation for the various test cases which were solved by Sun.

Menon et.al [56] extended the idea of correlated chemistry to correlated transport. In simulations transport properties are usually based either on one of the following models which include Mixtured Averaged Diffusion (MAD) or the Multi Species Transport (MST) or the lewis number transport. The MST method is the most expensive computationally as it involves an implicit solution a system of equations. On the other hand MAD and lewis number transport are simple and only depend on algebraic relations. Bruno et.al [8] compared different models of transport through a DNS simulation and concluded that MAD and MST predicted similar flow fields but the flow fields from lewis number transport were significantly different. Therefore the model should be preferred as it much cheaper computationally. Menon et.al mentions that even though the MAD model is faster computing it at every grid point and time step is still expensive. Hence the concept of correlated transport was introduced, Menon et.al point that diffusion coefficient also have space and time correlations which can be used identify cells with similar transport. Menon et.al formulate a similar correlation function as described by Sun et.al in [48] to determine correlation. Furthermore Menon suggest the use of the following parameters which are know to effect transport the most. These parameters include the mass fraction of the fuel, N_2, O_2, CO, CO_2, H_2 and $H2_O$ along with temperature. Menon et.al found that by using the correlated transport model calculation of the transported properties was 72 times faster as compared to the MAD model for all the species.

All these methods however depended on defining some key species based on which the dynamic reduction will be based. However, universal definitions of these key species can require some level of understanding by the user regarding the test case and the chemistry involved. A DAC method based on species time-scale and a Jacobian aided rate analysis proposed by Xie et.al [55] eliminates this issue and reduces species based on the reactiveness. Species are categorised as active, coupled or non-reacting through a timescale analysis and a Jacobian aided rate analysis. A species is said to be active if the criteria stated below is satisfied:

$$\left|\frac{\mathrm{d}Y_i}{\mathrm{d}t}\right| \geq min\left(\epsilon(|| S || + || M ||), \frac{Y_i + \theta}{\Delta t}\right). \tag{2.22}$$

where ϵ is an user specified threshold ,S and M are the magnitudes of the chemical production of transport fluxes of species respectively. θ is a very small number $\approx 10^{-12}$ is used in the term which includes intermediate species even if its production rate is low. The formulation above neglects slow reacting species as it categories them as non-reacting, however as Xie et.al points out that these slow reacting species have notable effects on flame. To check for this a Jacobian analysis of the species is performed based on the following formulation:

$$V_{i,j} = Y_j\frac{\mathrm{d}S_i}{\mathrm{d}Y_j} = \frac{\partial S_i}{\partial lnY_j}. \tag{2.23}$$

where i, j are the indices of the active and the non-reacting species respectively. This equation determines the effect of the non-reacting species on the complete system. A non-reacting species is added to the pool of the active species if $V_{i,j} \geq \epsilon(|| S || + || M ||)$. A reduced mechanism based on the active species is made and to validate the mechanism the following criteria is tested for all the species. Species which do not satisfy this condition are added to the list of active species to obtain a final validate reduced mechanism.

$$\left|S_i - S_{red,i}\right| \geq \epsilon(|| S || + || M ||). \tag{2.24}$$

where $S_{red,i}$ is the chemical production/consumption of species i in the reduced mechanism.

2.3.1. DAC with ISAT

Though the DAC method and other reduction methods such as the ISAT [42] reduce the computational cost of simulating reacting flows efforts were being made to accelerate this further. Contino et.al[12] came up with a method that combines DAC implementation with ISAT tabulation. The ISAT algorithm proposed by [42] was meant to be used for isobaric high temperature cases. It was shown by Pope et.al that the ISAT method accelerated (speed up factor 10^3) the simulation considerably, however for other operating conditions the storing and lookup from the binary table reduced the efficiency of the tabulation(speed up factor $\tilde{}$ 10). Contino implemented the ISAT algorithm such that an entry in the binary table can be removed according to two key parameters: number of growths (N_{mg}) and number of time steps(N_{ms}). To represent phenomenon like autoignition a very small threshold for ISAT is needed this makes the storing and retrieval expensive, however in Contino's implementation a point in the binary table is deemed to be redundant after N_{ms} time steps. This reduces the number of points present in the table. In a typical ISAT tabulation query points move towards high temperature and pressure conditions this leads to errors in lookup as the query points are still within the threshold of ISAT but are quite far in phase space from the initial condition to which the query points were mapped to. To overcome this the initial condition is redefined after a time interval of N_{mg} to account for the changes in the phase during the combustion process. Coupling between DAC and ISAT is viewed as interaction among successive layers. A query point Ψ_q received by ISAT is provided to the DAC algorithm which gives out a reduced mechanism Ψ_q^r based on some key pre-defined key species. The reduced mechanism is then integrated by an ODE solver to get the chemical rates R_q^r and this is stored by ISAT in the binary table mapped to the reaction rate of the complete mechanism R_q. This would mean the ISAT would need map query points to different reaction rates with varying number of active species. A set of new variables are introduced which store the data related to the inactive species, this is done by having identity matrices for the inactive species in the relation matrix used in the DAC reduction. It was found that this implementation of DAC had a speed up factor of 300 universally irrespective of the type of reacting flow begin solved.

A recent publication on the topic of dynamic tabulation of reduced schemes by An et.al [5] was presented in the August - 2019 edition of Combustion and Flame. The method follows a similar ideology to the one proposed in this study however, the implementation and extent of testing the model differ significantly. An et.al [5] proposed to tabulate schemes on error functions which were essentially changes in mass fractions of the oxidiser, fuel, O_2, OH, CH_2O and HO_2 and temperature of the mixture. Thresholds are set for each of the predefined error functions and tabulation is done if any of the error functions would be over the threshold. Thresholds were set at 5% and 15% in mass fractions and $10K$ and $100K$ in temperature to investigate the effect of the threshold. The methods was tested on two turbulent case, a 3D Sandia D flame and a 2D supersonic DLR jet to [5], it was reported that both the thresholds were able to predict flames accurately including the flame structure and the lift off length. The issue with this tabulation strategy would be that a table of size $n^{100/\epsilon}$ would be needed where n is the number of error functions and ϵ is the threshold in %. The size of the table could lead to issues with cpu memory, furthermore the requirement for a table that big is not necessary as reduced mechanism obtained by PFA for all possible thermodynamic states could be represented in a smaller table. [5] tested their model on complex turbulence flows solved with a 3D Unsteady RANS and a 2D LES solver, this could mean the errors in the reduction methods could be influenced by the turbulence models. This leaves a gap to determine the effect of reductions in the absence of turbulent models on flames which represent fundamental physics involved in various regimes of combustion. This gap would be the main focus of the current study.

Other methods of reducing computational costs are which are not based on chemical reductions are mentioned below, the play into the actual numerical solution of the reacting flows.

2.4. Jacobian calculation and stiffness removal

A Jacobian matrix needs to be computed for a solving an system of algebraic equations for an steady case and for integration of chemical source terms in unsteady problems. Lu et.al [37] mention two different strategies to optimise the computation of the Jacobian and remove some of the stiffness in the system of equations.

2.4.1. Analytic Jacobian with implicit solvers

Algebraic equations which arise with each implicit integration are non-linear in nature. Hence a Jacobian matrix is to be computed at every grid point to solve the set of non-linear Algebraic equations using the Newton-Raphson method. There are semi-implicit methods which treat only integration of chemistry to be implicitly, all the other terms are explicitly solved. These semi-implicit schemes use the Strang splitting algorithm (discussed below in detail Sec4.3) to separate the chemistry from transport and other terms. Jacobian's could be computed either numerically or analytically as mentioned earlier the numerical solution of is more expensive than the analytical solution. The following equation give the Jacobian of species i:

$$J = \frac{\mathrm{d}g}{\mathrm{d}y} = \Omega \cdot \Gamma, \Omega = \sum_{j=1}^{I} \left(\nu_j \frac{\mathrm{d}\omega_j}{\mathrm{d}c} \right), \Gamma = \frac{\mathrm{d}c}{\mathrm{d}y}. \tag{2.25}$$

where g is the chemical production rate, c is the concentration, y is the mole fraction, ν_j is the stoichiometric coefficient of species i in reaction j. The cost of the derivative with respect to temperature is negligible and is not mention here. The definition of matrix Ω is such that it is i^{th} value in the matrix is determined by the number of species participating in reaction i. Since this number is quite small and not all species take part in every reaction most (one species on an average takes part in five reactions) of its elements are zero and hence can be treated as a sparse matrix. It was also pointed out by Lu et.al that if Γ is evaluated in species mole concentration space it becomes an identity matrix and is much cheaper to factorise. For simulations in the mass fractions space Γ is not sparse and it is quite expensive to factorise it. In such cases explicit methods with stiffness reduction should be used.

2.4.2. Explicit Solvers

Explicit solvers usually need to take smaller time-steps due to stiffness in the system of equations that it solves. Numerical round-off error restricts the maximum number of time-steps that can be taken, which limits the accurate prediction of certain species with very high time-scales. A way to avoid this would be to reduced stiffness in the system by identifying fast species and eliminating them from transport equations.

2.5. Cost minimisation in computations

The following set of optimisations are based on the just the implementation of the methods discussed before. These methods have no physical significance as they are aimed at reducing cost with no or minimal loss in accuracy. These methods optimise computational strategies for example exponential and logarithmic functions are converted to multiplication/division as these operations are much cheaper. Lu et.al presents the following examples which aim to minimise computational overheads.

Rate Evaluation

Chemical rates are evaluated using the Arrhenius rate expression shown below:

$$K_f = AT^{\alpha} exp\left(-\frac{E}{RT}\right). \tag{2.26}$$

where A is the collision factor, E is the activation energy, T is the temperature, α is the temperature exponent (can be integer or a float value),R^o is the universal gas constant. This function needs to be evaluated for all species for every time step which can be expensive due evaluation of an exponent. For most reactions the activation energy is 0 and the value of α is usually equal to either 1 or 0. This function can then be modified as follows based on the values of E and α:

$$K_f = \begin{cases} A, & \text{if } \alpha = 0 \text{ E = 0} \\ exp(log(A) + \alpha logT), & \text{if } \alpha \neq 0 \text{ E = 0} \\ exp(logA + \alpha logT - E/RT), & \text{if } \alpha \neq 0 \text{ E} \neq 0 \\ exp(logA - E/RT), & \text{if } \alpha = 0 \text{ E} \neq 0 \\ A\overbrace{T...T}^{\alpha} & \text{if E = 0 and } \alpha \text{ is an integer} \end{cases} \tag{2.27}$$

This formulation reduces the number of times the logarithmic function is called. Values of $logA$ and E/RT can be stored as these are fixed values. A similar treatment can be done to obtain reaction rates of a backward reaction.

Caching
As mentioned earlier the most expensive part in evaluating species production rate is the computing the Arrhenius equation. Since the Arrhenius equation only depends on temperature a buffer of solutions for a given temperature can be maintained. These solutions can then be retrieved if solution for a similar temperature exists avoiding re-computation. Similar idea can be applied to cache pressure-dependent coefficients.

These are just few examples given by Lu et.al [36] to minimise computational overheads, however these techniques can be extended further. This type of optimisation has not been studied extensively in literature hence its impact needs to verified.

2.6. Research objective

The thesis focuses on the implementation of finite rate solver with detailed chemistry. The solver is then extended to include robust dynamic adaptive chemistry reduction techniques. This would facilitate design and evaluation of novel combustion systems at realisable computational costs.

Reduction methods based on truncating chemical pathways are robust and can be applied to all regimes of combustion with certain modifications to the algorithm. Tabulation strategies are very efficient at prediction of flames in a given regime, however when applied outside this specific regime they produce large errors. There is scope for a method which would combine the efficiency of the tabulation methods with the robustness of the truncation methods. The current study aims to fill this literature gap. The project proposes a new tabulated method of chemistry reduction and evaluates its performance and accuracy in various canonical combustion problems. The aim of the project can be laid out as:

To develop, implement and validate a high-fidelity reacting flow solver based on finite rate kinetics using dynamic adaptive chemistry

To achieve the aim the following are the research questions are to be addressed.

1. Identification of a reduction model which requires minimum user input.
   (a) What method of chemistry reduction should be chosen DRGEP or PFA?
   (b) Define procedures to make the reduction model globally applicable and work with minimal user input.
2. Can the computational cost and the impact of the ad-hoc tuning for the CODAC method be reduced?
   (a) Propose a new tabulation strategy for reduction.
   (b) What are the controlling variables and the distribution of the table?
   (c) How does the proposed model of tabulation compare to state-of-the-art reduction models?
   (d) What is the reduction in computational cost of using the TDAC method?

3
Theory

The following section presents theory behind reacting flow simulations, this includes description of chemical kinetics, conservation equations and modelling choices. Solution of reacting flow simulations involves solving of the highly coupled Navier-Stokes equations and the chemistry using the finite rate methodology. The theory is split into two sections which describe governing equations related to chemical kinetics and Navier-Stokes equations respectively.

3.1. Chemical Kinetics

Chemical kinetics are specified by reaction mechanisms, consider a reaction mechanism contains N species reacting through M reactions. The reactions of species can be represented as:

$$\sum_{k=1}^{N} \nu'_{kj}\chi_k \rightleftharpoons \sum_{k=1}^{N} \nu''_{kj}\chi_k, \qquad \text{for j = 1,}M. \tag{3.1}$$

Here χ_k is the chemical symbol for species k, ν'_{kj} and ν''_{kj} are the stichiometeric coefficient of species k in reaction j. For mass conservation to be satisfied:

$$\sum_{k=1}^{N} \nu''_{kj}W_k = \sum_{k=1}^{N} \nu'_{kj}W_k, \qquad \text{for j = 1,}M. \tag{3.2}$$

Where W_k is the molecular weight of species k. Net production/consumption ω_k of species k is given by the sum of rates $\omega_{k,j}$ for all reactions.

$$\dot{\omega}_k = W_k \sum_{j=1}^{M} \nu_{kj}Q_j \;\; = \sum_{j=1}^{M} \dot{\omega}_{k,j}, \qquad \text{with } \frac{\dot{\omega}_{k,j}}{W_k\nu_{kj}} = Q_j. \tag{3.3}$$

The rate of progress Q of reaction j is given as

$$Q_j = K_{fj}\prod_{K=1}^{N}[X_k]^{\nu'_{kj}} - K_{rj}\prod_{K=1}^{N}[X_k]^{\nu''_{kj}}. \tag{3.4}$$

K_{fj} and K_{rj} are the forward and the reverse rates of reaction j and $[X_k] = \rho Y_k/W_K$ is the molar concentration of species k. Rate constants K_{fj} and K_{rj} are expressed by the Arrhenius law as:

$$K_{fj} = A_{fj}T^{\beta_j}\exp\left(-\frac{E_{aj}}{RT}\right). \tag{3.5}$$

Here A_{fj} is the pre-exponential constant, β_j is the temperature exponent, E_{aj} is the activation energy and R is the universal gas constant. All molecular collisions do not result in reactions, a threshold for the level of kinetic energy is necessary. The exponent term in Equation 3.5 accounts for this factor and determines the fraction of all collisions that satisfy the minimum kinetic energy requirement. Constants A and E_a are determined through statistical measurements from experimental data. The description of these constants is provided in the chemical mechanism and influence the chemistry of the problem. Hence it is important to understand the validity and applicability of a chemical mechanism before it is used.

The reverse rate of reaction K_{rj} is computed from the forward rate of reaction K_{fj} as:

$$K_{rj} = \frac{K_{fj}}{\left(\frac{p_a}{RT}\right)^{\sum_{k=1}^{N} \nu_{kj}} \exp\left(\frac{\Delta S_j^0}{R} - \frac{\Delta H_j^0}{RT}\right)}. \tag{3.6}$$

Here p_a is the atmospheric pressure, ΔS_j^0 and ΔH_j^0 are the changes in entropy and enthalpy when the change from reactants to products is made respectively, in reaction j.

Reaction mechanisms formulated based on experimental data and aim to predict Q_j for specific thermodynamic states. Some of the reactions are well known and their respective rate of progress are universally accepted, however for other reactions one can obtain different rates of progress for the same reaction using different mechanisms. This means that reaction mechanisms must be chosen carefully to predict the chemistry accurately, for example lack of low temperature reactions for a N-heptane mechanism would fail to predict the negative temperature coefficient NTC region (further explained in section 5.1.1). Very small timescale and the stiffness associated with the computation Q_j is one of main challenges in numerical combustion. To accurately resolve Q_j meshes which are orders of magnitudes finer than the non-reacting flow cases are needed. Furthermore, E_j which is the activation energy of the reactions and determines when the reaction would become spontaneous, is exponential. Small deviations in its value could lead to massive changes in the activation energy. Thus requiring more number of computation points in the domain to accurately resolve such auto-ignition conditions. The combined effect of the stiffness, small length scales, the exponential dependence of the chemistry and the large number of species to be tracked are the responsible for the major expenses in a reacting flow simulation. In the following study Cantera [19] is used to solve the chemistry, more information on the structure and coupling of Cantera is given in section 4.

3.2. Conservation Equations

The following are the conservation equations solved in the context of finite rate kinetics solver. This study is focused on direct numerical simulations of fundamental combustion problems hence no simplification or modelling is applied to the following equations. This is done so that the pure impact of the different reduction strategies can be tested on without any influence from the computational modelling.

Mass

$$\frac{\partial \rho}{\partial t} + \frac{\partial \rho u_i}{\partial x_i} = 0. \tag{3.7}$$

Momemtum

$$\underbrace{\frac{\partial \rho u_j}{\partial t}}_{Temporal} + \underbrace{\frac{\partial \rho u_i u_j}{\partial x_i}}_{Convective} = -\underbrace{\frac{\partial p}{\partial x_j}}_{Pressure} + \underbrace{\frac{\partial \tau_{ij}}{\partial x_i}}_{Viscous} \tag{3.8}$$

The mass Equation 3.7 and the momentum equation Equation 3.8 are coupled through velocity and the pressure term only appears as a source term in the momentum equation. For compressible flows density is computed in the mass conservation equation which can be used to compute the pressure (P), in incompressible flows however, the density variations are not coupled with the pressure. This leads to system where the evolution of pressure is not known and the unknowns (ρ, P, V(x,y,z)) exceed the number of equations.

The fraction step method is used to solve the velocity-pressure coupling. First the velocity is approximated using only the temporal, convective and viscous terms in Equation 3.8 yielding u^*. Then the pressure is solved using Equation 3.9 which takes into account continuity. Finally the full time-step is computed using the known pressure.

Pressure

$$\frac{\partial}{\partial x_i}\left(\frac{\partial p}{\partial x_i}\right) = \frac{1}{dt}\frac{\partial u_i^*}{\partial x_i}. \tag{3.9}$$

Species

$$\frac{\partial \rho Y_k}{\partial t} + \frac{\partial(\rho u_i Y_k)}{\partial x_i} = -\frac{\partial \rho V_{k,i} Y_k}{\partial x_i} + \dot{\omega}_k. \tag{3.10}$$

Enthalpy

$$\frac{\partial \rho h}{\partial t} + \frac{\partial(\rho u_i h)}{\partial x_i} = \frac{\mathrm{d}p}{\mathrm{d}t} - \frac{\partial q_i}{\partial x_i}. \tag{3.11}$$

Molecular diffusion of the species is given by the extension of Fick's diffusion law to multiple species. The diffusivity D is a property of the species which changes with the thermodynamic state. The flux of the species is defined as

$$V_{k,i} Y_k = -D_k \frac{\partial Y_k}{x_i}.$$

Further simplification of the the diffusion D can be done by assuming unity Lewis numbers for all species which makes the diffusion coefficient of species k $D_k = \lambda/\rho C_p$. Enthalpy flux q_i in Equation 3.11 is given by

$$q_i = -\lambda \frac{\partial T}{\partial x_i} + \rho \sum_{k=1}^{N} h_k^0 Y_K V_{k,i}. \tag{3.12}$$

where the first part of Equation 3.12 is the Fourier law and the second part represents the diffusion of chemical enthalpy as a consequence of diffusion in species. The conservation equations are closed by the ideal gas equation.

$$\rho = \frac{PW}{RT}. \tag{3.13}$$

Here ρ is the density, P is the pressure, W is the molecular weight, R is the universal gas constant and T is the temperature. Temperature is calculated by inverting Equation 3.14 using a Newton-Raphson solver to obtain the temperature from the total enthalpy.

$$h = \sum_{n=1}^{5} \frac{a_n}{n} T^n + a_6. \tag{3.14}$$

Note: No additional steps like applying an averaging filter to obtain equations in the context of Reynold's Averaged Navier-Stokes (RANS) or Large Eddy Simulation (LES) are shown as all test cases presented in this study correspond to Direct Numerical Simulation (DNS) simulations.

3.2.1. Low-Mach Solver

Coupled Navier-Stokes equations mentioned in the previous section are solved with a low-Mach formulation, this makes it possible to solve variable density reacting flow simulations without the need for a relatively expensive fully compressible solver. Low-Mach flows are characterised by moderate Reynolds number, low Mach number and large density gradients, and thus fits in the description of reacting flow simulations. Since the Mach number of the flow is low there is an acoustic equilibrium, hence acoustic waves can be neglected by decomposing the pressure into a homogeneous thermodynamic pressure and a hydrodynamic pressure and decoupling density changes with the hydrodynamic pressure. This is done by computing the density solely based on the homogeneous thermodynamic pressure using the ideal gas law. The Poisson equation 3.9 is modified by accounting for changes in density by adding a time derivate of density as a source term in the Poisson equation. Equation 3.9 changes to Equation 3.15

$$\frac{\partial}{\partial x_i}\left(\frac{\partial p}{\partial x_i}\right) = \frac{1}{dt}\left(\frac{\partial u_i^*}{\partial x_i} + \frac{\partial \rho}{\partial t}\right). \tag{3.15}$$

where $\frac{\partial \rho}{\partial t}$ is approximated as:

$$\frac{\partial \rho}{\partial t} = \frac{\rho^n - \rho^{n-1}}{\partial t}. \tag{3.16}$$

Spatial Discretisation
The governing equations are solved with finite element discretisation with a fractional step method to include the low-Mach solver. The non-linear convective term in discretised with the EMAC [9] formulation, which conserves linear and angular momentum and kinetic energy.

Temporal Marching
Equations are solved explicitly using a third order Runge-Kutta scheme where one time-step is evaluated in 3 sub-steps. A non-incremental fractional step method is used which solves the pressure to maintain the pressure-velocity decoupling. The fractional step solves the momentum and the Poisson equation at every sub-step of the Runge-Kutta. The solution of the Poisson equation is quite expensive, to reduce the computational cost a approximation for the pressure based on the previous time-steps is used. The Poisson equation is only solved at the end of the last sub-step of the Runge-Kutta. More information on the coefficients for the Runge-Kutta scheme, implementation of the fractional step method, the low Mach solver and the approximation for the pressure equation can be found in [7]. The order in which the equations are solved is shown in algorithm 1.

$t = t_0$;
while $t \leq t_f$ **do**
  Compute δt (from CFL number using an eigen value based time step estimator [50]);
  $t = t + \delta t$;
  Initialise Scalars;
  $\ell = 2$;
  ${Y_k}^1 = {Y_k}^{n-1}$;
  while $\ell \leq s$ **do**
    Evaluate Y_k using (3.10) ;
    $\ell = \ell + 1$;
  end
  Combine RHS of sub-steps to get the time-step;
  Initialise Enthalpy;
  $\ell = 2$;
  $h^1 = h^{n-1}$;
  while $\ell \leq s$ **do**
    Evaluate h using (3.11) ;
    $\ell = \ell + 1$;
  end
  Combine RHS of sub-steps to get the time-step;
  $\ell = 2$;
  $u^1 = u^{n-1}$;
  while $\ell \leq s$ **do**
    Solve for Velocity u^* ;
    Evaluate Pressure solving (3.15) or approximate Pressure (extrapolation);
    Solve for Velocity using (3.8) ;
  end
  Combine RHS of sub-steps to get the time-step;
  Evaluate Pressure solving (3.15) ;
  Solve for Velocity using (3.8) ;
  Evaluate material properties;
end

Algorithm 1: Low Mach algorithm

Here t and t_f are the current and the final time, s is the number of sub-steps, l is an index for sub-step in the explicit Runge-Kutta scheme, Y_K, h and u are the unknowns of the problem, namely mass fraction of the species, total enthalpy and velocity .

4

Implementation

The following section details information on Alya and Cantera, the codes on which the current study was performed. The structure of the codes are presented, before moving on to the motivation and the actual implementation of the coupling strategy between them.

4.1. Alya

Alya is a parallel multi-physics software package developed at the Barcelona Supercomputing Centre. Alya is based on the finite element discretisation method to run Computational Fluid Dynamics (CFD) among a multitude of other applications. Alya is highly optimised and is independently tested and benchmarked on most European supercomputing platforms. Alya is a highly parallelized code and is designed to run on leading edge HPC systems, parallel performance of Alya on multi-physics applications can be found in [53]. Alya's parallelisation utilises both the MPI and OpenMP implementations and takes the advantage of distributed and the shared memory paradigms. Acceleration through GPUs is also exploited at the basic iterative solver level to further enhance the performance of the code. Load balancing techniques are implemented to better utilise the computational resources at the node level. Alya is one among the twelve simulation codes of the Unified European Applications Benchmark Suite and thus complies with the highest standards in HPC.

The structure of Alya is based on a modular approach wherein new models that are developed are integrated in the main code as modules. The current project which aims to develop and implement a finite rate kinetics solver will be tested on stand alone problems before integrating into Alya. This kind of modularity makes its easy to debug problems as validation is done at every stage of development. A typical finite rate solver would require the following sub-modules:

1. Chemical mechanism, thermodynamic and transport database reader.
2. Computation of reaction rates using the Arrhenius rate law.
3. A stiff ODE integrator to obtain the integrated chemical sources in a given interval.
4. Advection, diffusion and source transport equation solver.

Step 1,2,3 are tedious and require careful implementation as slight errors in code development would lead to unphysical solutions. These steps are then performed using the open source chemical kinetics solver Cantera.

The computational domain is represented as a series of independent homogeneous constant pressure ideal gas reactors, the thermodynamic state of these reactors is set every time-step. A time interval dt is specified and new mass fractions of the species are obtained after the chemical source integration. Cantera also provides the temperature of the mixture after integration, however this would mean that the total enthalpy would always remain constant as constant pressure reactors are used. To account for isothermal walls or a heat fluxes through the walls the enthalpy is obtained from the transported total enthalpy equation. This enthalpy along with the NASA polynomials and the specific heat of the mixture is used to compute the temperature using a Newton iterator. The initial guess for the Newton iterator is taken as the temperature obtained from the previous time-step.

4.2. Cantera

"Cantera is an open-source suite of tools for problems involving chemical kinetics, thermodynamics, and transport processes."

Cantera [19] is an open source chemical kinetics solver, which is used by numerous reacting flow solvers to compute chemistry. Cantera has python/cython, C++ and fortran interfaces. Cantera takes advantage of object oriented programming concepts for robust yet flexible phase models. This makes it easy for algorithms to be general so that developers can work on new models without affecting the main code.

Structure of Cantera is shown in Figure 4.1, the structure of Cantera is divided into two levels. The upper level is considered as a bookkeeping level which includes libraries for reading of chemical mechanisms, thermal and transport databases, and logistics of the program dealing with parsing or writing files. This layer of functionality is available in python, Fortran 77/90, Matlab and C++ api's. The second layer includes the numerics needed for source term integration and other related operations. The C++ interfaces use a Sundials library written in C to handle the numerics. The python and Matlab interfaces also use the Sundials library but other numerics packages like Scipy and inbuilt Matlab libraries could also be used. The numerics layer for C++, python and Matlab interfaces work right out-of-the-box, as the Sundials libraries are complied together with the complication of Cantera. The Fortran module however, has limited number of intrinsic functions and external numeric libraries should be complied and linked to Cantera. This makes the Fortran interface limited in its usage.

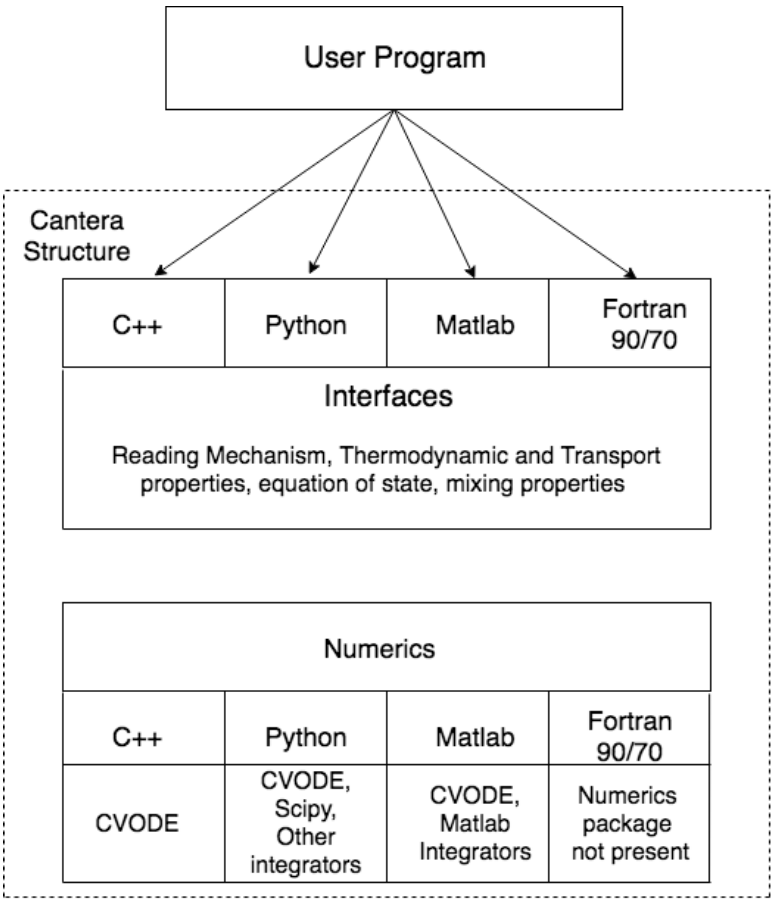

Figure 4.1: Cantera's structure

4.2.1. Coupling with Alya

The multi-physics code Alya is written in Fortran 90 and is to be compiled together with Cantera to compute chemistry. The bookkeeping functions layer of Cantera (available in the Fortran interface) is used as an intrinsic function in Alya. For the numerics layer there could be two major strategies, firstly, an external fortran numerics library can be used or, secondly a C++ wrapper could be used to port Cantera's C++ functions to Fortran 90. The second approach is used in this project as it reduces dependency on external libraries and gives more control to the user. Furthermore, no additional validation is needed as the Sundials package is validated extensively.

The C++ wrapper contains Cantera functionalities as external functions, the wrapper is then complied with the same complier as Alya. The object that is obtained after the compilation of the wrapper is linked with the executables of Alya. This makes it possible to port C++ functionalities to Fortran programs. For the wrapper to work as expected it is of critical importance that all the involved entities (Alya, Cantera and the wrapper) must be complied with the same complier using the same compilation flags. Any inconsistency in this may not result a fatal error but the functionality of the wrapper would be effected. The following Figure 4.2 shows the compilation strategy used for the wrapper.

Note: Cantera has its own format of chemical mechanism (*.cti), it can however read (*.xml) files as well. When using mechanisms of format *.cti in either the C++ or the Fortran 90 interface of Cantera python flags must be used. To avoid this mechanisms can be converted into *.xml format with the included xml writer in the standard distribution of Cantera.

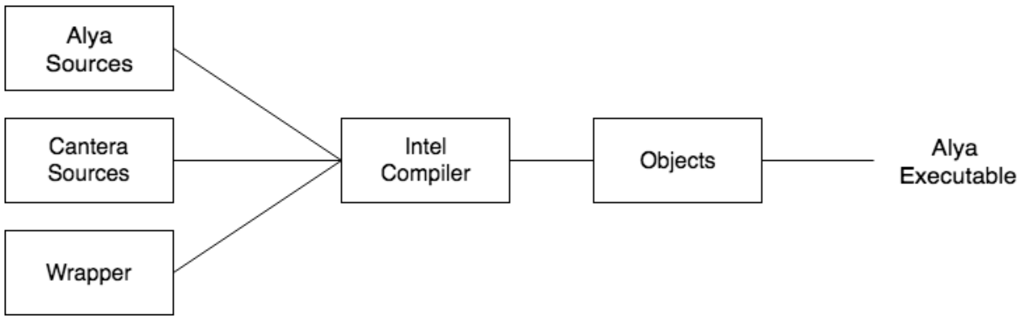

Figure 4.2: C++ Wrapper strategy

As mentioned earlier Cantera is an object based program and thus represents all its functions as objects. An object is initialised when a mechanism is read, subsequently the thermodynamic state is set by specifying temperature, pressure and mass fractions of the species. This object is then used to create a ideal constant pressure reactor object, which integrates the chemical source term for a given time interval. The creation of these objects is computationally expensive especially for large number of reactors. To overcome this empty pointer objects are created and operated on to avoiding the need for creating new objects for every operation. Additionally to take advantage of the massively parallel capabilities of Alya the entire process is vectorised, this includes the definition of a vector of empty objects which are operated on simultaneously. The size of the vector is controlled to prevent issues concerning lack of memory due to the pure implicit solver used by Cantera, the solution strategy discussed in section 4.2.2. Currently there are attempts being made to port the wrapper and the chemical source integration to GPU's which would accelerate the process exponentially.

4.2.2. Perfectly Stirred Reactor (PSR)

A PSR represents a simplified 0D reaction system where the thermodynamic state and all state variables are homogeneously distributed. Even though, the reactor is in a transient state as changes in the state are possible due to chemical reactions, the reactor is assumed to be in thermodynamic equilibrium at any given time instance. There are many ways in which a reactor can interact with its surroundings like mass, heat transfer, compression/expansion and effects of walls on the reactor. For the current implementation of simulating chemistry in a reacting flow an ideal gas constant pressure reactor is used, this means that the pressure inside the reactor is kept constant by varying the volume of the reactor which is computed from the ideal gas equation. This is done to make sure that the total enthalpy of the reactor stays constant. It is to be noted that the effect of thermal expansion due to the chemical reactions is computed as the time derivative of density $\mathrm{d}\rho/\mathrm{d}t$, this term is added as a source

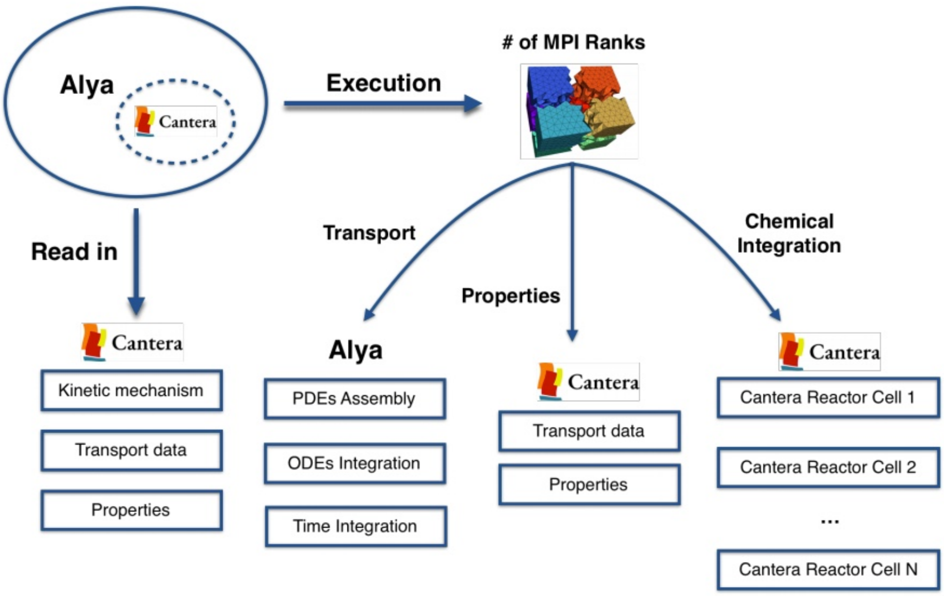

Figure 4.3: Alya-Cantera coupling

to the poisson pressure equation. The following are the governing equations for the PSR.

Mass conservation:

$$\frac{\mathrm{d}m}{\mathrm{d}t} = \sum_{\mathrm{in}} \dot{m}_{in} - \sum_{\mathrm{out}} \dot{m}_{out}. \tag{4.1}$$

Species conservation:

$$m\frac{\mathrm{d}Y_k}{\mathrm{d}t} = \sum_{\mathrm{in}} \dot{m}_{in}(Y_{k,in} - Y_k) + \dot{m}_{k,gen}. \tag{4.2}$$

Where $\dot{m}_{k,gen} = \rho\dot{\omega}_k$. As mentioned earlier Cantera uses a multi/single step BDF method with Newton iterations, the procedure is briefly explained here:

CVODE is a numerical solver written in C for initial value problem in ordinary differential equation (ODE) systems. The example below is specific to the chemical kinetics problem solved by Cantera. Chemical source of species k at a given time t_0 is given by:

$$\frac{\mathrm{d}Y_k}{\mathrm{d}t} = \dot{\omega}_k = f(T, P, Y_k) \quad \text{With } \; y_k(t_0) = y_{k0}. \tag{4.3}$$

A general form of a multi/single step BDF method is:

$$\sum_{i=0}^{K_1} \alpha_{n,i} Y_{k,n-i} + h_n \sum_{i=0}^{K_2} \beta_{n,i}\omega_{k,n-i} = 0. \tag{4.4}$$

Here K_1 varies between 1 and 5 depending on the state of the equation and the desired accuracy and $K_2 = 0$. The non-linear system in now represented as:

$$G(Y_{k,n}) \equiv Y_{k,n} - h_n\beta_{n,0} f(t_n, Y_{k,n}) - a_n, \quad \text{where} \quad a_n \equiv \sum_{i>0}(\alpha_{n,i}Y_{k,n-i} + h_n\beta n, i\omega_{k,n-i}). \tag{4.5}$$

Equation 4.5 is solved using a Newton iteration:

$$M(Y_{k,n+1} - Y_{k,n}) = -G(Y_{k,n}). \tag{4.6}$$

where

$$M \approx I - \gamma J, \quad J = \mathrm{d}\omega_k / \mathrm{d}Y_k \quad \text{and} \quad \gamma = h_n \beta_{n,0}. \tag{4.7}$$

The Jacobian J is computed by a direct dense method. This step is quite memory intensive as a matrix of $(N \mathrm{X} N)$ with real numbers is to computed and stored for every PSR reactor. The Jacobian once computed is hence used for multiple time-steps, until the convergence is bad. The user can also specify the methods to compute the Jacobian which are the numerical different-quotient method or the analytical Jacobian.

The temporal marching in Alya is explicit and hence to have a stable solution the Courant Friedrichs Lewy (CFL) criteria must be respected. This would mean to have a stable solution the size of the time-steps must be smaller than the smallest times-scales found in the problem. Chemical timescale can be defined as ω_k/ρ, where ω_k is the chemical source of species k and ρ is the density. The critical time-steps for the chemistry are usually orders lower that the flow time-scale and hence determines the critical time-step. This forces the solver to take very small time-steps which makes the solution expensive as more number of time-steps are to be computed. To avoid this issue a splitting methodology is applied where in the chemical source term is split from the transport and both these terms are solved separately. The time-step size for the transport of the chemical species is then determined by the CFL number based only on the flow. Chemical sources are then integrated over this time-step and the equations are updated for the next time-step. For this solution strategy to be applicable a robust solver which integrates chemical sources between arbitrary time-step sizes is needed. Cantera uses a pure-implicit solver and the the robustness of this solver is demonstrated by computing an homogeneous reactor case for a stichiometeric mixture methane/air at 1500K and atmospheric pressure using the GRI 3.0 [22] mechanism. A reference curve is generated by using an explicit solver (4th order Runge-Kutta) with very small time-steps (of the order of the chemical timescales). The same curve is then computed in 500, 100 and 10 intervals using the stiff implicit solver from Cantera shown in Figure 4.4.

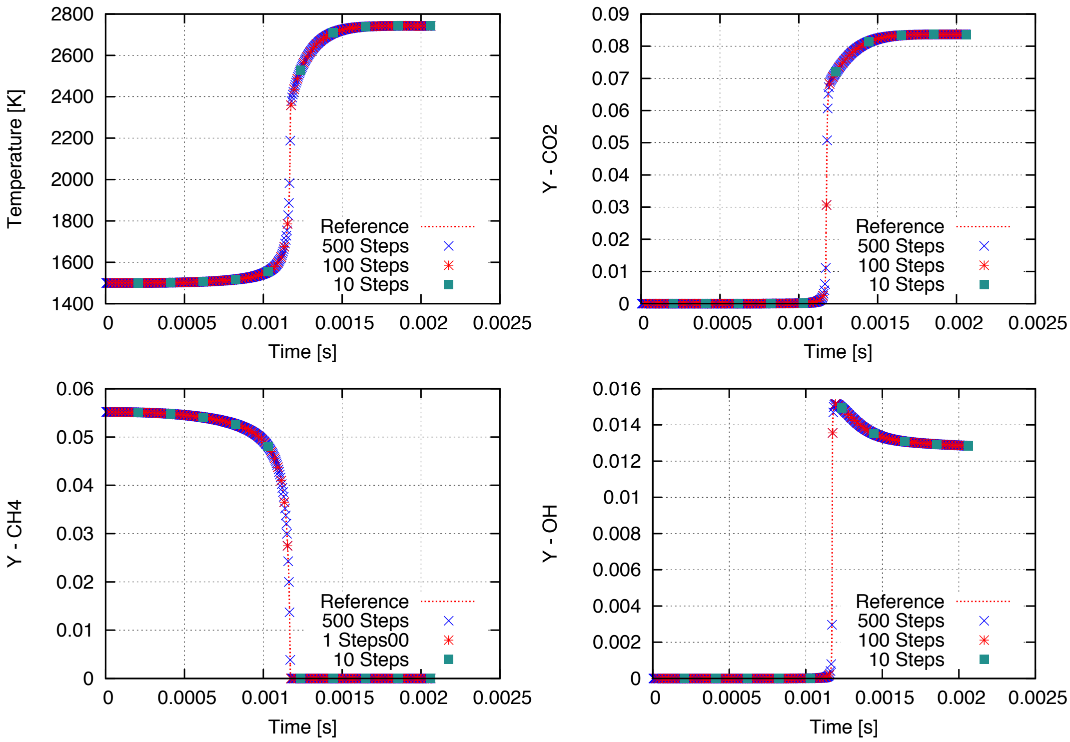

Figure 4.4: CVODE - time-step size test

It can be observed in Figure 4.4 that CVODE's solution is not affected by the size of the time-step taken, this gives motivation to use to splitting algorithm to improve computational efficiency. This improvement comes in form of ignoring chemical timescales and essentially removing the stiffness in the problem. The stiffness is passed on to the computation of the integrated chemical sources which are computed using a robust stiff solver.

4.3. Strang splitting algorithm

The scalar transport equation that is solved for every species contains an advection, a diffusion and a source term 3.10. The issue of solving this equation comes in the computation of the chemical source terms. These source terms are highly non-linear and often are computed from solving a stiff set of equations 4.2.2.

$$\frac{\mathrm{d}r}{\mathrm{d}t} = R(r,t), T(r,t). \tag{4.8}$$

where r is the primary variables such as mass fractions of the species. R and T represent the reaction terms and the transport terms respectively and t is the time.

The Strang splitting method splits the portions of an equation which are then solved separately. For reacting flows part of the equation which describes the transport (advection-diffusion) is separated from the chemistry (source) part. As shown by Ren et.al in [44] this splitting scheme leads to the accuracy of this method for solving the transport is second order in time. Ren et.al [44] developed different schemes of splitting based on the Strang method. The most simple method involves

Sub-step 1 : Integrating the reaction term between 0 and $\Delta T/2$.

$$\frac{\mathrm{d}r_{(0\rightarrow t/2)}}{\mathrm{d}t} = R(r,t). \tag{4.9}$$

Solution of the reactions obtained after this step is defined as R_b

Sub-step 2 : Integrating the transport terms over the total time step ΔT

$$\frac{\mathrm{d}r_{(0\rightarrow t)}}{\mathrm{d}t} = T(r_b,t). \tag{4.10}$$

Solution of the transport term obtained after this step is defined as $u(t_b)$

Sub-step 3 : Integrating the reaction term between $\Delta T/2$ and ΔT

$$\frac{\mathrm{d}r_{(t/2\rightarrow t)}}{\mathrm{d}t} = R(r_b,t). \tag{4.11}$$

Ren et.al [44] mentions that for $\Delta t \rightarrow 0$ the error is of the order of Δt^2. It was also mentioned by Ren that for stiff chemical systems with Δt being much larger than the small scales the Strang splitting fails. [44] proposes a predictor-corrector methods to obtain a more accurate solution for the transport integration. This method adds an additional corrector step in the calculation of the transport sub-step. Sub-step 2 mentioned before is modified to

Predictor step:

$$\frac{\mathrm{d}r_{(0\rightarrow t)}}{\mathrm{d}t} = T(r_b,t). \tag{4.12}$$

Solution of the transport term after this step is defined as $T(r_b,t)$

Corrector step:

$$\frac{\mathrm{d}r_{(0\rightarrow t)}}{\mathrm{d}t} = \frac{1}{2}T(r,t) + \frac{1}{2}R(r,t). \tag{4.13}$$

The accuracy of the splitting method is demonstrated in [44]. For the context of this project with the GRI 3.0 and Lu and law mechanism for methane and N-heptane it was found that higher order splitting effected only the Flame Vortex Interaction (FVI) case 6.2.6. A second order splitting was used for the FVI case, rest of the test cases were run with first order splitting scheme. The FVI case represents a highly strained flame and is not reproduced accurately with the first order splitting due to inconsistencies between the transported and the integrated scalars. This is mitigated by either using smaller overall time-steps or by increasing the order of integration.

4.4. Reacting flow solver validation

The reacting flow solver has been extensively tested and validated in problems belonging to various combustion regimes. Validation for canonical cases which represent flow conditions in combustion applications are presented here, namely, laminar premixed and counterflow diffusion flames. Details of these configurations are discussed in section 5.1.1. The premixed flame case was solved for a methane/air mixture at 300 K and one atmosphere at an equivalence ratio of 0.66. The counter flow diffusion flame was solved with air and methane as the fuel and oxidiser respectively. The mass flow rates of the oxidiser and the fuel and the distance between the inlets lead to a strain rate of $550\ s^{-1}$. This is considered high strain for methane/air diffusion flames at 300 K and one atmosphere. Both the cases were used the GRI 3.0 [22] mechanism for the description of chemistry.

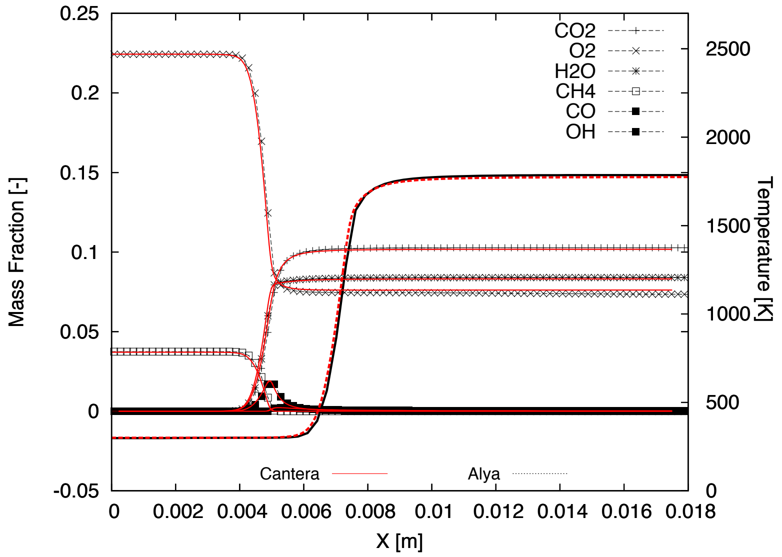

Figure 4.5: Premixed flame validation

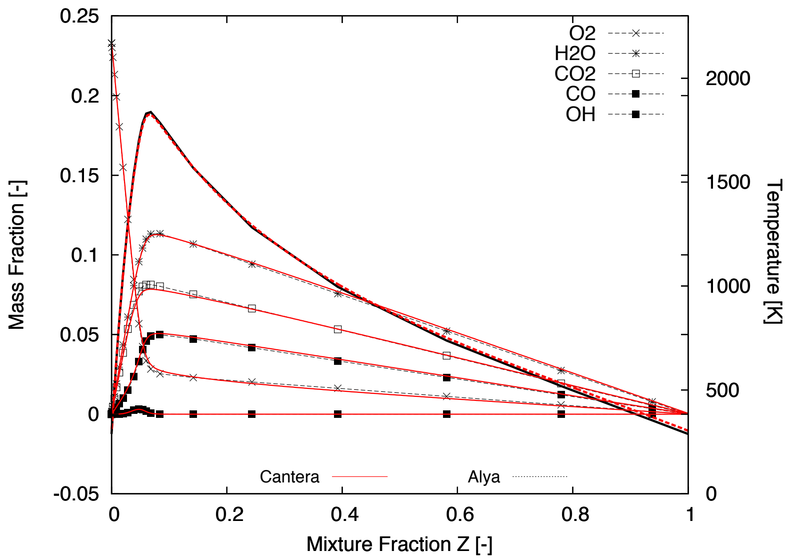

Figure 4.6: Diffusion flame validation

Figure 4.5 presents mass fractions of major species and temperature obtained across the flame from Cantera and Alya. Figure 4.6 shows the mass fractions and temperature across the centre line of the counterflow diffusion flame against mixture fraction (ref section 5.1.1). As seen in Figure 4.5 and Figure 4.6 that there is a good agreement between Alya and Cantera on these test cases. This validates the reacting flow solver implementation in Alya and ensures that the code is ready for testing chemistry reduction techniques. Following sections will discuss chemistry reduction techniques and discuss their performance.

5

Chemistry reduction

The following chapter deals with chemistry reduction strategies. The objective for chemistry reduction method in this study was to develop a reduction method which would be applicable to multiple combustion regimes with no necessary tuning. This means that user input has to be minimal and users need not have an *a priori* understanding of the chemistry. During the literature review two methods - DRGEP [40] and PFA [49] were identified which fulfilled these criteria, these methods were then tested for accuracy and their respective computational costs. These reduction methods provided accurate results at relatively low computational costs with minimal user input. This makes the DRGEP and the PFA models good candidates to be studied for static and dynamic adaptive chemistry implementations.

The computational cost and accuracy of these methods were computed by evaluating the temporal evolution of a Perfectly Stirred Reactor (PSR) reactor at various mixture temperatures, reduced schemes were then generated at every mixture temperature using the DRGEP and the PFA method. This case was computed using two test fuels namely, methane and n-heptane with the GRI 3.0 [22] and Lu and Law mechanism [35] respectively. The cost of reduction is shown normalised to the time taken for integration of source terms for a time interval of 0.1 ms and is shown in Figure 5.1. The time interval is representative of the time-step obtained in a typical LES simulation.

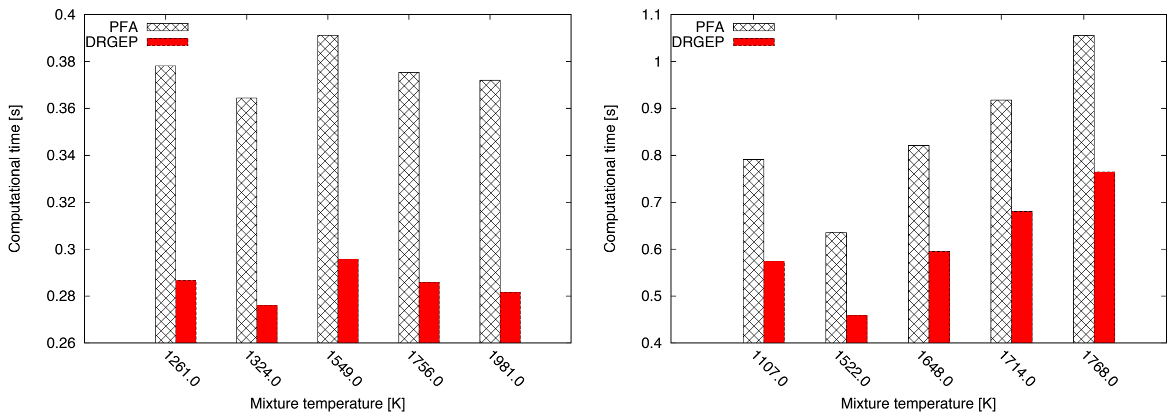

(a) Methane

(b) N-heptane

Figure 5.1: Reduction costs

It can be inferred from Figure 5.1 that for methane the cost of chemistry reduction through DRGEP and PFA is around 30 % and 40 % respectively, of the time needed for integration of the source terms for methane. For N-heptane reduction through DRGEP costs between 45 % and 80 % and with PFA costs between 65 % and 105 % of the time taken for integration. As the chemistry reduction procedure (DRGEP and PFA) is purely arithmetic its cost is independent of the state of the mixture and only depends on the size of the reaction mechanism (explained in section 5.1). However, the computational cost for integration of the chemical source terms strongly depends on the state of the mixture and is responsible for the trends in the relative cost for reduction, shown in Figure 5.1.

The accuracy of the reduction methods is computed in an auto-ignition delay test for n-heptane, as the differences in the computational costs for both these methods are more pronounced for n-heptane than for methane. Two reduced mechanisms with almost similar number of species were generated with the reduction methods DRGEP (104 S) and PFA (94 S). The accuracy of predicting the auto-ignition delay was then compared against the reference full mechanism (188 S). It is to be noted that the definition of the key species was the same in both these methods, but the threshold had to be different to generated reduced schemes with similar number of species.

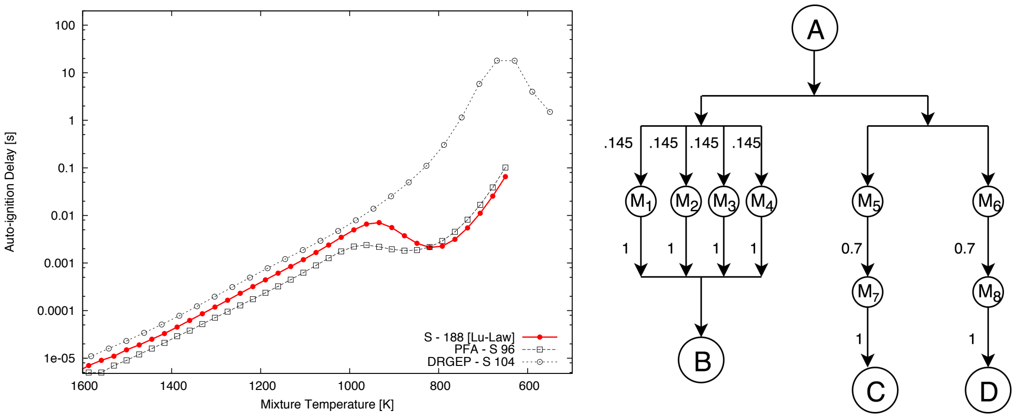

(a) Accuracy of reduction methods (b) Flux relation example

Figure 5.2: DRGEP vs PFA

As seen in Figure 5.2a the mechanisms obtained from DRGEP failed to predict the Negative Temperature Coefficient (NTC) region unlike the PFA generated mechanisms which was able to capture this complex phenomena. This shows that the PFA method is superior to the DRGEP method for the same simplistic definition of the key species, a better definition of which could lead to better predictions in both the methods.

The difference between the PFA and the DRGEP method can be understood in a intuitive way by the following example (adapted from [49]). Consider a reaction pathway shown in Figure 5.2b where A is the target/key species and B,C and D are the products formed through intermediate species M_{1-8}. If the objective was to reduce this reaction to about 5-6 species the DRGEP method which does not take into account overall flux contribution in multiple generations of intermediate species will yield a reduced mechanism containing species M_5, M_6, M_7, M_8, C and D. The overall flux contribution is computed by multiplying all the contributing fluxes $0.21 * 0.7 * 1 * 2$ = 29.4%. PFA on the other hand will yield a reduced scheme containing species M_{1-4} and B, the flux contribution of this mechanism is $0.145 * 4 * 1$ = 58 %. Reduction schemes which represent higher percentages of the overall species flux are more accurate and hence PFA would lead to a more accurate reduced mechanism than DRGEP for similar number of species, this was already observed in the auto-ignition delay tests on n-heptane where PFA could predict the NTC region with lesser number of species than the DRGEP method.

The accuracy and computational cost analysis presented PFA as the superior method, which even though is slightly more expensive than the DRGEP method but yields better accuracy and is hence chosen as the reduction strategy for this study.

The following sections test the PFA algorithm in more detail considering a wide range of classical combustion problems. Firstly, statically reduced schemes generated using the python interface of Cantera are presented before moving on to dynamically reduced schemes generated through Alya. Test cases were identified which represented fundamental combustion parameters like flame speed in premixed and stratified flames, diffusion flames and flames under high strain.

5.1. Path Flux Analysis (PFA)

PFA is based on identifying important reaction paths among a set of pre-defined ”Key Species”, these pathways are weighed by the reaction rates of the involved reactions. Key species in this study were chosen as the fuel, O_2 and major products occurring in combustion of hydrocarbons like CO, CO_2 and H_2O, the aim of the tests the follow is to understand the applicability of the PFA method. The results could be improved and more reduced schemes can be generated if chemical species specific to the problem were included as the key species. A threshold is then specified to cutoff reaction pathways. The process of reduction through PFA can be explained by assuming a chemical mechanism which contains N species and M reactions, K are the key species which are defined. The PFA algorithm starts by computing the production and consumption rates of N species through M reactions for a given thermodynamic state.

$$P_A = \Sigma_{i=1,M} max(0, v_{A,M}\omega_M). \tag{5.1}$$

$$C_A = \Sigma_{i=1,M} max(0, -v_{A,M}\omega_M). \tag{5.2}$$

where i is the index of reaction in the mechanism, $v_{A,i}$ is the stoichiometric coefficient of species A in reaction i, ω_i is the net rate of progress of reaction i. Then a matrix of size $K * N$ is computed which contains the production and consumption rates for all species K with respect to reactions involving species N.

$$P_{AB} = \Sigma_{(i=1,i)} max(0, v_{A,i}\omega_i\delta_{iB}). \tag{5.3}$$

$$C_{AB} = \Sigma_{(i=1,i)} max(0, -v_{A,i}\omega_i\delta_{iB}). \tag{5.4}$$

Here $\delta_{Bi} = 1$ or 0 if species B in involved in reaction i or not respectively. This relation matrix is then normalised by the absolute maximum between the production and consumption rates of species N through M reactions as obtained in step 1. This gives the 1^{st} generation of normalised reaction coefficients.

$$r_{AB}^{p-1st} = \frac{P_{AB}}{max(P_A, C_A)}. \tag{5.5}$$

$$r_{AB}^{c-1st} = \frac{C_{AB}}{max(P_A, C_A)}. \tag{5.6}$$

Here r_{AB}^{p-1st} and r_{AB}^{c-1st} are the first generation relation coefficients. The DRGEP formulation ends here and the threshold is applied to relation matrix obtained in this step. The PFA is however, designed to take into account multiple generations an addition step is done to computed second generation normalised coefficients. The second generation coefficients are computed as:

$$r_{AB}^{p-2nd} = \Sigma_{M_i \neq A.B}(R_{AM_i}^{p-1st} R_{MB_i}^{p-1st}). \tag{5.7}$$

$$r_{AB}^{c-2nd} = \Sigma_{M_i \neq A.B}(R_{AM_i}^{c-1st} R_{MB_i}^{c-1st}). \tag{5.8}$$

Here r_{AB}^{p-2nd} and r_{AB}^{c-2nd} are the first generation relation coefficients. This step can be repeated for as many generations as needed, the computational time scales as N^{Gen}. The overall relation matrix is then obtained by summing up all the reaction coefficients.

$$r_{AB} = r_{AB}^{p-1st} + r_{AB}^{c-1st} + r_{AB}^{p-2nd} + r_{AB}^{c-2nd}. \tag{5.9}$$

The relation matrix r_{AB} is of size AXB and contains the normalised production rates of species A in the presence of species B, the matrix could be formulated in any orientation. In this study A correspond to the predefined key species and B to all the species present in the mechanism. Relation between the same species is set to 0, $R_{A,A}$ or $R_{B,B} = 0$. Once the relation matrix is obtained a threshold is defined and chemical pathways are truncated accordingly. Finally a set of species to be removed is obtained however, the reduction is done in terms of reactions and not species to ensure mass conservation and to account for the temporal evolution of the species and their reactivities. All reactions where the species to be removed are present either as product or as reactant are removed from the mechanism. Third body reactions where the species that are to be removed act as collision bodies but do not react themselves are left unchanged.

The PFA method is based on the local thermodynamic and chemical states, which makes it hard to define an universal threshold. Defining a universal threshold would lead to over/under reductions of chemistry which is to be avoided. It was noticed that elements in the relation matrix r_{AB} followed a logarithmic scale, to come up with more intuitive and globally applicable thresholds, logarithm of the locally generated relation matrix is normalised by the maximum value in the matrix.

$$r_{AB} = \frac{log(r_{AB})}{max(r_{AB})}. \tag{5.10}$$

A relation matrix with values ranging from 0 to 1 is obtained for which there can be an universal definition of the threshold. The PFA algorithm is shown in 2. PFA can be used to generate mechanisms with reduced stiffness as less number of reactions with similar reaction rates have to integrated. Using the PFA method more carefully with knowledge of the chemistry it is possible to generate non-stiff reaction mechanisms which can integrated with less computational time using pure explicit methods.

Targeted reduced schemes for specific pollutants can be generated using PFA which would identify the set of reactions critical to predict the specific pollutant permitting the use of a section of the detailed mechanism which represents the area of interest for the specific case. The definition of key species will have to include NO_X species or precursors for soot, this would open up reaction pathways specific to those species. This kind of modularity in the use of the PFA method makes it not only a method for chemistry reduction but also allows users to truncate/include specific chemical pathways reducing the overall stiffness of the system. PFA algorithm is shown in Algorithm 2.

The following Figure 5.3 shows the reaction path diagram following the element C. This is generated from a stoichiometric mixture of methane in air at a temperature of 1000 K and atmospheric pressure. The GRI 3.0 [22] mechanism is used to determine the chemistry. The strength of the reactions are represented by the gradient of the colour, the threshold specified determines the pathways which are retained in the PFA. The solid line represents the basic skeletal mechanism and the dashed line show auxiliary pathways. The dotted pathways represent redundant chemical pathways between key species. It is to be noted that these redundant pathways might be necessary for other definitions of key species, but the current definition of key species is CH_4 and $CO2$ which represent major reactants and products in the current context. The definition of key species can be extended to include pathways necessary to other families of reactions, like reactions contributing to NO_X or to precursors of soot.

5.1.1. PFA tests

The following sections show the performance of statically generated (the reduction is static as the reduced schemes are generated based on a single state) PFA reductions on 0D auto ignition, 1D premixed and counter flow diffusion problems. The following cases were computed using the C++ and python interfaces of Cantera.

Auto-ignition delay

A mixture is said to be auto igniting if it reacts spontaneously without any external supply of energy such as a flame or a spark. This occurs when the energy/temperature of the mixture is higher than the activation energy required by the reactions. Autoignition delay time is defined as the time in which a reactable mixture reacts to form products. Auto-ignition delay times can be correlated with the Wolfer equation modified to account for equivalence ratio (ϕ) effects [30] shown in Equation 5.11.

$$t_i = 0.43P^{-1.19}exp(4650/T_m). \tag{5.11}$$

Here T_i is the auto-ignition delay in ms, A ,n and m are experimentally determined constants, P is the pressure in bars, T_M is the mixture temperature, E is the activation energy and R is the universal gas constant.

Auto-ignition delay is a key parameter which represents various chemical properties of the fuel for example, in lean-premixed combustion focused on low emissions auto-ignition delay of the mixture before reaching the combustion chamber must be high in order to avoid damaging the combustor and over-production of pollutants.

To test the effectiveness of the PFA reduction to predict auto-ignition delays a stoichiometric mixture of n-heptane and air is taken at temperatures ranging from 650 K to 1600 K and at pressures of 16 and 40 bar respectively. Chemistry is computed using a n-heptane mechanism [35] containing 188 species and 1719 reactions. A homogeneous mixture is set by defining temperature, pressure and mass fractions of fuel and air. This mixture is then added to a constant pressure gas reactor which

```
Result: Get_Removed(Gas,Key_Species,Tolorence)
Set_TPY(gas);
Get_Net_Rates_Of_Progress(gas);
for (i in N_Sp) do
    Get_PA(i) using (5.1) ;
    Get_CA(i) using (5.2) ;
end
for (i in N_Key) do
    for (j in N_Sp) do
        Get_PAB(i,j) using (5.3);
        Get_CAB(i,j) using (5.4);
    end
end
for (i in N_Key) do
    div = max(PA(i),CA(i)) ;
    for (j in N_Sp) do
        RP_1(i,j) = PAB(i,j)/div using (5.5);
        RC_1(i,j) = CAB(i,j)/div using (5.6);
    end
end
for i in N_Key do
    for j in N_Sp do
        for k in N_Sp do
            RP_2(i,j) = RP_2(i,j) + RP_1(i,k) * RP_1(k,j) using (5.7);
            RC_2(i,j) = RC_2(i,j) + RC_1(i,k) * RC_1(k,j) using (5.8);
        end
    end
end
for i in N_Key do
    for j in N_Sp do
        R_mat(i,j) = RP_1(i,j) + RP_2(i,j) + RC_1(i,j) + RC_2(i,j) using (5.9);
    end
end
Logarithmic Normalisation of R_mat using (5.10);
for i in N_key do
    if max(i,:) < tol then
        Remove = i ;
    else
end
```

Algorithm 2: PFA Algorithm

solves the following transient equation for species mass fractions Y_k. The chemical source $\dot{\omega}_k$ is computed from Arrhenius rate laws and the chemical mechanism, the procedure is described in detail in section 3.1. Once the temporal evolution is known the auto-ignition delay time can be extracted by defining a criteria to identify completion of the reaction. In this study auto-ignition delay is defined at a point where the temporal gradient of temperature is maximum. This process in then repeated for a series of temperatures and pressures.

$$\frac{\mathrm{d}Y_k}{\mathrm{d}t} = \dot{\omega}_k. \tag{5.12}$$

A seen in Figure 5.4 there is a region of in the curves where increase in temperature does not result in smaller ignition delays, this is called the negative temperature coefficient region. This phenomenon is extensively studied and documented [13]. This is explained by the competition among radicals to form cyclic ethers, olefin etc, these reactions are of the chain propagating type and result in reduced overall reactivity of the mixture [13]. Once the temperature is increased the radical pool becomes well

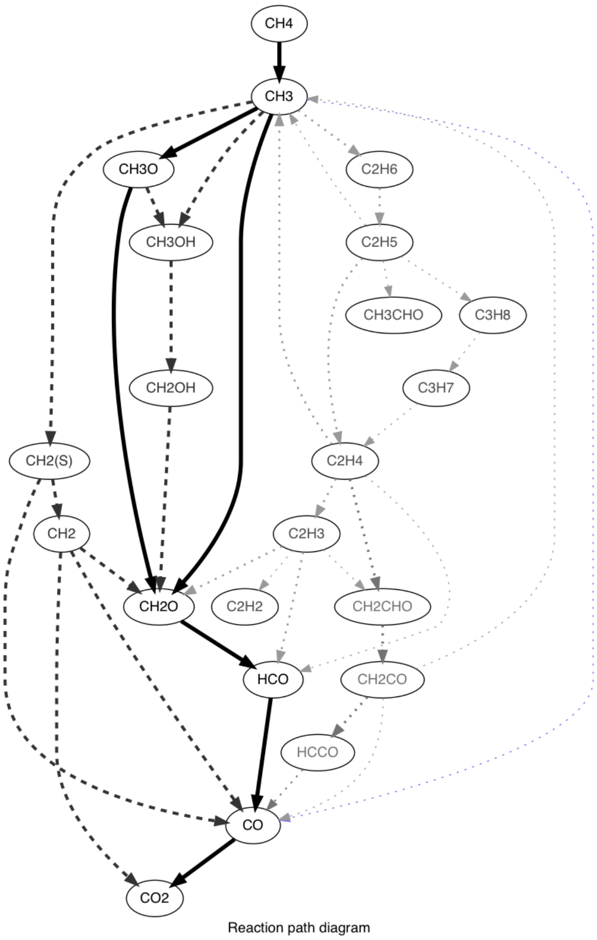

Figure 5.3: Reaction path diagram - C

established and competition in the radical pool stops restoring normal behaviour where the auto-ignition delay reduces with increase in mixture temperature. The nature of this complex chemical phenomenon was one of the reasons to choose n-heptane as a fuel for this case. Also seen in Figure 5.4 that reduced chemical schemes predict auto-ignition delays with acceptable errors. Greater reduction can be through PFA by including species responsible for the NTC behaviour as key species. This however would require extensive knowledge on the chemistry of n-heptane and is not explored in this study.

1D Premixed flames

A series of one-dimensional laminar flame propagating into a premixed gas mixtures at different equivalence ratios are computed. This is fundamental test case which is used to measure the accuracy of a chemical mechanism against experimental data. Laminar flame speed, is a measure of the heat release and is key to predict flame dynamics. Flame speed or burning velocity of a flame is a measure of the rate of propagation of a plane flame through a flammable gaseous mixture it can be defined as the velocity of the plane with which the flame front moves orthogonally to the unburnt gases. This propagation is determined by heat release through chemical reactions in the thin reaction zone formed between the reactants and products and the heat/mass transfer through it. Reactions in the unburnt gases are initiated through heat transfer through conduction and radiation from the reaction layer. Thus the flame speed of a mixture is affected by temperature and local mixture properties like viscosity ,conductivity and density. Temperature, equivalence ratio and pressure are the parameters that effect the flame speed most.

Equivalence ratio ϕ [-]

Change in the equivalence ratio of the mixture changes the chemistry and the strength of the mixture, in most cases the maximum strength is observed close to stichiometeric conditions ($1.05 < \phi < 1.10$)

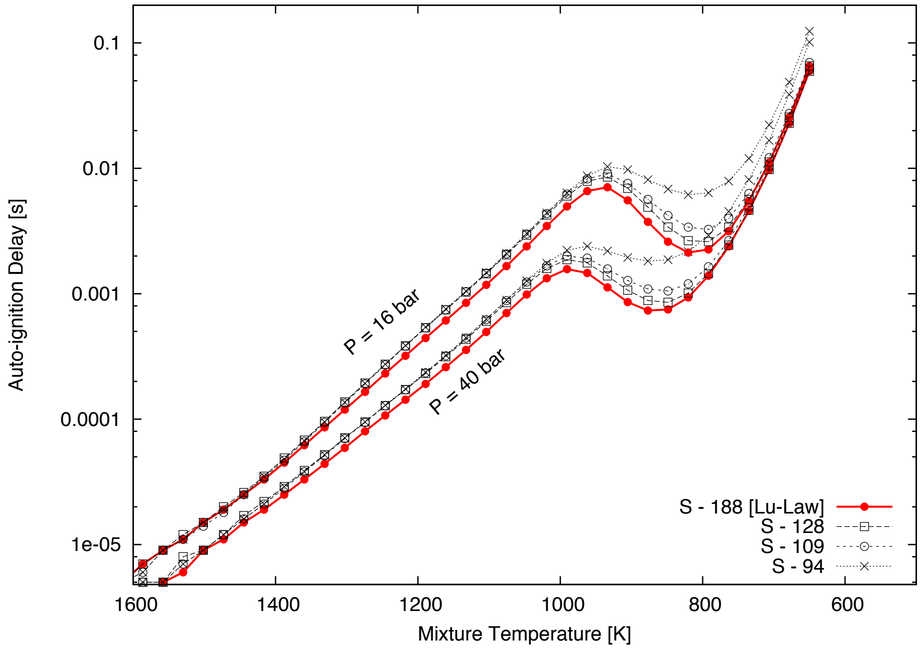

Figure 5.4: Autoignition delay - n-heptane

with hydrogen and carbon monoxide being the exceptions [30].

Initial temperature T_0 [K]
Studies [15] show that flame speed increases with increase in temperature for methane experimental data was fitted to an empirical equation shown in Equation 5.13.

$$S_L = 0.08 + 1.6 * 10^{-6} T_o^{2.22}. \tag{5.13}$$

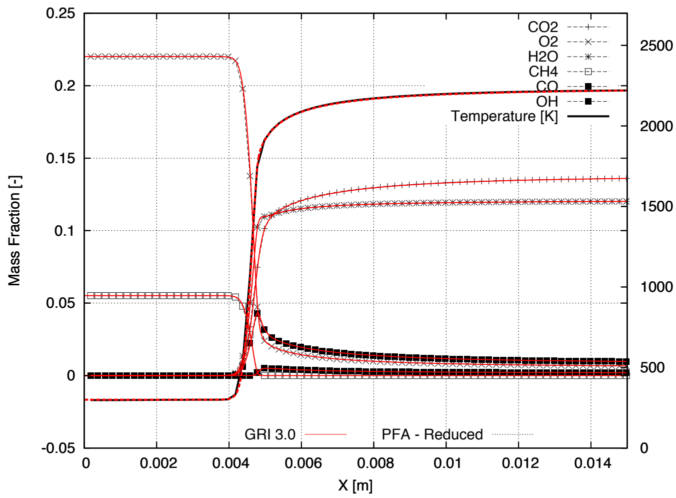

Figure 5.5: Laminar premixed Flame - CH_4 - $\phi = 1$, P = 1 bar

Pressure [Pa]
Pressure effects the reaction order as given in Equation 5.14 [47],

$$S_L \propto P^{n-2}/2. \tag{5.14}$$

For simple bimolecular fuels the reaction order is independent of pressure but for more complex fuels like kerosene and natural gas the effect of pressure can be expressed as Equation 5.15, where x takes a values between 0.1 to 0.5 [15].

$$S_L \propto P^{-x}. \tag{5.15}$$

Flame temperature and speed are identified as the key parameters which represent the chemistry as well as the transport of a premixed flame. Flame temperature is a measure of the thermal expansion factor $\tau = (T_b - T_{ub})/T_u)$ where T_b and T_{ub} are the burnt and unburnt mixture temperature respectively. Reduced schemes generated by PFA will be tested for these two parameters. Tests were run on methane/air and N-heptane/air premixed flames, from equivalence ratios ranging between their respective flammability limits. A solution of a stichiometeric mixture of methane/air 1D laminar premixed in shown in Figure 5.5.

It is important to mention that these test were done to show how the reduced schemes generated by the PFA algorithm work in a very primitive way. The reduced schemes presented here were generated at the same thermodynamic and chemical state for different values for the threshold. The performance of these schemes can be improved by using a dynamic implementation of the PFA algorithm (discussed in section 6.1.1). Also the key species chosen were the reactant and products, a better definition of these keys species based on the chemistry of the fuel would lead to more accurate reduced schemes. The reduced schemes generated for methane with the GRI 3.0 [22] are given in the appendix .1.

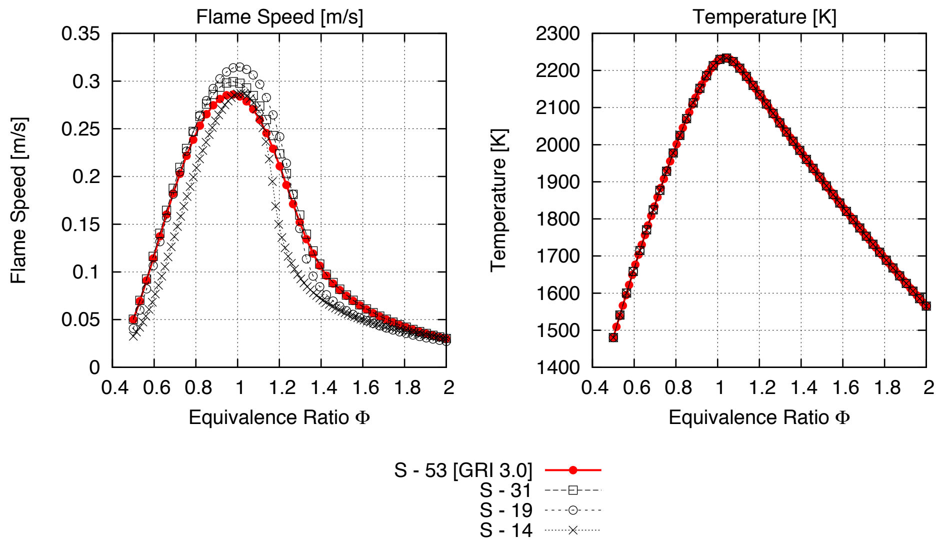

Figure 5.6: Laminar premixed flame - CH_4 between $\phi = 0.4$ and $\phi = 2$

Before moving on to diffusion flames the concept and formulation of mixture fraction is discussed, this is an important scalar quantity which is used to represent flames.

Bilger's mixture fraction

Mixture fraction is a non-dimensional quantity representing mass fraction of the fuel with respect to the oxidiser, definition of mixture fraction based on the mass fraction of the fuel is not well defined in the flame region as the mass fraction of the fuel changes due to reactions. On the other elemental mass fractions are conserved in chemical reactions and can be used to define mixture fraction. The elemental definition of mixture fraction makes it act like a passive scalar without source terms. In the current study mixture fraction is defined based on Bilger's definition [6], which for hydrocarbons is

$$b = 2\frac{Y_C}{W_C} + 0.5\frac{Y_H}{W_H} - \frac{Y_O}{W_O}. \tag{5.16}$$

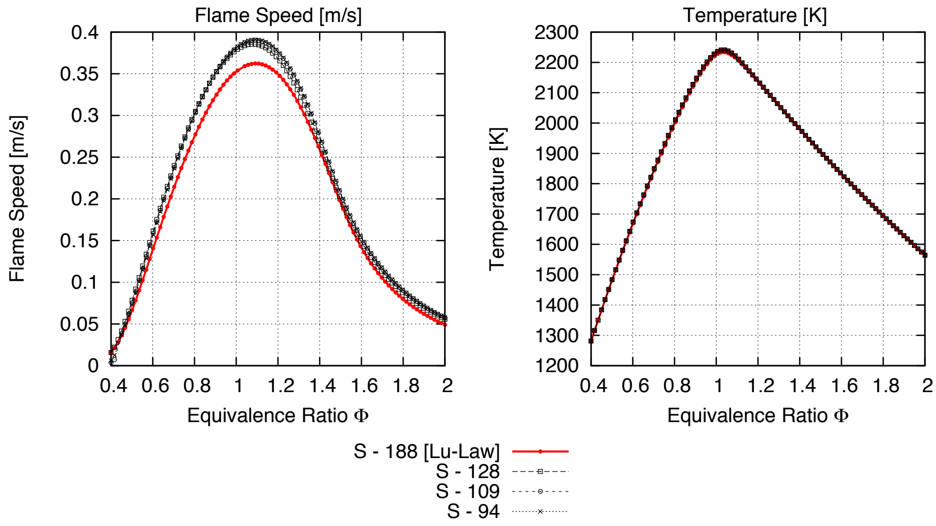

Figure 5.7: Laminar premixed flame - n-heptane

Here Y_C, Y_H and Y_O are the elemental mass fraction and W_C, W_H and W_O are the elemental weight of carbon, hydrogen and oxygen respectively. b is then normalised by boundary values b_f and b_o which are obtained by computing b of the fuel and oxidiser respectively.

$$Z = \frac{b - b_o}{b_f - b_o}. \tag{5.17}$$

Counter flow diffusion flames

Laminar premixed or non-premixed (if the mixing is fast compared to the chemistry) systems are characterised as a homogeneous processes. In cases where the mixing is not fast, mixing time would control the chemical rates and the burning rate. In such configurations the fuel and oxidiser are not mixed before and have opposing inlets, this makes it necessary for the fuel and to mix before combustion can take place. Fuel and oxidiser mix and form a reaction zone through molecular and turbulent diffusion. A typical configuration in shown in Figure 5.9.

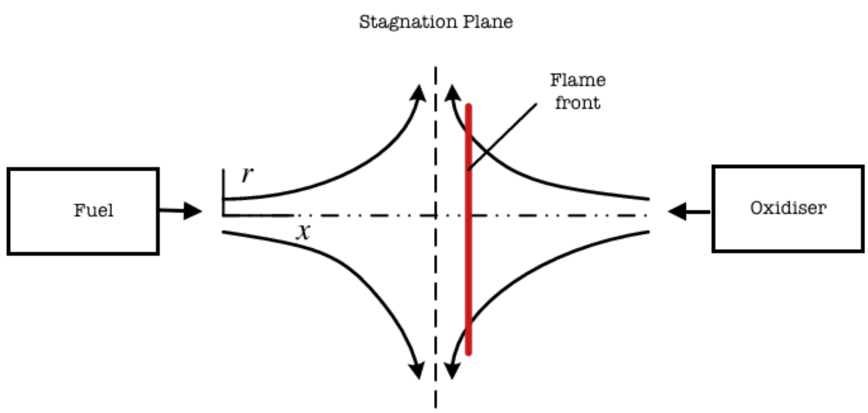

Figure 5.8: Schematic of a counter flow flame

The axisymmetric stagnation flow governing equations solved by Cantera to compute such flames are listed in Equation 5.21 to Equation 5.21. Diffusion flames are characterised by a small region of reaction, outside of which reactions are not possible to excessive presence of fuel or oxidiser. The flame is strained in this case and effects how the combustion process takes place. In this study strain is defined as $(V_{fuel} + V_{Oxy})/D$, where V_{fuel}, V_{Oxy} are the absolute velocities of the fuel and the oxidiser respectively and D is the distance between the two inlets. A flame can either lead to a equilibrium solution under very low strain or extinguish under high strains. Unlike premixed flames diffusion flames do not have a characteristic flame speed and is stagnant, this makes such flames more sensitive to turbulence and disturbances. Also diffusion flames are considered to be more safer from an industrial perspective as they do not propagate, all these reasons make such flames a suitable fundamental test case [54].

The following Figure 5.9 shows a typical solution of a counter flow flame, the strain can be varied by either increasing the velocity of the reactants at the inlets or by reducing the distance between them. The flames are plotted against mixture fraction which is defined using Bilger's formula 5.1.1.

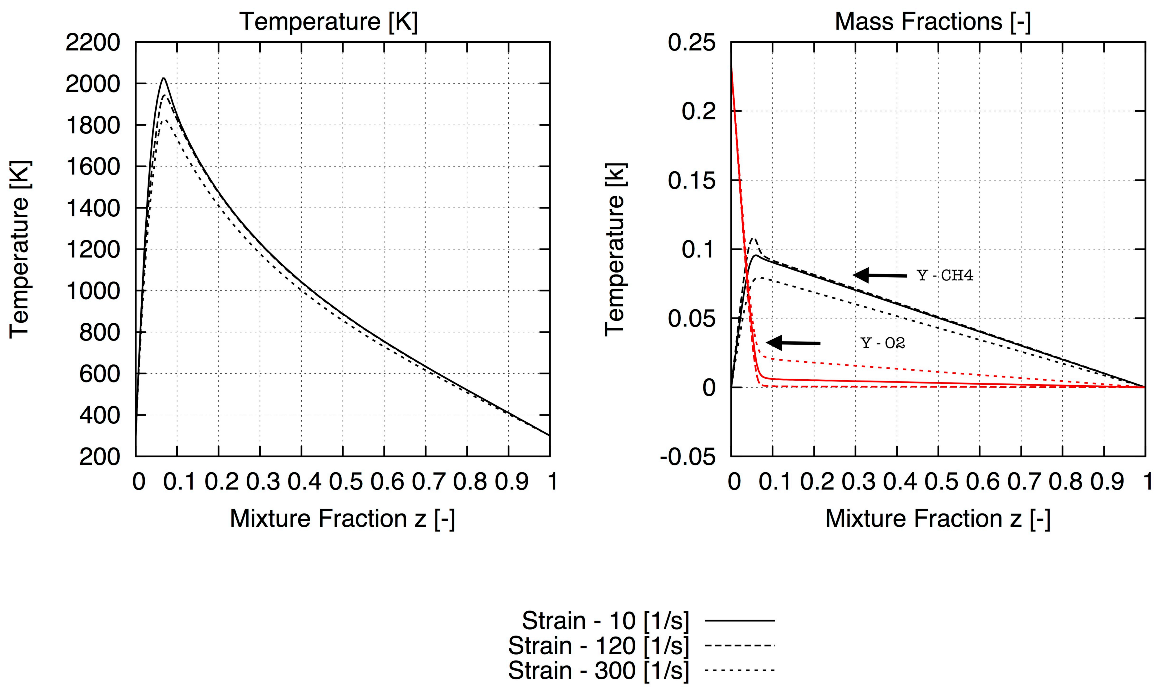

Figure 5.9: Counter flow flame solution

Cantera solves 1D flames based on axisymmetric stagnation flow conditions, along stagnation streamlines. The following equations are the governing equations:

$$\frac{\partial \rho u}{\partial z} + 2\rho V = 0. \tag{5.18}$$

$$\rho u \frac{\partial V}{\partial z} + \rho V^2 = -\Lambda + \frac{\partial}{\partial z}\left(\mu \frac{\partial V}{\partial z}\right). \tag{5.19}$$

$$\rho C_P u \frac{\partial T}{\partial z} = \frac{\partial}{\partial z}\left(\lambda \frac{\partial T}{\partial z}\right) - \Sigma_k j_k c_{p,k} \frac{\partial T}{\partial z} - \Sigma h_k W_k \dot{\omega}_k. \tag{5.20}$$

$$\rho u \frac{\partial Y_k}{\partial z} = -\frac{\partial j_k}{\partial z} + W_k \dot{\omega}_k. \tag{5.21}$$

Here u, v and $V = v/r$ are the axial, radial and the scaled radial velocity respectively, ρ is the density, Λ is the pressure eigenvalue, c_p is the heat capacity, T is the temperature, μ is the dynamic viscosity, Y_k are the mass fractions, j_k are the diffusive fluxes, W_k is the molecular weight, and ${}_k$ are the sources of species k. Cantera has implementation for both real and ideal gases, in the current context the mixture is assumed to be an ideal gas. Diffusive fluxes j_k are closed by Lewis number unity assumption.

Canter tests are run on methane/air and n-heptane/air counter flow configuration, both the fuel and the oxidiser are admitted at 300 K and atmospheric pressure. To find the extinction point of the flame the scalar dissipation rate and temperature at the stichiometeric surface are plotted, this gives the iconic 'S' curve for diffusion flames. Scalar dissipation rate χ is defined as shown in Equation 5.22, it has a dimension of $(1/s)$ and gives a measure of the gradients of mixture fraction (z) and the molecular fluxes of the species towards the flame front.

$$\chi = 2D\left(\frac{\partial z}{\partial x_i}\frac{\partial z}{\partial x_i}\right). \tag{5.22}$$

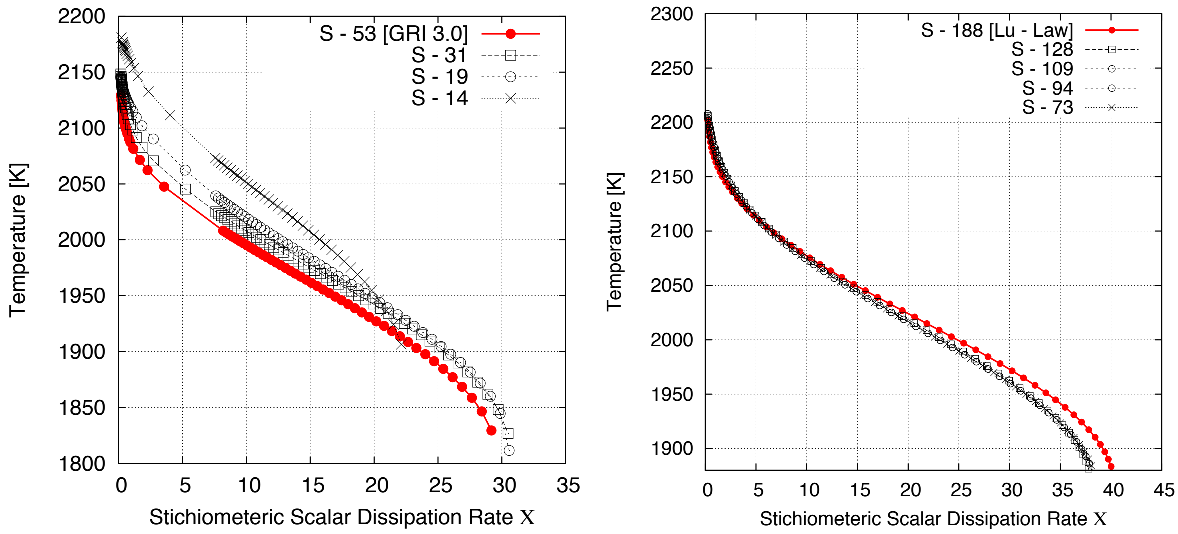

Figure 5.10: Counterflow diffusion flames

The aforementioned tests show the effectiveness of the PFA applied to various fundamental steady state combustion problems. PFA has demonstrated excellent efficiency and accuracy in the reduction, and therefore can be considered to be incorporated in Dynamic Adaptive Methods (DAC).

It is noticed that not all combustion regimes are represented with the same degree of accuracy. This is a result of the reduction being done statically on one thermodynamic state. If the reduction were to be done dynamically on the fly based on the current thermodynamic state the accuracy of the reduced mechanism could be improved. This dynamic implementation of chemistry reduction DAC has be explored by [32] and is talked about in the following section of the report.

6

Dynamic Adaptive Chemistry (DAC)

Though statically *a priori* generated reduced schemes were able to predict flames in various combustion regimes, this type of reduction does not take into account the temporal evolution of the chemistry of the problem. Use of such static schemes leads to large errors in the prediction of flames and are not applicable in problems which deal with multi-regime combustion problems. To account for these temporal changes reduced schemes then need to be relatively large to include all possible reaction pathways which could be encountered this however, beats the purpose of using reduced chemistry. To avoid this a dynamic implementation of the reduction method is to be employed which would take into account the temporal changes in the problem and truncate reaction pathways accordingly. The reduction would extend the use of the PFA [49] by computing reduced mechanisms at given points and time steps in the problem. There are various methods in which the dynamic reduction can be performed, literature on such methods is presented in 2.3. After the literature review DAC and CODAC were found to be suitable for applications which are of interest in the current project. The PFA and the on-the-fly reduction algorithms were implemented in Alya and is used to evaluate the performance and accuracy of the reduction strategies on the following tests.

6.1. DAC methodology

The following section outlays the different dynamic adaptive chemistry models and presents their implementation in the current work. The current study differs from the literature in terms of the error function definition for CODAC and the actual quantity which is being reduced. Most of the studies found in literature reduce the number of species this would mean that an additional step is to be performed to ensure mass conservation. To overcome such issues and to ensure mass conservation without any additional computations the current study reduces the number of reactions. This satisfies mass conservation and reduces the computational time as less number of reactions have to computed.

6.1.1. Dynamic Adaptive Chemistry (DAC)

The most simple implementation of the adaptive chemistry is to computed reduced schemes in specified intervals of computational time on every computational point in the domain irrespective of its relative importance to the flow. If the interval between successive reductions is low the solution obtained would be the upper limit for the accuracy of what can be achieved with dynamic reductions. The computational cost of reducing chemistry was computed to be around 40 % of the time needed to compute the integrated chemical sources, furthermore the cost scales exponentially with the number of species in the reaction mechanisms (presented in section 5). This to lead to a scenario where the reduction become more expensive than the chemistry itself, this can be avoided by specifying larger time-steps between reductions, this however would effect the accuracy.

6.1.2. Correlated Dynamic Adaptive Chemistry (CODAC)

As mentioned in 2 the simple DAC method was improved by Gou et.al [20] which included an error function to the chemistry reduction process. This error function is used to determine correlation of thermodynamic states between the same point in time, the correlation would then decided if a new reduced scheme is to be generated or an existing scheme can be used. The definition of the correlation function was adapted from [20] and was modified to:

$$\Delta = max\left(\frac{T_{n+1} - T_n}{\epsilon_t}, \frac{lnY_{Fuel_{n+1}} - lnY_{Fuel_n}}{\epsilon_{Fuel}}, \frac{lnY_{CH_2O_{n+1}} - lnY_{CH_2O_n}}{\epsilon_{CH_2O}}, \frac{lnY_{OH_{n+1}} - lnY_{OH_n}}{\epsilon_{OH}}, \frac{lnY_{HO_{2n+1}} - lnY_{HO_{2n}}}{\epsilon_{HO_2}}, \frac{lnY_{CO_{n+1}} - lnY_{CO_n}}{\epsilon_{CO}}\right). \tag{6.1}$$

CO was added to the correlation function to account for post-ignition kinetics, which would identify correlation in burnt mixtures, furthermore the error function is to be tuned for specific cases to achieve better predictions.

6.1.3. Tabulated Dynamic Adaptive Chemistry (TDAC)

CODAC was based on the assumption that reducing chemistry for mixtures at similar thermodynamic and chemical state would yield similar reduced schemes. This makes it redundant to run the expensive reduction procedure for all the points at similar states. In practical reacting flow simulations there could be many points where the mixtures are in similar states and computation costs can be reduced if the reduced schemes were tabulated against controlling variables which determine the state. This concept is the fundamental basis of the TDAC method, the TDAC method improves on the CODAC method on two aspects, firstly the expensive process of reduction is tabulated and secondly the TDAC method removes the dependence on an error function. This makes the TDAC method applicable for a wide range of applications and combustion regimes without the need for any 'ad hoc' tuning. Definition of the controlling variables was chosen to be mixture fraction, chemical progress variable and scaled temperature for problems involving auto-igniting/re-igniting problems. The choice of the controlling variables was inspired from classical definition of controlling variables in combustion problems solved with the flamelet model found in [52] [41] [25]. Mixture fraction is computed by the Bilger's formula 5.1.1 and the definitions of the progress variable is given in Equation 6.2.

$$Y_c = 4.0 * Y_{CO_2} + 2.0 * Y_{H_2O} + 1.0 * Y_{CO} + 0.5 * Y_{H_2}. \tag{6.2}$$

The following shows the algorithm of the reduction strategies implemented, tested and validated in this study. The methodologies are summarised in Figure 6.1

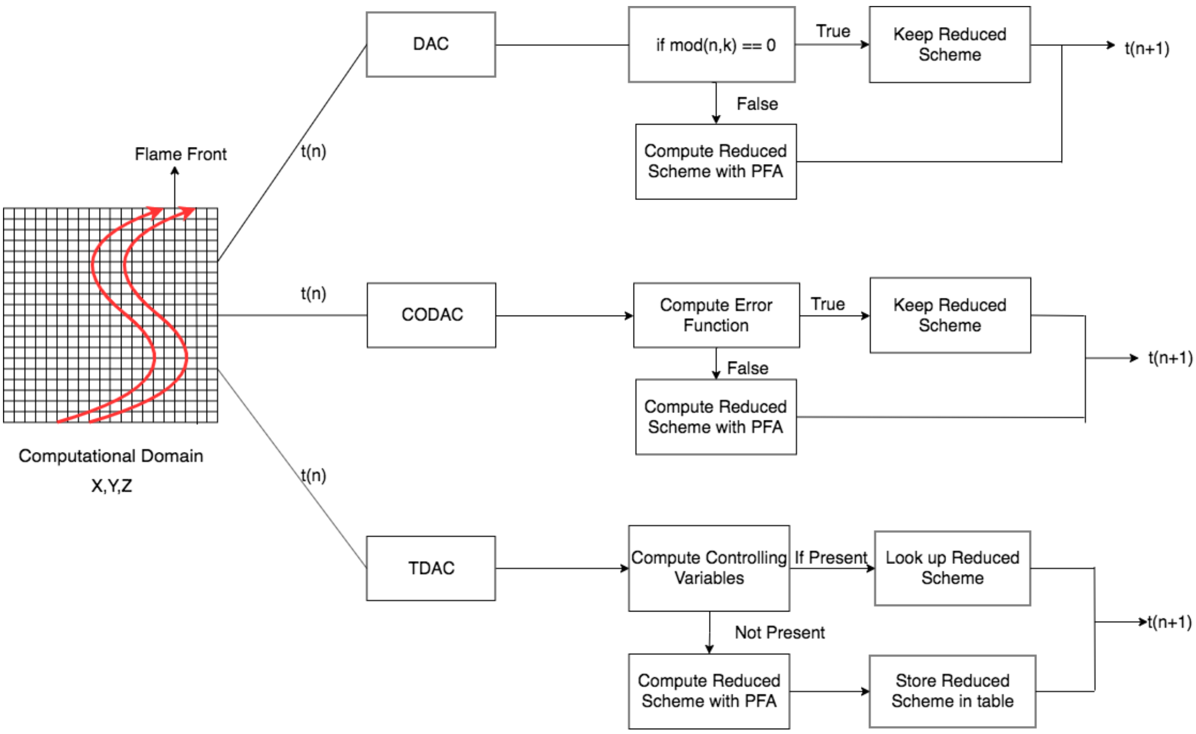

Figure 6.1: DAC methedology

```
Result: Dynamic Adaptive Chemistry (DAC)
if (Method == DAC) then
    if mod(n,k) == 0 then
        call Get_Removed ;
        call Cantera_Integrate ;
    else
        call Compute_Removed ;
        call Cantera_Integrate ;
else if (Method == CODAC) then
    call Get_Correlation;
    if Correlation == True then
        call Get_Removed ;
        call Cantera_Integrate ;
    else
        call Compute_Removed ;
        call Save_Removed ;
        call Cantera_Integrate ;
else if (Method == TDAC) then
    call Get_Mixture_Fraction ;
    call Get_Progress_Variable ;
    call Check_Table ;
    if If Z exists then
        call Get_Removed_Table ;
    else
        call Compute_Removed ;
        call Save_Removed_Table ;
    call Cantera_Integrate ;
```

Algorithm 3: Dynamic adaptive chemistry algorithm

Algorithm 3 shows the implementation of the reduction strategies here Compute_removed represents computing the reduced scheme, Get_Removed represents obtaining a previously reduced scheme, Cantera_Integrate represents the integration of the chemical source terms, Get_Correlation represents computing the correlation using section 6.2, Get_Mixture_Fraction computes the mixture fraction using Bilger's mixture fraction Equation 5.17, Get_Progress_Variable computes the chemical progress variable using Equation 6.2 and Check_Table, Get_Removed_Table and Save_Removed_Table represent the look up, retrieval and storage of reduced schemes in the TDAC.

6.2. DAC test cases

Test cases for DAC which are mentioned below were performed with the finite rate solver implemented in Alya. To be consistent in terms of chemistry reduction all test cases were run with same definition of key species, thresholds for PFA and correlation function. Number of entries and the distribution in the table for TDAC were also kept constant in all the cases. The objective of these cases is to present the application of the reduction methodology, higher accuracies can be achieved in all the problems with specific definitions the key species and the thresholds based on the chemistry of the problem. The following parameters were set:

- PFA
  - Key species - CH_4, CO_2, H_2O, CO, O_2
  - Threshold - 0.85 (Normalised)
- DAC
  - Frequency - 100 time-steps (relatively frequent)
- CODAC
  - Correlation function -
  - Correlation threshold - 0.05 (5 % of correlation)
- TDAC
  - 100, 500 points in mixture fraction (z)and progress variable (Y_c) respectively (all cases expect pure auto-ignition).
  - Distribution is based on a geometric distribution around stichiometeric conditions shown in Figure 6.2.

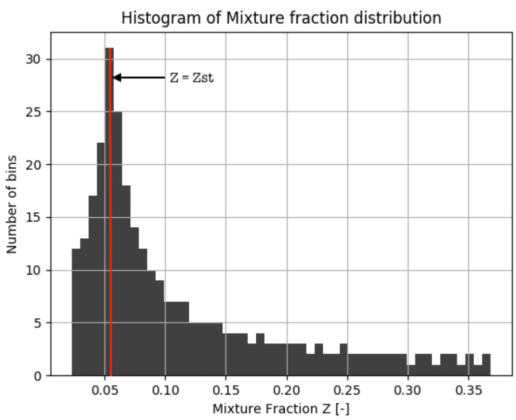

Figure 6.2: Mixture fraction Z [-]

6.2.1. Auto-ignition

Auto-ignition in homogeneous mixtures were computed for a stichiometeric methane/air mixture at $1500[K]$ and atmospheric pressure. The following plot Figure 6.3a shows the temporal evolution of the constant pressure Perfectly Stirred Reactor (PSR). It is seen that DAC fails to predict the autoignition of the mixture, however, the CODAC and the TDAC model successfully predict it. The DAC method has no information of the state of the mixture and hence reduces chemistry at all computational point with the same degree causing over/under reduced mechanisms. This could be mitigated by reducing the frequency of the DAC method, this would make this method computationally expensive not feasible for use in complex flows. CODAC and TDAC reduce the chemistry based on local conditions and are hence more effective in predicting autoignition.

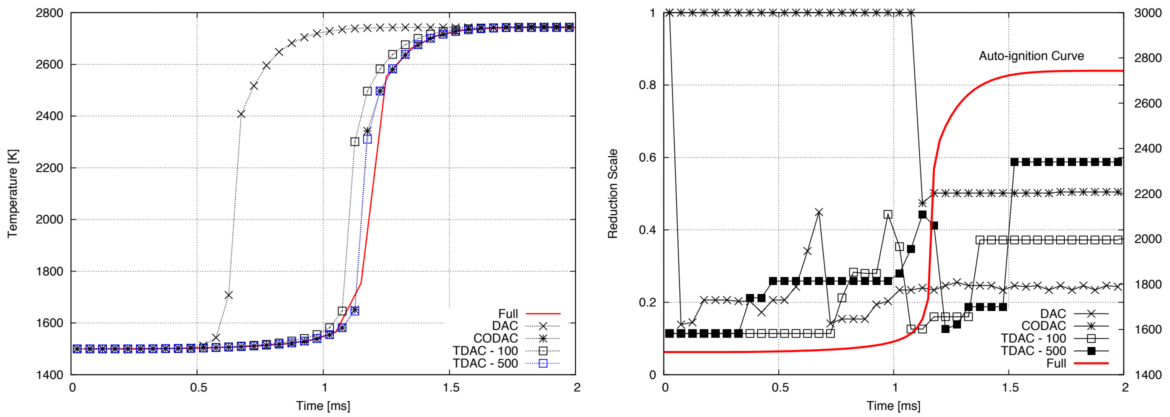

(a) Autoignition (b) Chemistry reduction autoignition

Figure 6.3: PSR - Autoignition

The evolution of the chemistry reduction factor (number of reaction active to total number of reactions) is shown in Figure 6.3b. It is observed that CODAC reduced the chemistry only when the autoignition process was completed, this is because the composition of the mixture evolves quite sharply and the correlation only fails when the auto-ignition process is completed where mass fractions in the mixture remain constant. The TDAC however, is able to both predict autoignition delay and also reduce chemistry accordingly. It can be observed that the chemistry reduction with TDAC method evolves with the chemistry as more reactions are made available during dissociation of species to produced radicles which in-turn trigger the autoignition process. The effect of the size of the table on the solution was checked by using tables with 100 and 500 divisions in scaled temperature. It is seen that the size of the table has a small effect on the solution, and leads to better predictions. The auto-ignition process occurs over a small change in both progress variable and temperature and hence to capture the exact point of ignition more points are needed in the table. The size of the table would not effect the computational time as once generated, reduced schemes can be look-up for subsequent runs.

Note: Problems that deal purely with auto-ignition of homogeneous mixtures pose a specific problem to the TDAC method. As the case is homogeneous the mixture fraction is constant hence the tabulation only happens against the progress variable. Typical evolution of the Progress Varibale (PV) is shown in Figure 6.4, the evolution has a sharp jump. This is due to the auto-ignition process being dominated by radicals which after being created trigger the ignition process. This effect of radicals is not captured by the progress variable. Hence tabulation against just the progress variable would result in very poor results, to overcome this an additional controlling variable in temperature is needed Equation 6.3. This additional variable would make sure that the actual process of the ignition is captured. A finer table in progress variable would also achieve the result but defining table intervals in temperature is more intuitive and universally works for different mixtures conditions and at various thermodynamic states.

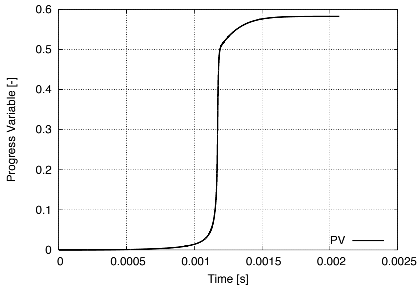

$$T_C = \frac{T - T0}{T_{E_Z} - T0}. \tag{6.3}$$

Figure 6.4: Evolution of progress variable

Here T_C is the scaled temperature T_0, is the temperature at boundary and T_{E_Z} is the equilibrium temperature at a mixture fraction Z.

6.2.2. Premixed flame

1D premixed laminar flames were computed using the GRI 3.0 [22] mechanism for methane/air mixtures at equivalence ratios that lie between the flammability limits ($\phi = 0.4$ to $\phi = 2$) .The computational domain for this case is show in Equation 5.22. Premixed mixture of air and fuel at specified equivalence ratios at 300 K and one atmosphere pressure are admitted into the domain from the left boundary. The flame is initialised by enforcing equilibrium states obtained from Cantera for the specific state of the mixture, there is a linearly interpolated region between the unburnt and the equilibrium state to have a smooth initial solution. Cases are run till convergence is observed and the flame speed (w.r.t the unburnt gas) is computed by Equation 6.4:

$$S_L = \frac{u_b - u_u}{(\rho_u/\rho_b) - 1}. \tag{6.4}$$

here S_L is the laminar flame speed, u_b and u_u are the velocities and ρ_b and ρ_u are the densities of the burnt and the unburnt mixture respectively.

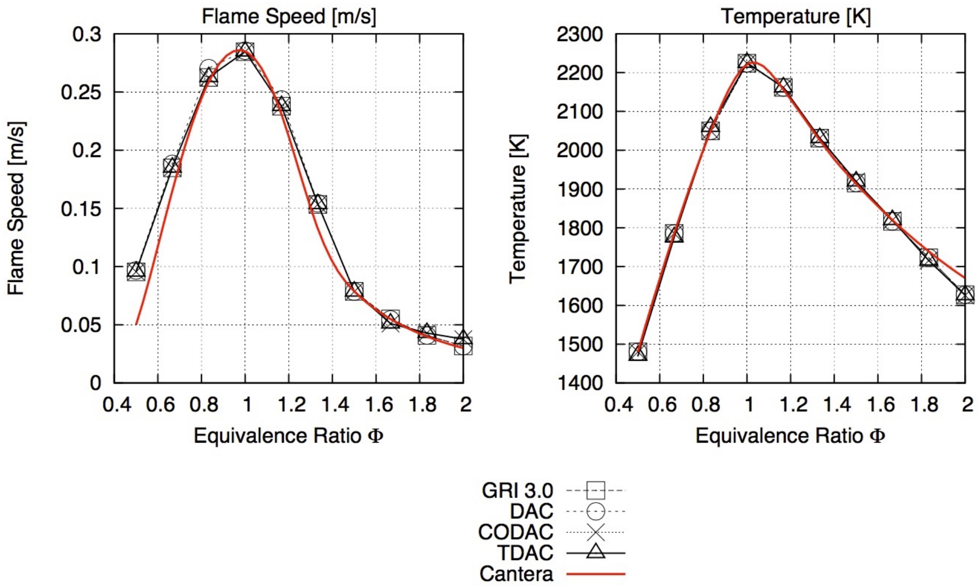

Figure 6.5: Premixed flames with DAC

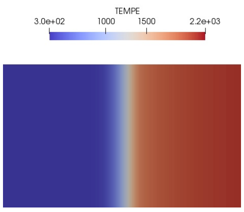

(a) Premixed flame - temperature [K]

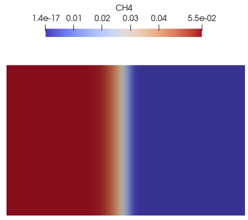

(b) Premixed flame - Y-CH_4

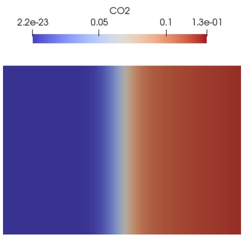

(c) Premixed flame - Y-CO_2

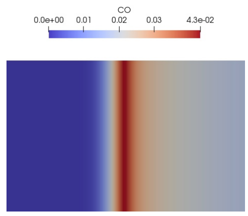

(d) Premixed flame - Y-CO

Figure 6.6: Laminar flame profile (ϕ = 1)

It is seen in Figure 6.5 that, reduced schemes predict the flame speed and the adiabatic flame temperature accurately.

6.2.3. Counter flow diffusion flame

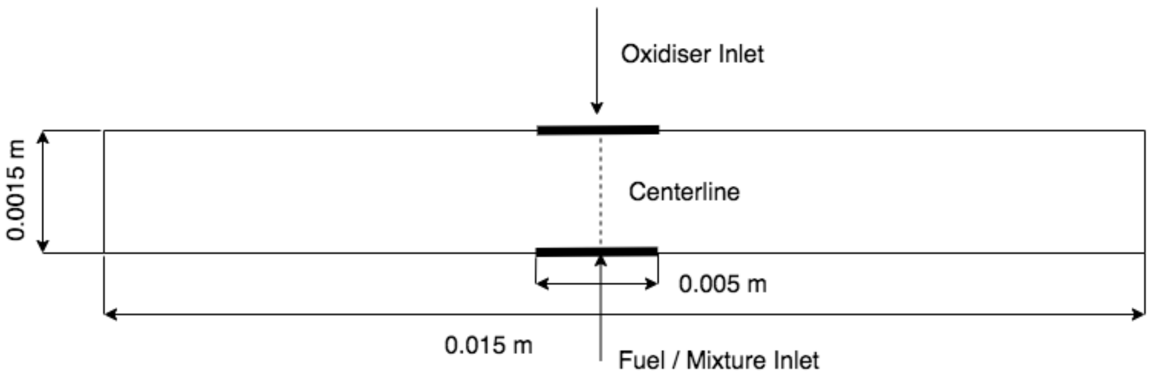

Figure 6.7: Counter diffusion flame

To evaluate DAC methodologies in strained flames a set of counter flow diffusion flames at varying strain rates are computed. The counterflow diffusion test case used in this study consists of a opposing streams of oxidiser and fuel separated by a distance, a schematic is shown in Figure 6.7. Calculations were performed at various strain rates by varying the mass flow rates of the oxidiser and fuel inlets (a similar effect can also be obtained by reducing the distance between the inlets). The oxidiser stream is fixed to the composition of air and the fuel stream to methane at 300 K and atmospheric pressure. The test flames were run using different reduction strategies (DAC, CODAC, TDAC) and were compared with solutions obtained with the full GRI 3.0 mechanism. Three strains rates were considered 200, 333.33 and 466.66 $[s^{-1}]$, respectively these correspond the low, medium and high strain respectively.

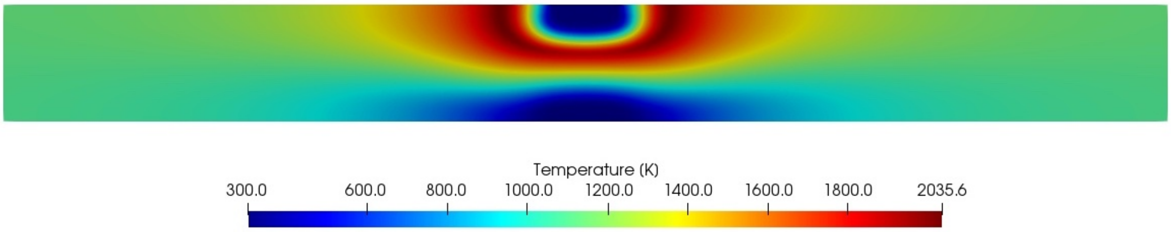

Figure 6.8: Counter diffusion flame - temperature [K]

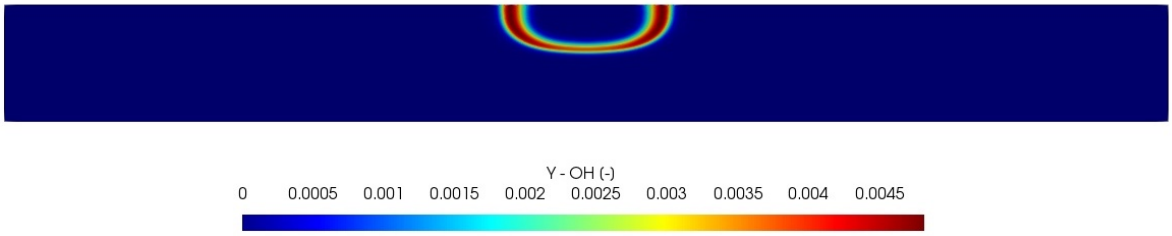

Figure 6.9: Counter diffusion flame - $Y_O H$ [-]

Figure 6.8 and Figure 6.9 show the temperature and the mass fraction of OH respectively. Here the oxidiser (Air) is admitted from the top and fuel (CH_4) from the bottom, once a pure mixing solution is obtained the mixture is ignited at the iso stichiometeric line by specifying equilibrium conditions. The results that follow are obtained at the centre line of the domain and are presented against mixture fraction (Z) computed from Bilger's formula 5.1.1.

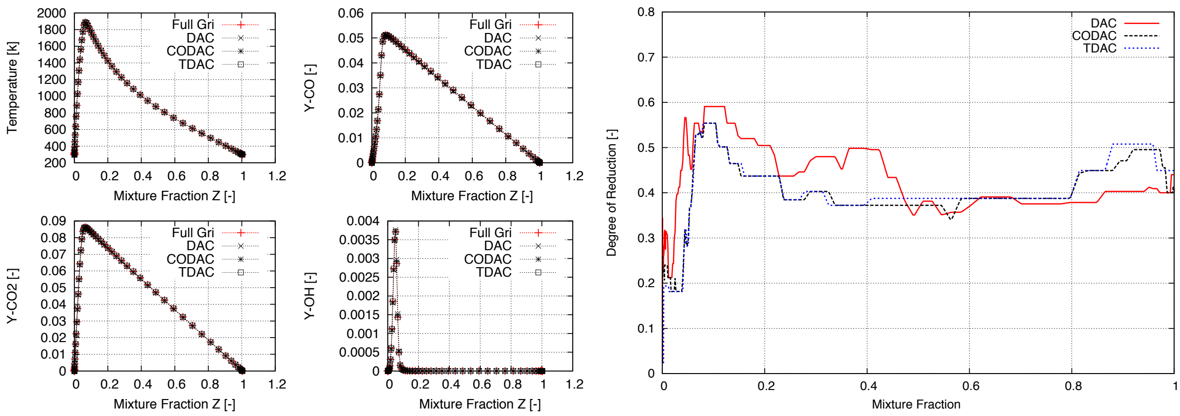

(a) Medium strain

Figure 6.10: Degree of reduction - medium strain

Figure 6.10 represents the degree of reduction which is the ratio between the number of active reactions to the total number of reactions plotted against mixture fraction along the centre line of the domain. It is seen that all methods provide more number of reactions around the stichiometeric point which for methane/air is around 0.055. Plots for the low and high strain case are shown in appendix .2.

6.2.4. Counter flow partially premixed flame

Combustion systems in practical application hardly run in one regime of combustion usually most practical combustion systems operate across multiple regimes. Partially premixed flames occurs when a flame cannot be called purely premixed or non-premixed, this could be due to a priori mixing of exhaust gases with the reactants or improper mixing of the fuel and oxidiser among other reasons. Partially premixed flames can be divided into an oxidiser-rich and an oxidiser-lean region. The reactants are partially oxidised in the oxidiser-lean region and intermediate species and remaining fuel are transported to the oxidiser-rich region where the reactions are completed this leads to a system with a double flame structure [43]. In turbulent flames, lift-off of the flame occurs due to extinction and re-ignition leading to a partially premixed mode of combustion. The applicability and complexity of partially premixed flames makes it a suitable test case to investigate the impact and evaluate the performance of the chemistry reduction methods. The computational domain and the numerical setup was same as in the case of the counter-diffusion type flame 6.7. However, in the partially premixed flame regime a priori mixing between the fuel and air is enforced. This is done by introducing a mixture at a given state into the burner rather than pure fuel. Three distinct regimes can be defined based on the equivalence ratio of the mixture introduced in such cases. For $\phi_{mix} = 1$ a stichiometeric stagnated flame is observed between the air and methane/air inlets. For $1.0 < \phi_{mix} =< 1.8$ a double flame structure is obtained, a rich premixed flame is followed by a diffusion flame. The diffusion flame is sustained by burning the products obtained after the rich premixed flame. This behaviour is observed up-to $\phi_{mix} \approx 1.8$ and for mixtures which are richer the premixed flame front extinguishes and a diffusion flame is observed, the strength of which keeps increasing with richer mixtures. In the context of reduction strategies two cases were considered - case 1 $\phi = 1.8$, and case 2 $\phi = 3.0$. These cases are of interest as they represent transition regimes between premixed flame propagation and diffusion flame regimes.

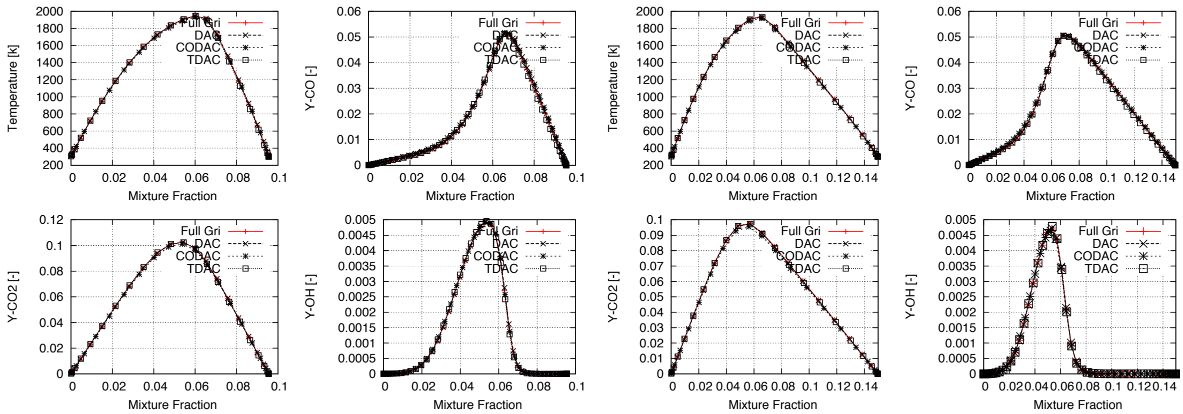

(a) Case 1 (b) Case 2

Figure 6.11: Partially premixed flame - Medium strain

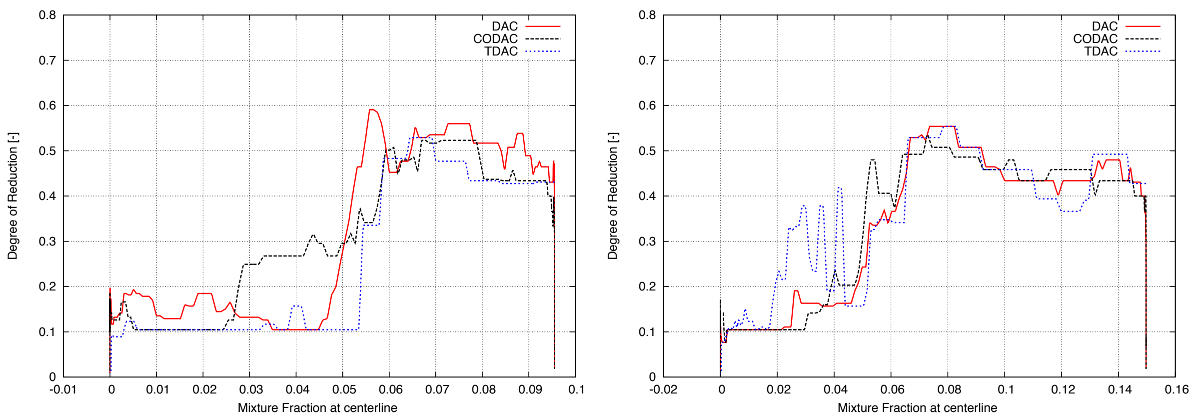

(a) Case 1 - Medium strain (b) Case 2 - Medium strain

Figure 6.12: Degree of reduction - Partially premixed flame

Figure 6.12 shows the degree of reduction along the centreline of the domain, it is seen that all methods yield higher reactions near the stichiometeric region. This is expected as the fuel is most reacting at stichiometeric conditions and the normalised threshold makes its possible to capture this.

The test cases mentioned above were steady state cases, it is seen that all the reduction methods reproduce solutions obtained from the complete detailed mechanism. Plots for the low and high strain case are shown in appendix .3. It seen that all the reduction methods perform with equal accuracy in all the steady-state cases mentioned above. To evaluate the reduction methods in constantly evolving problems, the DAC methods are applied to the following transient cases.

6.2.5. Stratified flame

A stratified flame is observed when a flame front propagates through a stratified domain, which essentially is a non-homogeneous field with fuel/oxidiser pockets. In traditional spark ignition engines fuel is admitted into the manifold and mixed with air and is then ignited with a spark, as the fuel and air are mixed throughly before the ignition the combustion is premixed in nature. Direct ignition spark ignition (DI-SI) engines are known to be more efficient as they use less fuel and can be run more leaner [33]. In such (DI-SI) engines the interval between injection of the charge and spark might be not sufficient for the charge to be homogenised. Though the average mixture is lean there could be certain pockets of rich mixtures, this leads to the spark travelling/propagating in a highly non-homogeneous field. The field can also contain mixtures beyond the flammability limits this would cause incomplete combustion and volumes with locally high concentration of oxidiser causing the combustion to occur in a partially premixed regime. Thus in a conventional IC engine or a gas turbine there can be volumes in the combustion chamber which are locally lean, stichiometeric or rich which lead to a multi-regime combustion problem. Hence solution of such flames provides useful insight into the real multi-mode combustion, furthermore this case also demands the presence of complex chemical reaction pathways to predict the multi-mode combustion.

A segregation factor is defined using Equation 6.5. The segregation factor defines the gradients between the corresponding fuel and air pockets, higher the segregation factor, steeper are the gradients between the fuel and air pockets. The random fields of mixture fraction were generated using Rogallo's procedure [46]. The code for generating the fields was used a tool, intricate details of which were not studied. Case 1 (ϕ = 0.4 - ϕ = 2.0) and Case 2 (ϕ = 0.75 - ϕ = 4) were studied at the respective conditions leading to a segregation of 1.5. The following Figure 4 show the generated initial fields. The domain is a square of side equal to $4cm$ and is divided into a gird of 256*256 points. The flame kernel was initialised with a stichiometeric mixture at equilibrium as a circle of diameter $0.4cm$ in the centre of the domain. Flame propagation is observed by computing the temporal evolution of the area of the flame kernel. The definition of the flame kernel can done in various ways, in the following study the flame kernel is defined at 75% of the stichiometeric adiabatic flame temperature. The temporal evolution of the area is then compared in solutions obtained by different reduction strategies in Figure 4.

$$S = \frac{Z_{mean}}{Z_{var}}. \tag{6.5}$$

Here Z_{mean} and Z_{var} are the mean and the variance of the mixture fraction respectively.

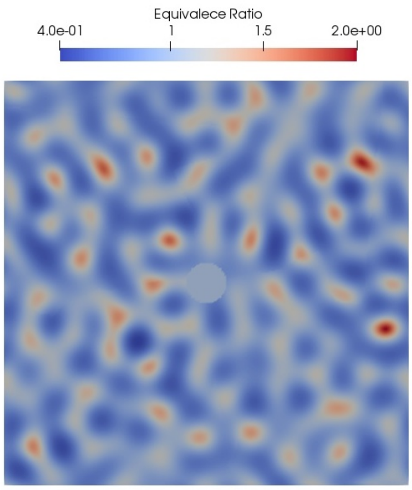

(a) Case 1 - Initial stratified field

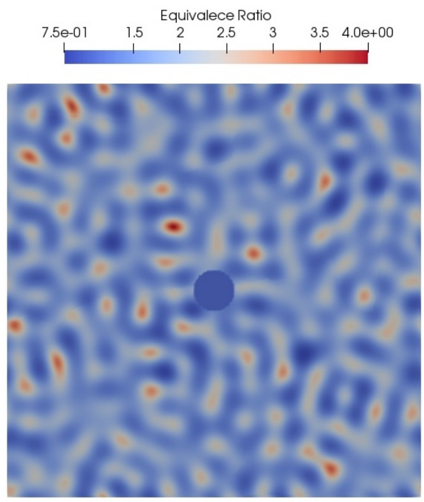

(b) Case 2 - Initial stratified field

Figure 6.13: Stratified flames

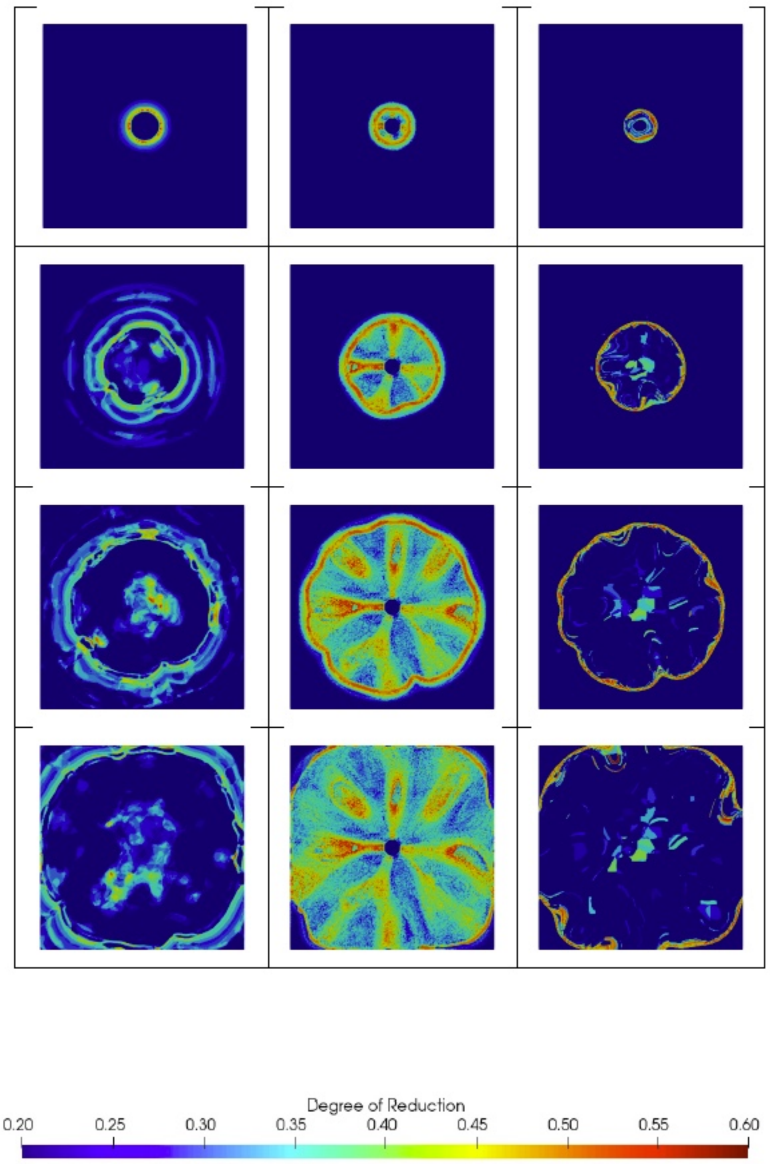

Figure 6.14: Degree of reduction - Case 1 - from left to right DAC, CODAC and TDAC

It is seen that for the lean conditions (Case 1) all the reduction strategies perform similarly, however in rich conditions (Case 2) the CODAC model fails to predict evolution of the flame kernel accurately. The CODAC method is based on the definition of an error function to determine correlation, the definition of this function effects the reduction. The error function fails to predict correlation in the rich conditions causing the CODAC method to fail, a better definition of the error function would mitigate this, but this would require the user to have a good understanding of the chemistry of the fuel and physical phenomena involved in the problem. The TDAC method, though similar to the CODAC method is based on universal definitions of physical parameters like the mixture fraction and chemical progress variable. This makes TDAC better at predictions on a wide range of combustion regimes. The degree of reduction and its temporal evolution is shown in Figure 6.14 for Case 1.

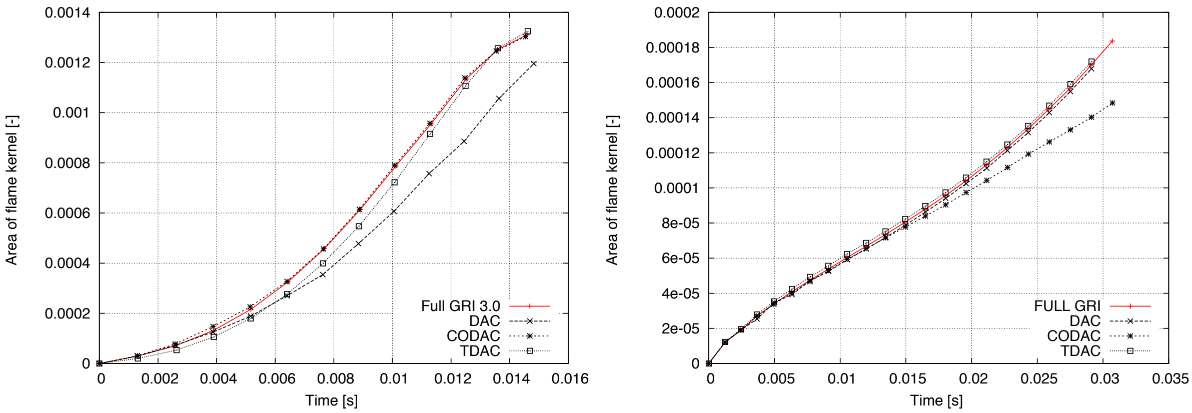

(a) Flame kernel evolution - Case 1 (b) Flame kernel evolution - Case 2

Figure 6.15: Flame kernel area

It is observed from Figure 6.14 that the DAC method, which is not aware of the chemistry of the flow and reduces the chemistry at all points in the domain deviates slightly from the reference. Changing the frequency at which the reduction is performed would lead to better predictions. Classic definition of the threshold in the PFA method which defines a threshold on a non-normalised relation matrix would cause over/under reduction is cases like this and cause the reduction methods to fail. This issue mitigated in this study by normalising the relation matrix leading to a uniform degree of reduction. The CODAC and the TDAC method are based on the chemistry and hence are able to capture the exact shape of the flame front. This makes these methods very effective as detailed mechanisms are only used at regions closer to the flame front.

6.2.6. Flame Vortex Interaction (FVI)

Vortices are present in all modes and applications of reacting flows from IC engines to gas turbines. Mixing of the fuel and oxidiser in non-premixed systems is controlled mainly by vortex motions by large scale vortices which are developed in highly sheared flows [4]. Turbulent combustion can then be perceived as a process which is dominated by extension, distortion, production and dissipation of the the flame structure by vortices of varied scales.

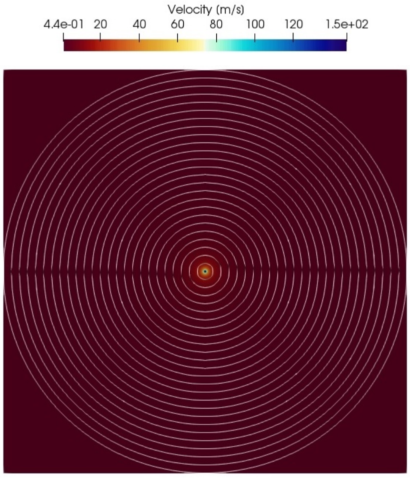

(a) FVI - Velocity streamline

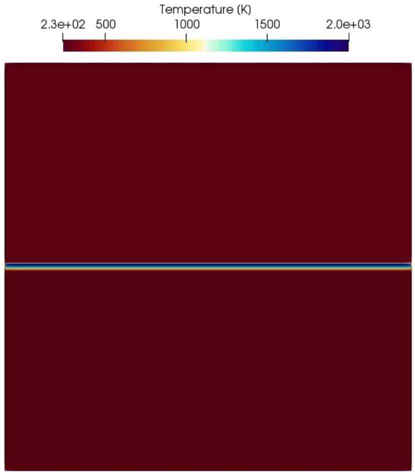

(b) FVI - initial temperature field

Figure 6.16: FVI

The aviation industry is moving towards low temperature combustion of lean mixtures, which would result in reduction in production of NO_X, CO and soot among other pollutants. The main issue with safe and efficient operations of such burners is instabilities caused due to thermo-acoustic effects. Swirling and the use or 'V' shaped gutters to create vortices to stabilise the flame come up as good options to have stable lean flame. Poinsot et.al [54] showed that most of the thermo-acoustic instabilities are driven and controlled by large vortices. The effect of flame vortex interactions through a theoretical analysis of a diffusion flame in the presence of viscous vortex core were mentioned by Marble et.al [4]. The results showed significant relations between the heat release and the fluid dynamics involved as the reaction rates are effected by the strain and cannot reach equilibrium. This case portrays fundamental combustion behaviour and is used to study transient behaviour of flames in high strain environments. Key understanding from such studies could be applied to development of burners with enhanced mixing, optimal flame shape and configuration and improved flame stabilisation. A shear layer is observed between the fuel and the oxidiser due a positive straining effect by of the vortex, the intensity of this shear layer would result in extinction and re-ignition of the flame front.

Presence of all these complex phenomena and wide range of applications for the flame vortex case made it a fundamental case where the reduction strategies are tested. The case is simplified to one viscous vortex core interacting with a diffusion flame. The computational domain is a square of side = 0.1 m, discretised by 500 and 200 points in the x and y direction respectively. The initial field is shown in Figure 6.16, a vortex core is defined in the centre of the domain using a thermo-diffusive approximation where in the purely azimuthal velocity field is given by Equation 6.6

$$V_0 = \frac{\Gamma_0}{2\pi r}\left(1 - exp\left(\frac{-r^2}{4tD_T}\right)\right). \tag{6.6}$$

Cases were run at a Peclet numbers - 20 which in context is defined in Equation 6.7.

$$Pe = \frac{\Gamma_0}{2\pi D_T}. \tag{6.7}$$

The temporal evolution of the flame vortex case is shown in Figure 6.21, visually solutions obtained from all the reduction methods were similar and hence only the evolution of reference case is shown.

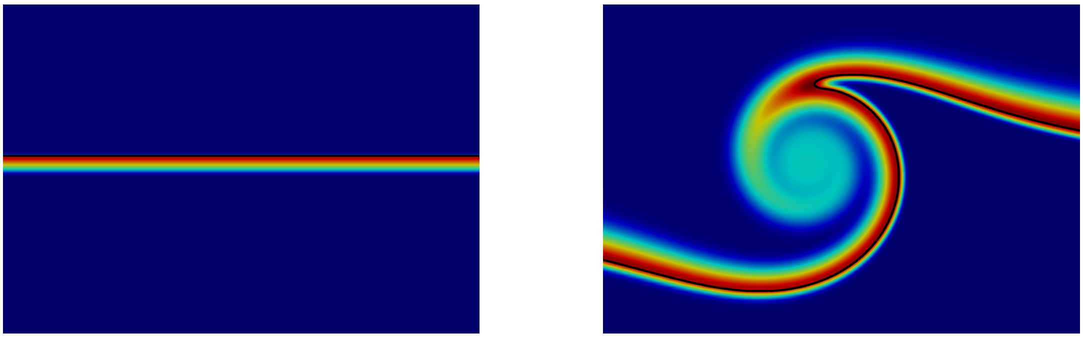

(a) T = 0.0 ms (b) T = 0.2 ms

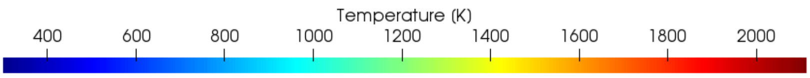

Figure 6.18: FVI - Pe 20 - Black line indicates stichiometeric mixture

The different reduction strategies are evaluated by a quantitative analysis which is defined by integrating values of scalars over iso-contour lines of constant equivalence ratio. Three equivalence ratios were chosen 0.6, 1, 2 to represent lean, stichiometeric and rich mixtures respectively.

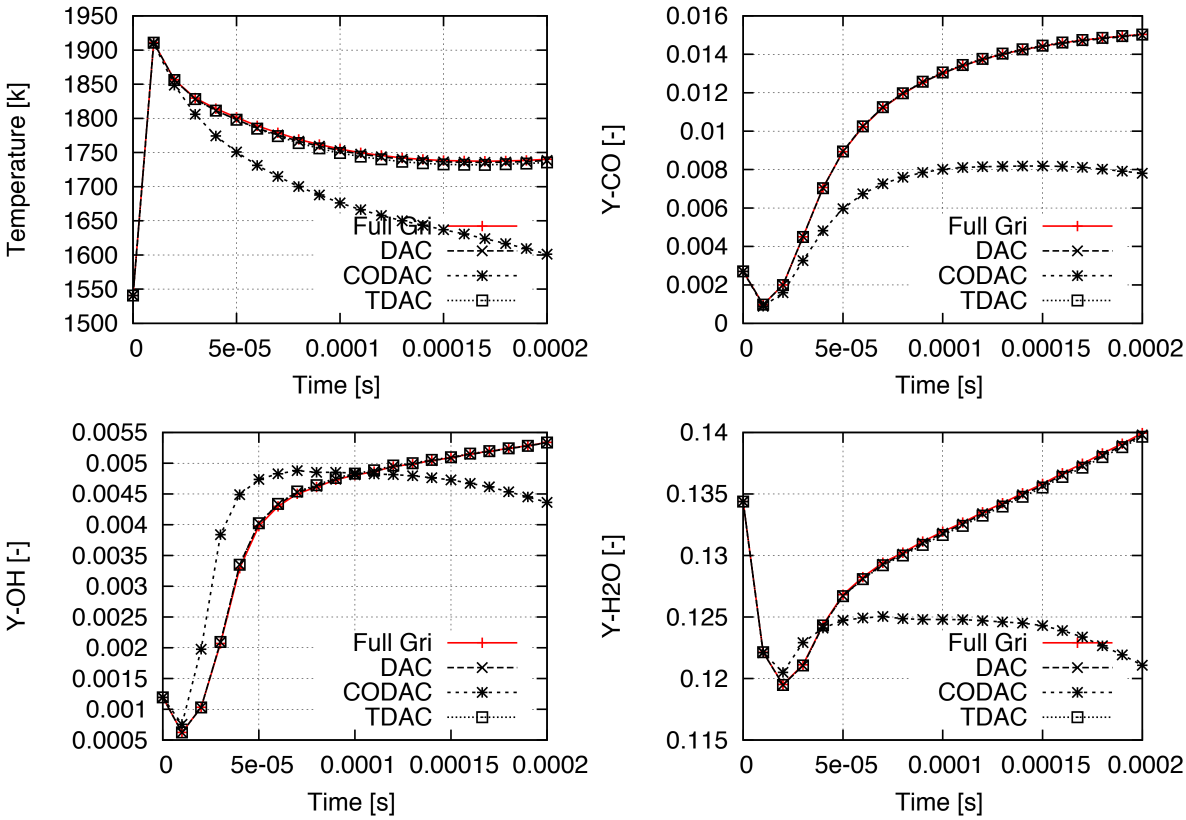

Figure 6.19: FVI - integrated scalars on iso $\phi = 1$ line

Figure 6.20: FVI - Stichiometeric line

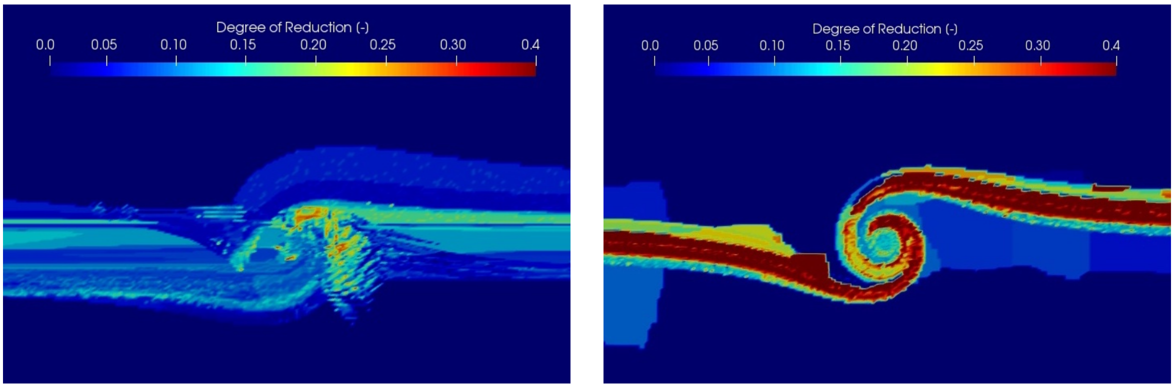

.

(a) CODAC (b) TDAC

Figure 6.21: FVI - Pe 20 - Degree of reduction

As seen in the figures above, the CODAC fails to predict the temporal evolution with the same accuracy as the other models, this is due to poor definition of the correlation error function. The current definition of the error function as given by Sun et.al [48] was derived for cases in the absence of significant strain. The error function does not have a scalar which would account for strain, adding a chemical progress variable to the definition of the error function would result in a more accurate solution from the CODAC method. Integrated scalars at lean ($\phi = 0.6$) and rich ($\phi = 2.0$) iso-equivalence ratio lines are given in the appendix .4.

6.3. Taylor Green Vortex (TGV)

A turbulent Taylor-Green Vortex case (TGV) is computed to investigate the effects and evaluate the performance of chemistry reduction techniques in a 3D turbulent flow regime. This case has been widely studied in detail to validate various solvers with detailed chemistry and to understand turbulence chemistry interactions. Turbulence chemistry interactions occur between eddies and chemical species, this interaction changes the evolution of chemistry. Fine grids used in DNS simulations capture this complex phenomenon however, to capture the same in LES or RANS simulations there are various approximations available in literature. In this study a DNS of the TGV case is computed which aims to evaluate the effect of the reduction strategies in absence of such turbulence models.

A square domain of dimension of 2π [mm], discretised by 256 points in X,Y and Z directions respectively, resulting in a mesh with approximately 16 M elements. This configuration represents a constant pressure case as all boundaries are set to open. The dimensions, grid size and length scale of the initial vortex field were obtained from [2]. The initial field for the velocity is set using the Taylor-Green vortex equations, which essentially initialise the flow with a vortices in the X-Y plane at a specified length scale Equation 6.10. As the flow evolves these vortices break and result in a decaying turbulent flow, the length scale of the initial vortex determines the kinetic energy of the system.

$$u(X,Y,Z) = U_0 \sin\left(\frac{2\pi x}{L_x}\right)\cos\left(\frac{2\pi y}{L_y}\right)\cos\left(\frac{2\pi z}{L_z}\right), \tag{6.8}$$

$$v(X,Y,Z) = -U_0 \cos\left(\frac{2\pi x}{L_x}\right)\sin\left(\frac{2\pi y}{L_y}\right)\sin\left(\frac{2\pi z}{L_z}\right), \tag{6.9}$$

$$w(X,Y,Z) = 0.0. \tag{6.10}$$

Here U_0 is the velocity at the core of the vortex, L_x, L_y,L_z are the dimensions of the domain and u,v,w are the components of the velocity. For the species, a band of fuel is set at the centre at 300 K, the rest of the domain is set to the oxidiser at 300 K. Equilibrium solutions are obtained for this mixture at constant pressure and enthalpy from Cantera. The thermodynamic state and mixtures obtained from the equilibrium solutions are then set as the initial condition. These fields are smoothed out using an hyperbolic tangent equation given by Equation 6.14 [2]

$$R_d = \sqrt{(x - 0.5L_x)^2}. \tag{6.11}$$

$$\Phi = 0.5\left[1 + tanh\left(\frac{c(R_c - R)}{R}\right)\right]. \tag{6.12}$$

$$Y_{CH_4}(x) = Y_{CH_4}(1 - \Phi). \tag{6.13}$$

$$Y_{O_2}(x) = \Phi. \tag{6.14}$$

Where R is the half-width of the central band and c is the stiffness parameter, which defines the intensity of the transition between the central band of fuel and the surrounding oxidiser.

The initial solution on the X centreline is shown in Figure 6.22

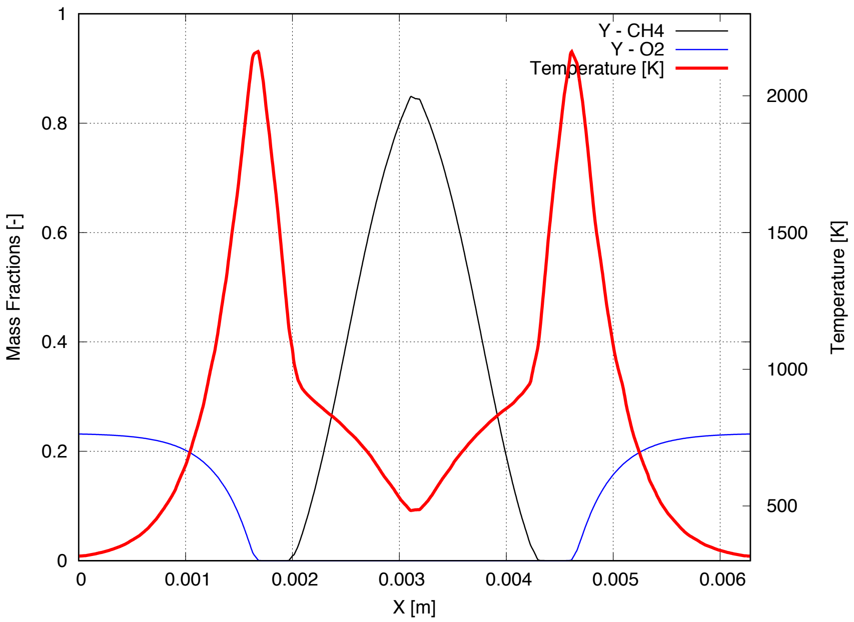

Figure 6.22: Initial Solution at X centerline

Figures 6.24 show the temporal evolution of the TGV problem, the vortices stretch the initial flame front which results in a mixing layer between the fresh gases and products. The central band is composed of pure fuel and hence no reactions can take place until there is sufficient mixing between the fuel central band and the surrounding oxidiser. Once the fuel and oxidiser are mixed combustion takes place and products are formed. The case is transient and once the all the fuel gets burnt the reactions stop this however, would need the simulation to be run for a longer time. Cases were run on 2400 processors for a period of 48 hours to advance around 2.5 ms in physical time. This time is considered appropriate as most phenomenon of interest like turbulence, mixing, autoignition take place during this time. Turbulence decays over time and so does the intensity of mixing, hence running the case longer would not have resulted in more data of interest.

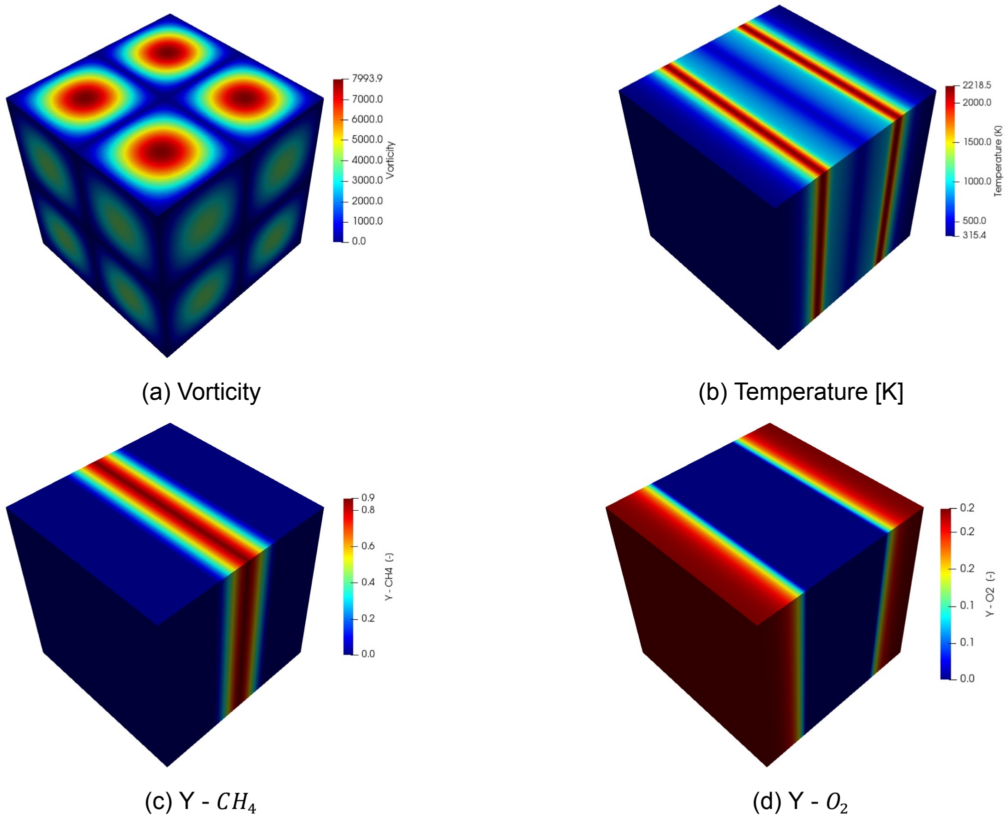

(a) Vorticity

(b) Temperature [K]

(c) Y - CH_4

(d) Y - O_2

Figure 6.23: TGV initial field

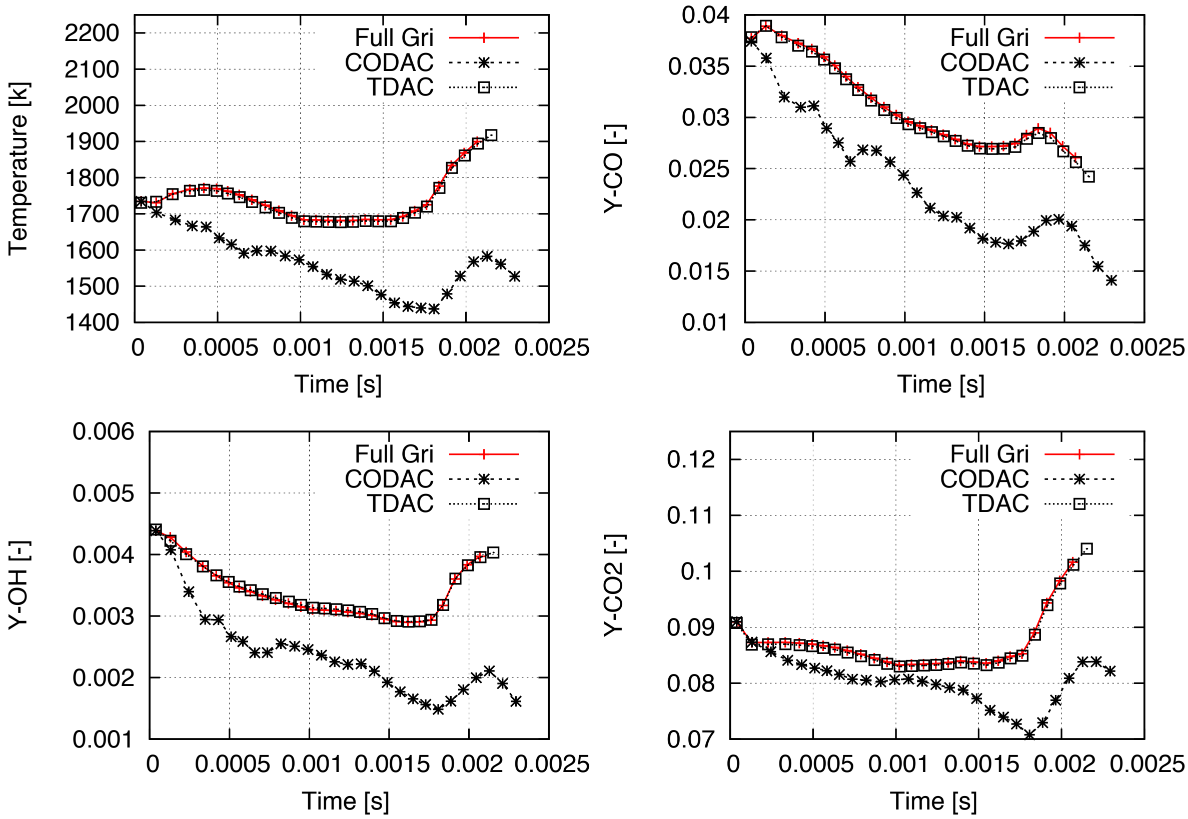

Figure 6.25: TGV - Temporal evolution of scalars on iso $\phi = 1$ line

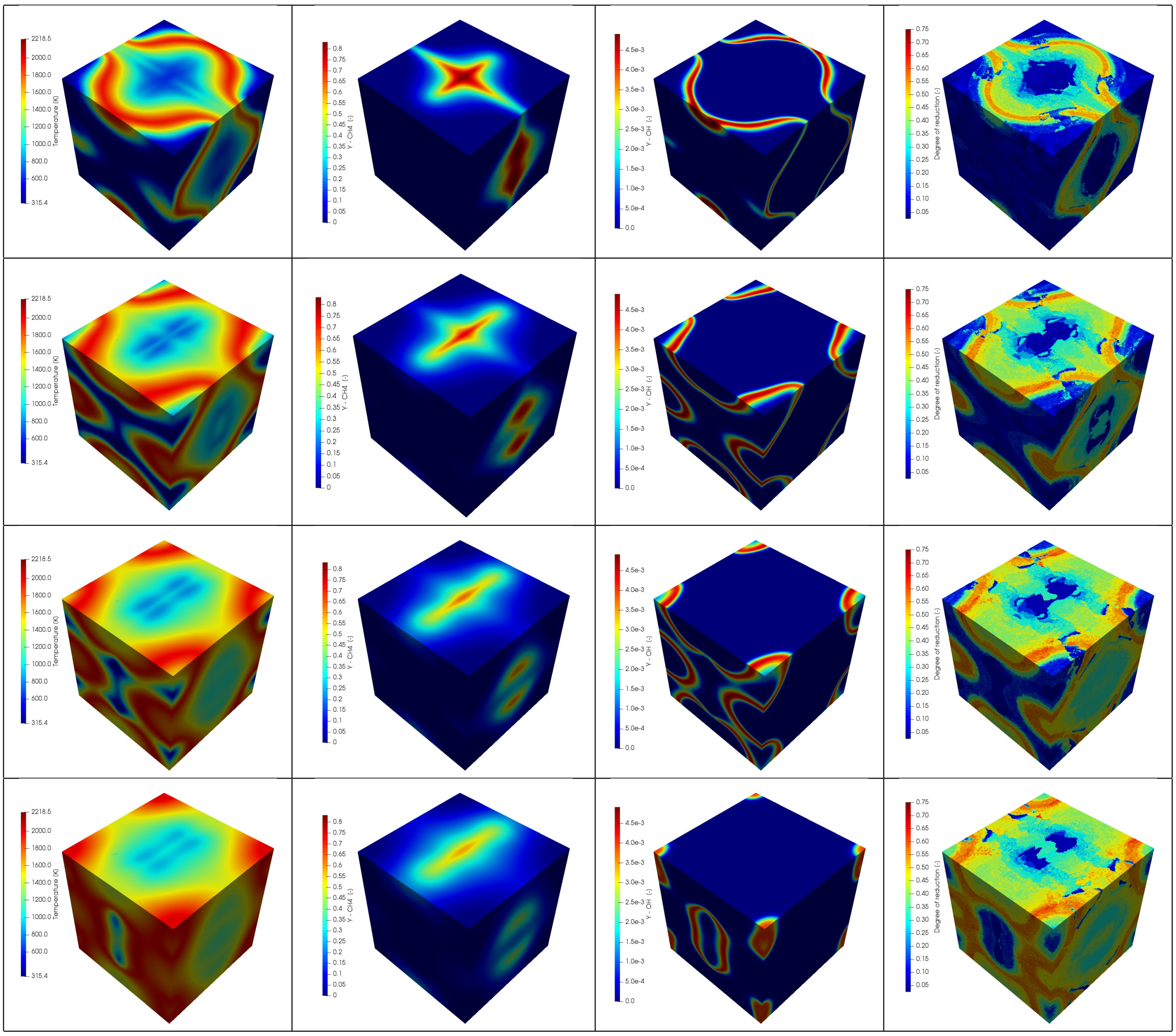

Figure 6.24: TGV case temporal evolution at 0.5, 1, 1.5 and 2 ms respectively and is represented by the rows , - from left to right temperature [K], Y - CH_4, Y - OH, Degree of reduction (TDAC)

It can be observed from Figure 6.24 the TDAC method follows the flame kernel evolution and reduces chemistry accordingly, in the last steps most the domain is mixed and reactions take place through out the domain, hence the degree of reduction is not significant. This is hardly the case in a practical flame where the reactions are limited to a thin zone and most the domain is not reacting.

To get a more quantitative analysis of the performance and accuracy of the reduction strategies scalars were integrated on lean, stichiometeric and rich iso-contours of the mixture fraction. This quantity would represent how the scalars evolve over time through the various reduction methods. The integration procedure can hide some differences as the quantities are essentially averages, to get more data the profiles of the flames are compared at various time steps. Finally, to understand the effect of the reduction methods on the heat release, the flame propagation velocity is compared among the various methods. These quantities should provide insight on the mechanism and the performance of the reduction methods.

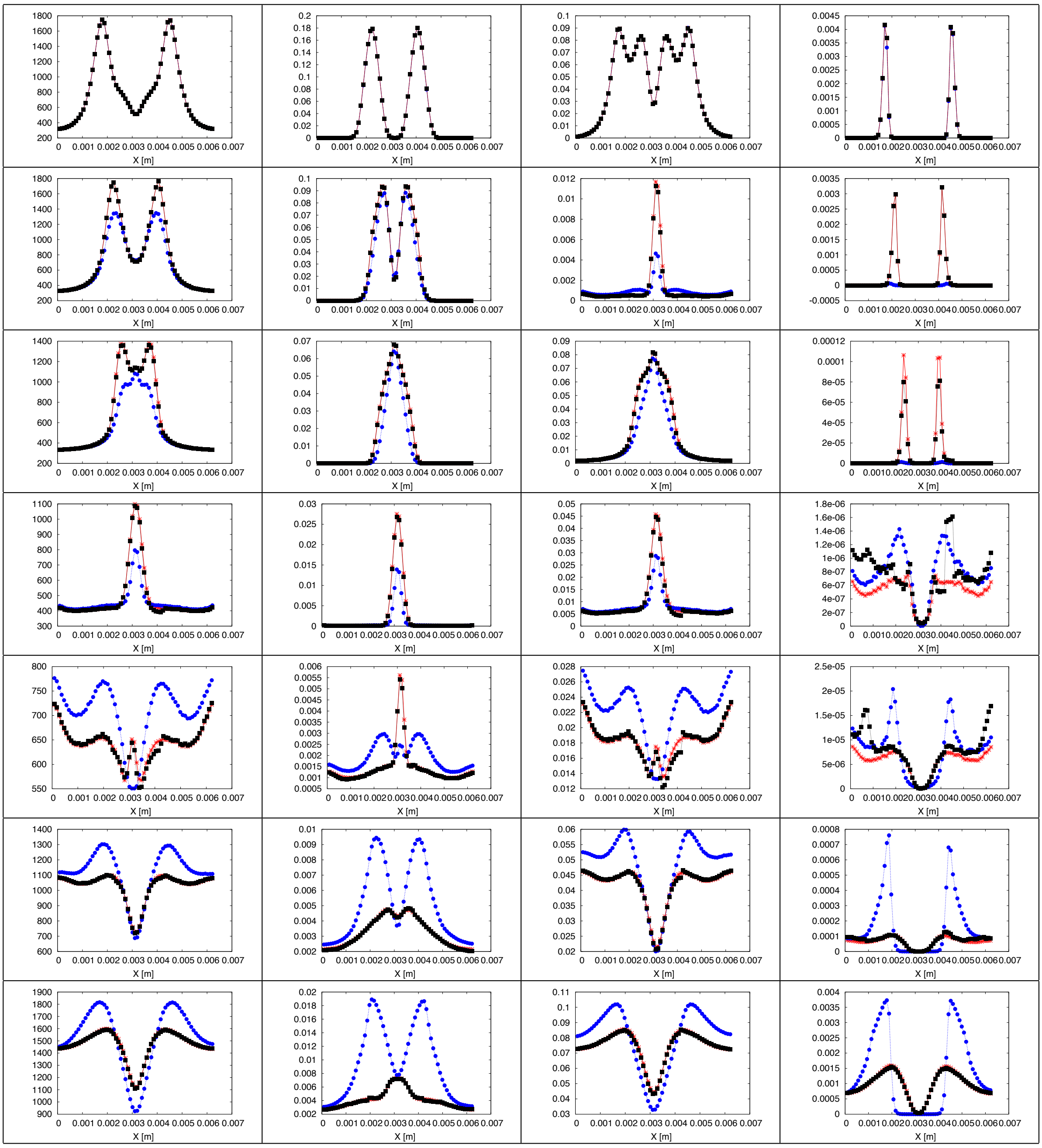

Figure 6.27: TGV case evolution at 0.28, 0.57, 0.85, 1.14, 1.42, 1.71 and 2 ms respectively and is represented by the rows - From left to right temperature [K], Y - CO_4, Y - OH, Y - CO, red - reference, blue - CODAC, black - TDAC

The propagation of the flame front is computed by defining a chemical progress variable using Equation 6.2. Spatial gradient of the progress variable is computed and an iso-contour of the gradient is obtained. The iso-value of the contour can be arbitrary as this is just used to define a propagating surface, the average shift/displacement of the surface is computed by taking an integral over the surface with respect to a predefined reference surface. Figure 6.28 shows the average speed of the iso-surface in time obtained with the TDAC and the CODAC reduction strategy. The propagation velocity is a function of the heat release which in turn is a function of the chemical reactions. As seen in Figure 6.28 that TDAC predicts the propagation speed accurately, the CODAC method however, follows the trend closely but does not show the accuracy as obtained from TDAC method.

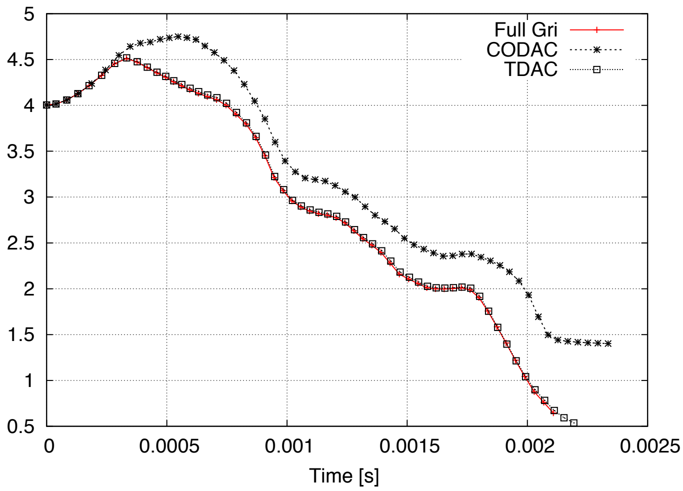

Figure 6.28: Flame propagation velocity

Plotting the scalars - temperature and mass fractions of CO, CO_2 and OH at the X centreline of the domain gives a more quantitative analysis of the solution obtained and the effect of the reduction strategy on it. OH is a very fast reacting radical and hence is more difficult to capture as seen in Figure 6.27. All the reduction methods show some degree of deviation from the actual solution. The deviation is more pronounced in the CODAC rather than the TDAC method, showing that the error function defined in CODAC fails to capture the evolution of OH.

To mitigate this OH could be added into the list of the correlation species definition for CODAC but as mentioned earlier that OH evolves rapidly the error function would fail more often leading to higher frequency of chemistry reduction making the CODAC method more expensive. Integrated scalars at lean ($\phi = 0.6$) and rich ($\phi = 2.0$) iso-equivalence ratio lines are given in the appendix .5.

6.4. High Performance Computing (HPC)

The current work is focussed on implementing a finite rate solver with state of the art dynamic reduction methods in Alya. Alya is optimised to run in massively parallel computing systems hence it is relevant to evaluate the performance of the code in the HPC framework. The following section presents data/results of the computational performance of the finite rate implementation.

6.4.1. Parallel scaling

Parallel scaling is an important parameter to be considered when developing applications optimised for HPC environments. An ideal scaling would be when the computational time reduces by the same factor as the increase in the number of processors. Scaling for the finite rate solver was evaluated in a swirling turbulent premixed case with 54 million cells solved with 2 step chemistry. The following scalability was observed 6.29

As seen in Figure 6.29 ideal scaling is observed until the case is run on 3840 cores where the actual curve slightly deviates from the ideal. This deviation is due the low number of fluid sub-domains per processor which reduces the impact of parellisation due to the increase in MPI communication among nodes. This could be mitigated by using the appropriate number of processor or by having a node shared memory to avoid this type of communication. Having said this the MPI internode communication is very efficient especially on newer processors and rarely forms the bottle neck in the computation process. The bottle-necks mainly comes due the highly non-uniform loads on the processors in the chemistry integration step. The local thermodynamic state has a huge impact on time taken to integrate chemical sources, this causes a high load imbalance in the processor where in some processors are idle and are waiting for other processors to complete their computation. Dynamic load balancing (DLB) can be used to make sure that the idle time of a processor is reduced by sharing the computational load equally among all the processors present. Load imbalance can be visualised by a trace of the process shown in Figure 6.30 which shows the operation being with respect to time. The trace was obtained using HPC toolkit which provides an integrated set of tools like the trace computing and viewer which

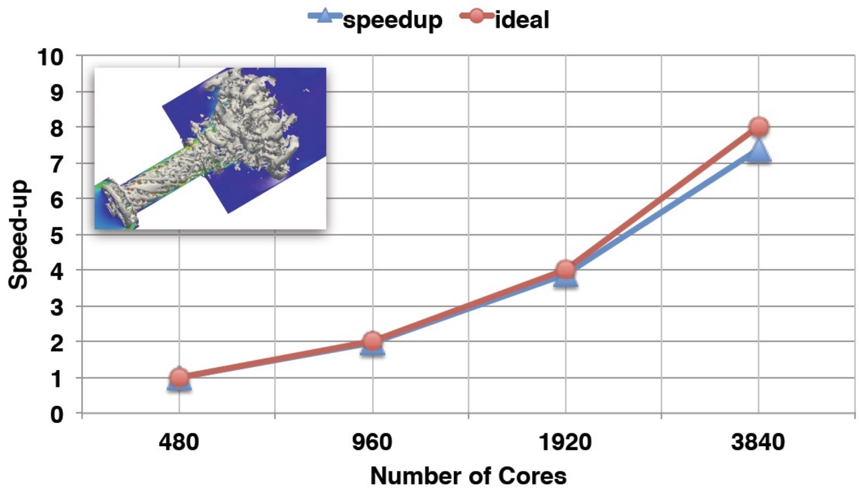

Figure 6.29: Parallel scaling of the finite rate solver

can be use to characterise a program on cluster systems.

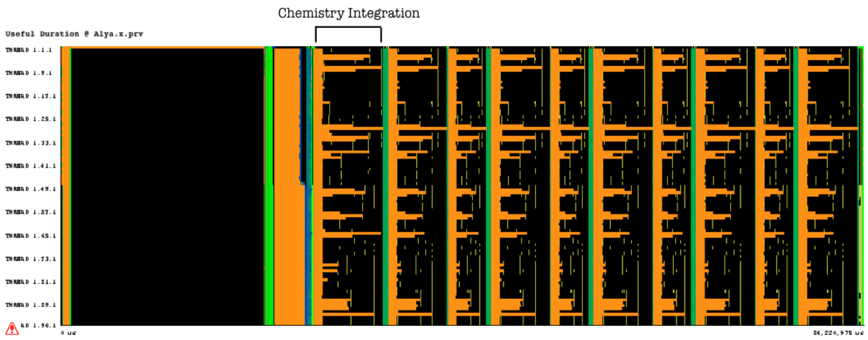

Figure 6.30: Trace - Finite rate chemistry

Each horizontal bar in Figure 6.30 represents a processor and on the x axis is the time take by a specific operation. The coloured sections in this case represent useful duration. The useful duration is defined as the time when the MPI's are executing a task. Each strip represents one time-step in the computation, time taken by the integration of the source terms can be seen as the highly non-uniform section between the strips. Significant part of the computational time is spent waiting for other processors to complete the task. The computational performance of such systems can be vastly improved by introducing dynamic load balancing (DLB) algorithms. A DLB algorithm would redistribute resources in run-time to ensure that the time spent by an processor between

Transport of the scalars, integration of the chemical source term and reducing the chemistry using PFA were identified to be most computationally expensive process. Since the reduction is based on eliminating reactions and not the number of species, the reduction strategy will have no effect on the transport step, and hence will not be shown.

6.5. Computational performance

The accuracy of the reduction strategies were discussed in 6.2, the following section presents an analysis of the computational cost of the reduction methods. The cost was obtained by using the intrinsic Fortran function called CPU_TIME, two instances of the function are called before and after the target function and the computational time is obtained as the difference between them averaged over the run of the entire simulation. Key procedures in any low Mach reacting flow simulation would include solution of Navier-Stokes, enthalpy equations and the chemistry. Computational costs were computed in the turbulent TGV case which represents most phenomenon found in practical simulations. Costs were computed on a TGV case discretised with 32 points in x,y and z directions respectively. The following table Table 6.1 shows the performance.

Table 6.1: Cpu cost analysis on the TGV case (32^3)

CASE	Total	Chemistry/Total	Integration/Total	PFA/Total	PFA/Chemistry	PFA/Integration
Full	1.0	0.512	0.44160	-	-	-
DAC	1.27	0.746	0.398	0.221	0.375	0.706
CODAC	1.08	0.55	0.397	0.075	0.15	0.207
TDAC - Unfilled	0.832	0.411	0.3036	0.0316	0.0663	0.086
TDAC -Filled	0.678	0.4474	0.2983	8.13e-05	0.000122	0.000183

Total - Total CPU cost (Navier-stokes + enthalpy + chemistry).

Chemistry - Chemistry cost (Integration + transport + reduction).

Integration - Chemistry integration.

PFA - Chemistry reduction through PFA.

To have a clear outlook and be able to draw relevant conclusions all computational times are normalised with respect to the total time obtained by the reference full GRI 3.0 case. It was mentioned earlier in section 6.1.1 that DAC method represents the upper threshold for the degree of reduction that can be achieved, this reduction however comes at a very high cost for reduction. For the DAC method PFA takes about 22 % of the total CPU cost, making the DAC method more expensive than the reference case. Results show that the ratio between the cost of integration and the total cost is least for the TDAC method, this is expected as expensive process of reduction is tabulated.

The CODAC method is more efficient that the DAC method in terms of the reduction. The cost of reduction is around 7 % of the total time, this is due to the localisation of the reduction, which is defined by the error function. Better and more suited definition of the error function would lead to improved performance, moreover due to the transient nature of the case the reaction zone is always evolving. This means the correlation between points in time is often not possible forcing the CODAC method to reduced chemistry more often. The cost of TDAC is computed in two instances, (1) starting from an empty table and, (2) when the table is almost filled with the reduced schemes. The cost of PFA in the TDAC methods reduces steadily as the simulation progress, this happens until the table is filled with reduced schemes that can obtained for all possible thermodynamic states. Once the table is filled the cost of PFA is reduced to the cost of look-up which is trivial compared to the actual reduction process. In terms of the overall computational cost TDAC is found to be around 17 % faster than the reference case when the cost of filling up the table is taken into account. This cost then drops by around 32 % of the reference case when the table is relatively filled with the reduced schemes. This improvement in computational cost comes at a very minute or no compromise in accuracy as seen in section 6.2.

7

Conclusions and Recommendations

The following chapter draws and summarises relevant conclusions obtained through the study and presents answers to the research questions mentioned in section 2.6

7.1. Conclusions

- A quantitative analysis of the accuracy, performance and computational costs of the DRGEP [20] and the PFA [49] chemistry reduction methods is performed. The PFA method is more expensive as it takes into account simultaneously occurring multiple generation reaction pathways, this is not present in the DRGEP method. The cost of reduction through PFA was found to be on average 20 % higher than the DRGEP method for both the tested fuels. The accuracy of the method was compared through an example of an autoignition delay case for N-heptane, where in the PFA method with fewer species was able to predict the complex NTC region. The DRGEP method however, was not able to capture this region even with more number of species. Methane is a simple fuel and the reaction mechanism (GRI 3.0 [22]) is absent of complex simultaneously occurring pathways, hence PFA and DRGEP produce similar reduced schemes. To have a more robust implementation of the reduction PFA was chosen as the method for reduction due to its accuracy which comes at a small increase in the computational cost.

- A threshold applied to the relation matrix obtained from the reduction method is normalised with respect to the local maximum value. The normalisation makes the definition of the threshold applicable to all combustion regimes and levels of chemical reactivity. This prevents under/over reduction of chemistry as the level of reduction is always scaled.

- The CODAC method relies completely on the definition of the correlation function which has to be representative of the considered case. This adds an aspect of ad-hoc tuning to the reduction procedure. Moreover, to capture radicals and fast reacting/moving species the correlation function must include these species, this would make the reductions more frequent and lead to higher computational costs.

- As the reduction only depends on the thermodynamic state of the mixture, similar mixtures would yield the same reduced scheme. This means that if the mixture can be represented by a low dimensional manifold, reduced schemes can be tabulated against the manifold. The expensive process of reduction is then reduced to linear look-up for the reduced scheme based on the manifold, the cost which is negligible as compared to the reduction, this forms basis of the TDAC reduction strategy.

- The controlling variable or the manifold was chosen to be mixture fraction (from Bilger's definition) and a chemical progress variable shown Equation 6.2. These variables were shown to represent the thermodynamic state in all of the combustion regimes the method was tested in. In pure homogeneous auto-ignition delay problems the mixture fraction is fixed so the tabulation needs to be done only against the progress variable. This raises an issue as the auto-ignition process happens over a very short time and the change in the progress variable is step-like. To capture this region an additional variable in temperature is defined 6.3. The scaled temperature takes into account the rapid changes in the auto-ignition zone and captures the process accurately.

- Mixtures close to stichiometery are more sensitive to the degree of reduction, thus the distribution of the table should be finer in this region to ensure that this behaviour is well captured. Linear distributions would lead to sparse tabulation around sitchiometery reducing the accuracy of the method.

- Solutions obtained from the TDAC method were compared in static problems like laminar premixed, counter diffusion and partially premixed flames. TDAC was also tested in transient cases like homogeneous auto-ignition, stratified flame propagation and a flame vortex interaction problem. Finally a 3D turbulent TGV case was computed to evaluate effect of turbulence on the reduction method. These analyses provide fundamental understanding of the reduction method in absence of sub-grid models which could smooth out the effect of the reduction procedure. These problems represent all possible combustion regimes that can be encountered in practical combustion problems. Validating the reduction method in all these test cases suggests that the model would have similar performance in any multi-regime problem that it is applied to.

- The TDAC method was compared with the same PFA threshold against DAC and CODAC which are considered state of the art reduction methods. It is to be mentioned that the definition of the correlation function for CODAC was adapted from literature, this function was formulated for a laminar non-premixed case. For better results with the CODAC method, knowledge of the chemistry of the problem can be used to define the error function, but this is not discussed in the context of this study. TDAC replicated the results of the full GRI 3.0 in all the steady and the unsteady cases. CODAC however, performed well in static cases but failed in some of the non-homogeneous transient cases this is due to the poor definition of the error function.

- The computational costs of the reduction strategies were compared in 6.5, its was found that the TDAC method was 33 % faster than the reference case without any reduction. The cost of chemistry reduction reduces as the solution progress and the table is filled with reduced schemes. Once most of the table is filled the expensive process of chemistry reduction is reduced to look-up of schemes.

In conclusion a new strategy for dynamic adaptive chemistry was proposed (TDAC) , formulated and evaluated for performance and accuracy. It was found the tabulating reduced mechanisms on-the-fly against controlling variables proved to be good strategy to mitigate the expensive process of chemistry reduction. TDAC was found to be around 33 % faster than the reference solution, this speed up was achieved while maintaining accuracy.

7.2. Recommendations

The following section outlines scope for future studies

- Cantera uses a pure implicit solver which solves the system of stiff equations using an implicit Euler backward differentiation(BDF) for time marching and a Newton solver for the non-linear problem. The Newton solver computes a Jacobian and this is treated by default as dense. This is done to make sure that the integration of the chemical sources is robust and any arbitrary time-step should yield physical results. Reduction in this study is done by reducing the number of reactions this would not change the size of the Jacobian as the size depends on the number of species, which are constant. However, the reduction method reduces the overall stiffness of the system, a reduced mechanism would lead to a less dense Jacobian but since the Jacobian is always treated as dense the effect of reduction is not strictly proportional to the number of reactions. The effect of the reduction could be increased by using a semi-implicit solver which would treat the Jacobian to be sparse. ODEPIM a semi-implicit solver was found to be 40 times faster than the pure implicit solver used in Cantera [56]. The only sacrifice would be in-terms of the robustness of the solver as large time-steps could lead to unphysical solutions hence care must be taken to limit the time-step size when using a semi-implicit solver.

- The effect of static *a priori* chemistry reduction on complex fuels like N-heptane were studied. The study did not consider N-heptane as a test fuel to validate the DAC implementations, this was due to time and CPU limitations. Further studies can be done with complex fuels like N-heptane and N-Dodecane to check the accuracy of the DAC methods. Changes would have to be made in the CODAC implementation as the error function is specific to the case and the fuel. Conversely, the TDAC method which is based on global parameters could be used without any changes.
- As mentioned earlier, that the reduction is done in terms of the number of reactions and not species, turning-off all reactions involving a particular species would mean that the chemistry of the particular species is considered frozen. This would open the possibility of reducing the cost of the transport step of the solver. The transport of the species forms the second major expense in finite rate simulations and this can be reduced by lumping/grouping frozen species and transporting them together. This would reduce the number of transport equations that are to be solved and result in higher efficiency.
- The time taken for the integration of the chemical source terms is strongly dependent on the state of the mixture, this leads to a load imbalance in the computation shown in Figure 6.30. This means that certain processors spend a significant amount of time idle waiting for other processors to complete the task. Hence Dynamic Load Balance (DLB) techniques could be implemented to share computational resources to increase the overall computational efficiency.
- It can be concluded that mixture fraction in addition to a chemical progress variable are able to represent the thermodynamic state of the mixture. The tabulation strategy can be extended to include the integrated chemical sources of minor species which are tabulated based on canonical flame configurations. The most common choice is the 1D laminar premixed flame where in the minor species can be tabulated based on the controlling variables. Similar approaches were presented in [45], this was however, done in context of using the flamelet model for combustion. Extension of this to the finite rate model with the TDAC reduction should result in substantial reduction in the computational costs.

8

Appendix

.1. Methane reduced schemes

Refer section 5.1.1

Number of Species	Species
31	CH2(S), CH3OH, HCNN, CH2O, CO, N2, CH3O, H2O2, NNH, O2, CH2, CH3, CH4, HO2, CH, N2O, H, O, N, CH2OH, C2H6, CH3CHO, C2H4, HCN, HCO, CO2, OH, H2, NO, H2O, C2H5
19	CO, H2O2, OH, H2, CH2(S), H2O, O, CH3OH, C2H6, CH2, CH3, HO2, H, CH2O, CH4, N2, CH3O, O2
14	CO2, OH, H2, CH2(S), H2O, O, CH2, CH3, HO2, H, CH2O, CH4, N2, O2

.2. Opposite counter flow diffusion

Refer section 5.1.1

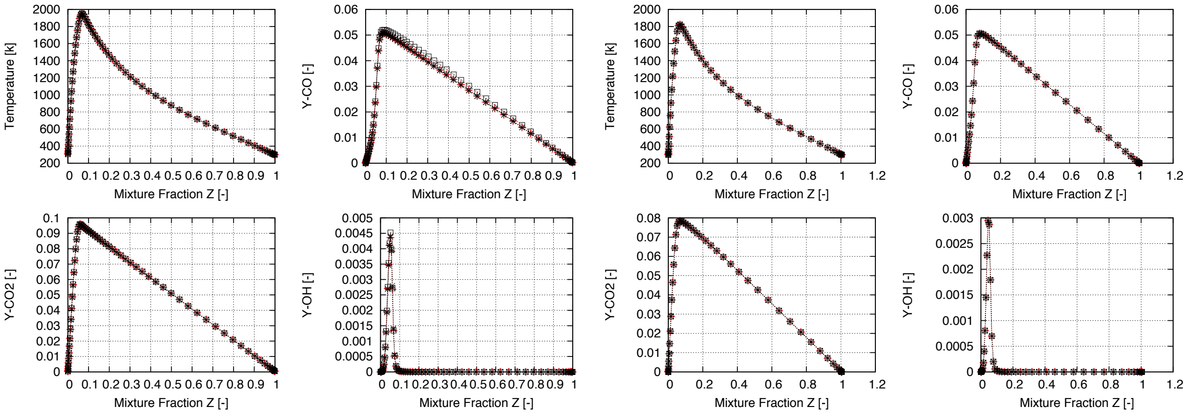

(a) Low strain (b) High strain

Figure 1: Diffusion flames

.3. Opposite counter flow partially premixed flames

Refer section 6.2.4

.3.1. case 1

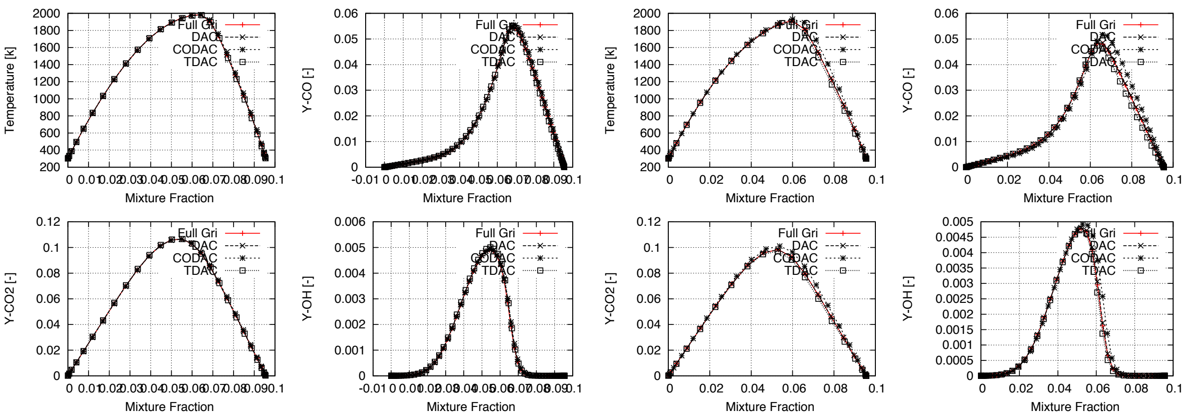

(a) Case 1 - Low strain (b) Case 1 - High strain

Figure 2: Partially premixed flames - case 1

.3.2. case 2

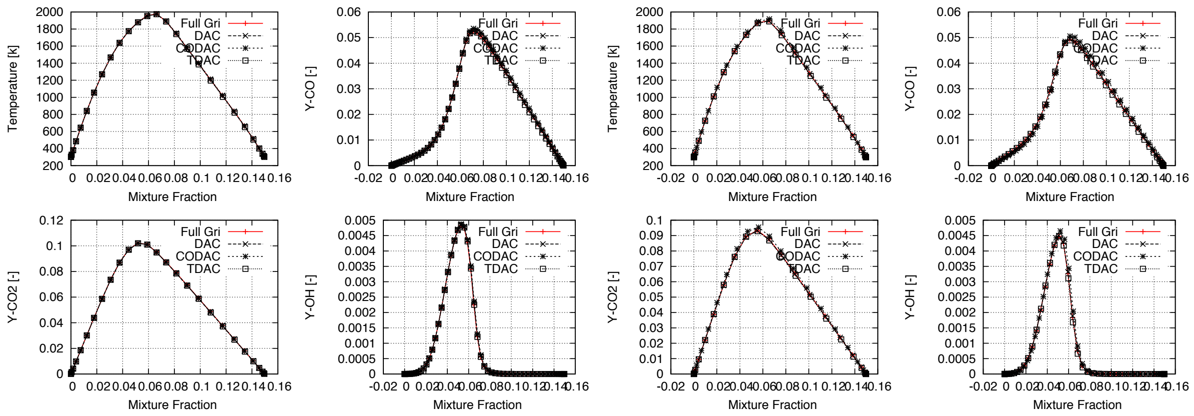

(a) Case 2 - Low strain (b) Case 2 - High strain

Figure 3: Partially premixed flames - case 1

.4. Flame Vortex Interaction (FVI)

Refer section 6.3

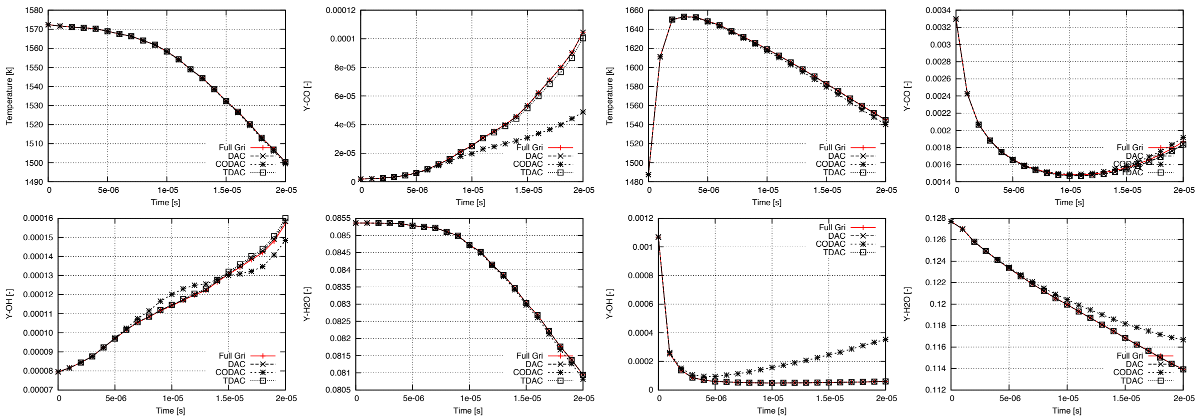

(a) FVI - integrated scalars on iso $\phi = 0.6$ line (b) FVI - integrated scalars on iso $\phi = 2$ line

Figure 4: Flame Vortex Interaction (FVI)

.5. Taylor Green Vortex (TGV)

Refer section 6.3

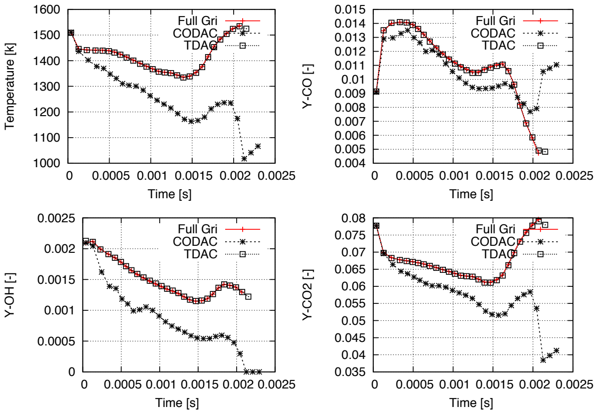

(a) TGV - integrated scalars on iso $\phi = 0.6$ line

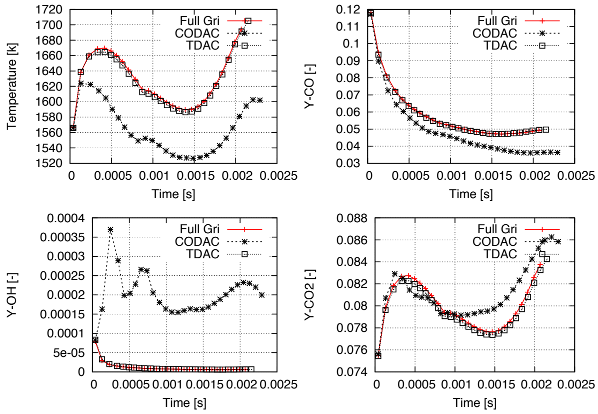

(b) TGV - integrated scalars on iso $\phi = 2$ line

Figure 5: TGV - Taylor-Green Vortex

Bibliography

[1] United nations framework convention on climate change.

[2] Ghislain Lartigueb Matthias Ihmed Jacqueline H. Chene B. Cuenotf Dominique Thevenina Abouelmagd Abdelsamiea, c. Mini-symposium on verifcation and validation of combustion dns. *17th Int. Conference on Numerical Combustion, Aachen, Germany*.

[3] International Energy Agency. Iea - annual report, 1999. URL `https://www.iea.org/tcp/`.

[4] M Alain and Sebastien M Candel. A numerical analysis of a diffusion flame-vortex interaction. *Combustion science and technology*, 60(1-3):79–96, 1988.

[5] Jian An, Guoqiang He, Fei Qin, Xianggeng Wei, and Bing Liu. Dynamic adaptive chemistry with mechanisms tabulation and in situ adaptive tabulation (isat) for computationally efficient modeling of turbulent combustion. *Combustion and Flame*, 206:467–475, 2019.

[6] RW Bilger. The structure of diffusion flames. *Combustion Science and Technology*, 13(1-6):155–170, 1976.

[7] A Both, O Lehmkuhl, and D Mira. Low-dissipation finite element strategy for low mach number reacting flows. *Computers & Fluids*, 2019 (under review).

[8] Claudio Bruno, Vaidyanathan Sankaran, Hemanth Kolla, and Jacqueline H Chen. Impact of multicomponent diffusion in turbulent combustion using direct numerical simulations. *Combustion and Flame*, 162(11):4313–4330, 2015.

[9] Sergey Charnyi, Timo Heister, Maxim A Olshanskii, and Leo G Rebholz. On conservation laws of navier–stokes galerkin discretizations. *Journal of Computational Physics*, 337:289–308, 2017.

[10] Jacqueline H Chen. Extreme scale direct numerical simulation of turbulent combustion-fundamental insights towards next generation engines. Technical report, Sandia National Lab.(SNL-CA), Livermore, CA (United States), 2017.

[11] John Conti, Paul Holtberg, Jim Diefenderfer, Angelina LaRose, James T Turnure, and Lynn Westfall. International energy outlook 2016 with projections to 2040. Technical report, USDOE Energy Information Administration (EIA), Washington, DC United States, 2016.

[12] Francesco Contino, Hervé Jeanmart, Tommaso Lucchini, and Gianluca D'Errico. Coupling of in situ adaptive tabulation and dynamic adaptive chemistry: An effective method for solving combustion in engine simulations. *Proceedings of the Combustion Institute*, 33(2):3057–3064, 2011.

[13] Henry J Curran, Paolo Gaffuri, William J Pitz, and Charles K Westbrook. A comprehensive modeling study of n-heptane oxidation. *Combustion and flame*, 114(1-2):149–177, 1998.

[14] Frederick L Dryer. Chemical kinetic and combustion characteristics of transportation fuels. *Proceedings of the Combustion Institute*, 35(1):117–144, 2015.

[15] Gordon L Dugger and Sheldon Heimel. Flame speeds of methane-air, propane-air, and ethylene-air mixtures at low initial temperatures. 1952.

[16] Ahead Project Europe. Project description, 1999. URL `http://www.ahead-euproject.eu/project-description/`.

[17] Xiang Gao, Suo Yang, and Wenting Sun. A global pathway selection algorithm for the reduction of detailed chemical kinetic mechanisms. *Combustion and Flame*, 167:238–247, 2016.

[18] Olivier Gicquel, Nasser Darabiha, and Dominique Thévenin. Liminar premixed hydrogen/air counterflow flame simulations using flame prolongation of ildm with differential diffusion. *Proceedings of the Combustion Institute*, 28(2):1901–1908, 2000.

[19] David G. Goodwin, Raymond L. Speth, Harry K. Moffat, and Bryan W. Weber. Cantera: An object-oriented software toolkit for chemical kinetics, thermodynamics, and transport processes. `https://www.cantera.org`, 2018. Version 2.4.0.

[20] Xiaolong Gou, Zheng Chen, Wenting Sun, and Yiguang Ju. A dynamic adaptive chemistry scheme with error control for combustion modeling with a large detailed mechanism. *Combustion and Flame*, 160(2):225–231, 2013.

[21] D Goussis, S Lam, and P Gnoffo. Reduced and simplified chemical kinetics for air dissociation using computational singular perturbation. In *28th Aerospace Sciences Meeting*, page 644, 1990.

[22] Michael Frenklach Nigel W. Moriarty Boris Eiteneer Mikhail Goldenberg C. Thomas Bowman Ronald K. Hanson Soonho Song William C. Gardiner Jr. Vitali V. Lissianski Gregory P. Smith, David M. Golden and Zhiwei Qin. Gri-mech 3.0. `http://www.me.berkeley.edu/gri_mech`.

[23] Inside HPC. What is hpc?, 2018. URL `https://insidehpc.com/hpc-basic-training/what-is-hpc/`.

[24] IATA. Iata forecasts, 2018. URL `https://www.iata.org/pressroom/pr/Pages/2018-10-24-02.aspx`.

[25] Matthias Ihme, Chong M Cha, and Heinz Pitsch. Prediction of local extinction and re-ignition effects in non-premixed turbulent combustion using a flamelet/progress variable approach. *Proceedings of the Combustion Institute*, 30(1):793–800, 2005.

[26] Mehdi Jangi and Xue-Song Bai. Multidimensional chemistry coordinate mapping approach for combustion modelling with finite-rate chemistry. *Combustion Theory and Modelling*, 16(6):1109–1132, 2012.

[27] Trupti Kathrotia, Sandra Richter, Clemens Naumann, Nadezhda Slavinskaya, Torsten Methling, Marina Braun-Unkhoff, and Uwe Riedel. Reaction model development for synthetic jet fuels: Surrogate fuels as a flexible tool to predict their performance. In *ASME Turbo Expo 2018: Turbomachinery Technical Conference and Exposition*. American Society of Mechanical Engineers Digital Collection, 2018.

[28] Hideaki Kobayashi, Akihiro Hayakawa, KD Kunkuma A Somarathne, and Ekenechukwu C Okafor. Science and technology of ammonia combustion. *Proceedings of the Combustion Institute*, 37(1):109–133, 2019.

[29] Katharina Kohse-Hinghaus, Patrick Oßwald, Terrill A Cool, Tina Kasper, Nils Hansen, Fei Qi, Charles K Westbrook, and Phillip R Westmoreland. Biofuel combustion chemistry: from ethanol to biodiesel. *Angewandte Chemie International Edition*, 49(21):3572–3597, 2010.

[30] Arthur H Lefebvre. *Gas turbine combustion*. CRC press, 1998.

[31] Kristin C Lewis et al. Commercial aviation alternative fuels initiative. 2010.

[32] Long Liang, John G Stevens, and John T Farrell. A dynamic adaptive chemistry scheme for reactive flow computations. *Proceedings of the Combustion Institute*, 32(1):527–534, 2009.

[33] Andrei N Lipatnikov. Stratified turbulent flames: Recent advances in understanding the influence of mixture inhomogeneities on premixed combustion and modeling challenges. *Progress in Energy and Combustion Science*, 62:87–132, 2017.

[34] Tianfeng Lu and Chung K Law. A directed relation graph method for mechanism reduction. *Proceedings of the Combustion Institute*, 30(1):1333–1341, 2005.

[35] Tianfeng Lu and Chung K Law. Linear time reduction of large kinetic mechanisms with directed relation graph: n-heptane and iso-octane. *Combustion and flame*, 144(1-2):24–36, 2006.

[36] Tianfeng Lu and Chung K Law. Strategies for mechanism reduction for large hydrocarbons: n-heptane. *Combustion and flame*, 154(1-2):153–163, 2008.

[37] Tianfeng Lu and Chung K Law. Toward accommodating realistic fuel chemistry in large-scale computations. *Progress in Energy and Combustion Science*, 35(2):192–215, 2009.

[38] Ulrich Maas and Stephen B Pope. Simplifying chemical kinetics: intrinsic low-dimensional manifolds in composition space. *Combustion and flame*, 88(3-4):239–264, 1992.

[39] Kyle E Niemeyer, Chih-Jen Sung, and Mandhapati P Raju. Skeletal mechanism generation for surrogate fuels using directed relation graph with error propagation and sensitivity analysis. *Combustion and flame*, 157(9):1760–1770, 2010.

[40] Perrine Pepiot-Desjardins and Heinz Pitsch. An efficient error-propagation-based reduction method for large chemical kinetic mechanisms. *Combustion and Flame*, 154(1-2):67–81, 2008.

[41] Charles D Pierce and Parviz Moin. Progress-variable approach for large-eddy simulation of non-premixed turbulent combustion. *Journal of fluid Mechanics*, 504:73–97, 2004.

[42] Stephen B Pope. Computationally efficient implementation of combustion chemistry using in situ adaptive tabulation. 1997.

[43] Ishwar Puri and Suresh Aggarwal. Partially-premixed flames: Applications and issues. In *45th AIAA Aerospace Sciences Meeting and Exhibit*, page 597, 2007.

[44] Zhuyin Ren and Stephen B Pope. Second-order splitting schemes for a class of reactive systems. *Journal of Computational Physics*, 227(17):8165–8176, 2008.

[45] Guillaume Ribert, L Vervisch, P Domingo, and Y-S Niu. Hybrid transported-tabulated strategy to downsize detailed chemistry for numerical simulation of premixed flames. *Flow, turbulence and combustion*, 92(1-2):175–200, 2014.

[46] Robert Sugden Rogallo. Numerical experiments in homogeneous turbulence. 1981.

[47] SP Sharma, DD Agrawal, and CP Gupta. The pressure and temperature dependence of burning velocity in a spherical combustion bomb. In *Symposium (International) on Combustion*, volume 18, pages 493–501. Elsevier, 1981.

[48] Weiqi Sun, Xiaolong Gou, Hossam A El-Asrag, Zheng Chen, and Yiguang Ju. Multi-timescale and correlated dynamic adaptive chemistry modeling of ignition and flame propagation using a real jet fuel surrogate model. *Combustion and Flame*, 162(4):1530–1539, 2015.

[49] Wenting Sun, Zheng Chen, Xiaolong Gou, and Yiguang Ju. A path flux analysis method for the reduction of detailed chemical kinetic mechanisms. *Combustion and Flame*, 157(7):1298–1307, 2010.

[50] FX Trias and O Lehmkuhl. A self-adaptive strategy for the time integration of navier-stokes equations. *Numerical Heat Transfer, Part B: Fundamentals*, 60(2):116–134, 2011.

[51] TU Berlin TU Delft. Ahead project. 2010.

[52] Jeroen Adrianus van Oijen. *Flamelet-generated manifolds: development and application to premixed laminar flames*. Technische Universiteit Eindhoven Eindhoven, 2002.

[53] Mariano Vázquez, Guillaume Houzeaux, Seid Koric, Antoni Artigues, Jazmin Aguado-Sierra, Ruth Arís, Daniel Mira, Hadrien Calmet, Fernando Cucchietti, Herbert Owen, et al. Alya: Multiphysics engineering simulation toward exascale. *Journal of computational science*, 14:15–27, 2016.

[54] Denis Veynante and Luc Vervisch. Turbulent combustion modeling. *Progress in energy and combustion science*, 28(3):193–266, 2002.

[55] Wenwen Xie, Zhen Lu, Zhuyin Ren, and Lingyun Hou. Dynamic adaptive chemistry via species time-scale and jacobian-aided rate analysis. *Proceedings of the Combustion Institute*, 36(1):645–653, 2017.

[56] Suo Yang, Reetesh Ranjan, Vigor Yang, Suresh Menon, and Wenting Sun. Parallel on-the-fly adaptive kinetics in direct numerical simulation of turbulent premixed flame. *Proceedings of the Combustion Institute*, 36(2):2025–2032, 2017.

[57] Zhuyin Ren Tianfeng Lu Yang, Hongtao and Graham M. Goldin. Dynamic adaptive chemistry for turbulent flame simulations. *Combustion Theory and Modelling*, 17(1):167–183, 2013.